THESIS

VOLATILE ORGANIC COMPOUND AND METHANE EMISSIONS FROM WELL DEVELOPMENT OPERATIONS IN THE PICEANCE BASIN

Submitted by

Noel G. Hilliard

Department of Atmospheric Science

In partial fulfillment of the requirements

For the Degree of Master of Science

Colorado State University

Fort Collins, Colorado

Summer 2016

Master's Committee:

Advisor: Jeffrey L. Collett Jr.

Emily V. Fischer
Jay M. Ham
Arsineh Hecobian

ABSTRACT

VOLATILE ORGANIC COMPOUND AND METHANE EMISSIONS FROM WELL DEVELOPMENT OPERATIONS IN THE PICEANCE BASIN

The natural gas industry in Colorado has experienced significant growth in the last decade due to widespread use of unconventional natural gas extraction technologies. Garfield County is located in the Rocky Mountain Region on the western slope of Colorado above the Piceance Basin. Natural gas wells in this region penetrate the William's Fork formation, located approximately 4,000 ft. below the surface, which is a tight sand formation known to be rich in natural gas. Horizontal drilling increases the extraction potential of natural gas stored in several sandstone lenses. Hydraulic fracturing is a stimulation technique used to maximize the flow and efficiency of natural gas transport to the surface from unconventional reservoirs. Once the formation is adequately cracked, 10-50% of the hydraulic fluid flows back to the surface .

Our field team collected samples in Garfield County between 2013-2015 to measure methane, ozone precursors, and air toxics associated with natural gas extraction activities. Very few studies have provided direct observations of VOC emissions from individual well development activities. Emission rates of 48 VOCs and methane were determined using the tracer ratio method for three well development operations: drilling, hydraulic fracturing (fracking), and flowback for a subset of samples collected. Methane had mean emission rates of 1.57, 6.78, and 25.6 g s^{-1} for drilling, hydraulic fracturing, and flowback operations respectively, while toluene had mean emission rates of 1.24, 0.469, and 0.437 g s^{-1} for these operations. Measured emission rates were used to determine if specific VOCs were well correlated with each

other and/or methane emission rates. Strong correlations between individual VOC emission rates and methane were investigated to assess whether methane emission rates might serve as useful surrogates for emission rates of individual VOCs, which are less easily measured. We found that methane and ethane appear to be emitted from the same sources for all operation types indicating that methane emission rates may be useful surrogates for ethane emission rates. Methane emission rates appear not to be very useful surrogates for heavier VOCs, including C_5-C_{10} alkanes, alkenes, and aromatics. Concentration ratios of source-specific tracer compounds were investigated to determine the source signatures of individual operation types. We found that drilling emissions appear to be primarily influenced by combustion, while flowback emissions are primarily influenced by the release of natural gas and other substances from the well.

ACKNOWLEDGEMENTS

The field measurements conducted for this study were crucial for completion of this thesis. Special recognition goes to the field team: Arsineh Hecobian, Andrea Clements, Kira Shonkwiler, Landan MacDonald, Bradley Wells, Yuri Desyaterik, Yong Zhou, and Derek Weber. Kira Shonkwiler had primary responsibility for the tracer release system and the meteorological station. Dr. Andrea Clements had primary responsibility for GC-FID canister analysis and associated chromatogram analysis. Dr. Yong Zhou had primary responsibility for the 5-channel canister analysis. Dr. Arsineh Hecobian had primary responsibility for coordinating field measurements, mobile measurements, data validation and participated in 5-channel chromatogram analysis. Derek Weber assisted with 5-channel chromatogram analysis and collection of canister samples. Landan MacDonald and Bradley Wells had responsibility for collecting canister samples, and Landan MacDonald performed the extensive analysis on the real-time methane data.

A very special acknowledgement goes to Arsineh Hecobian and Andrea Clements for their guidance and support throughout the last two years. I would also like to give a special acknowledgement to my advisor: Jeff Collett. Thank you so much for this opportunity and for your guidance the past three years.

TABLE OF CONTENTS

LIST OF TABLES

LIST OF FIGURES

CHAPTER 1

INTRODUCTION

1.1 Motivation

The United States (U.S.) contains a large amount of oil and natural gas (O&NG) energy resources in the form of coalbeds, shale, and tight sands [API, 2015]. In the last decade the U.S. O&NG industry has experienced significant growth due to technological improvements in the processes associated with the unconventional extraction of natural gas from tight sand and shale reservoirs [Thompson et al., 2014]. Key advances include improvements in hydraulic fracturing and horizontal drilling. These technological advances have allowed for more effective retrieval of natural gas and increased the use of natural gas as an energy resource [Swarthout et al., 2013]. The use of unconventional natural gas extraction practices, such as horizontal drilling and hydraulic fracturing are projected to increase from 42% of the total U.S. natural gas production in 2007 to 64% by 2020 [API, 2015]. Figure 1.1 shows the projected increase in tight sand and shale reservoirs compared to the other reservoirs [EIA, 2015].

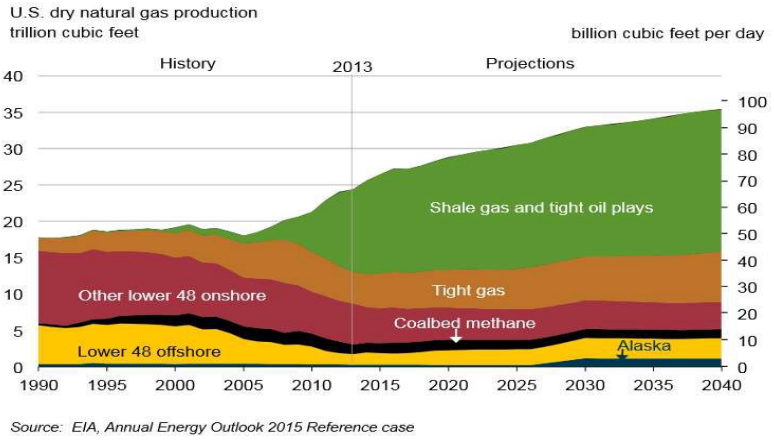

Figure 1.1 Sources of dry natural gas production in the U.S. The white line represents the year that this information was published. This information was provided by the U.S. Energy Information Administration.

As of 2012, 46% of domestic U.S. natural gas production was from shale and tight sand reservoirs [Gilman et al. 2013]. Currently 25% of U.S. natural gas production occurs in the western U.S. [WEA, 2015]. Colorado is one of the highest natural gas producing states, ranking 6th nationally in 2013 [EIA, 2015]. Colorado's distinctive geology allows for significant natural gas reserves with 11 of the largest natural gas fields residing in the state [EIA, 2014]. The highest producing basins in the state are the Denver-Julesburg Basin, a shale formation in northeastern Colorado and the Piceance Basin, a tight sands formation in northwestern Colorado. Figure 1.2 shows a map with the two basins identified.

Figure 1.2. Map identifying the Piceance Basin and the Denver-Julesburg Basin [Jaffe, 2012]. This information was obtained from the U.S. Geological Survey and U.S. National Oceanic and Atmospheric Administration.

Between 2000 and 2011, the number of active gas wells in Colorado increased by 34% and by 2011, 6% of U.S. producing natural gas wells were in Colorado [Swarthout et al., 2013]. Figure 1.3 demonstrates the overall increase in the number of producing gas wells in Colorado since 1990. This plot was made using information provided by the U.S. Energy Information Administration [EIA, 2015].

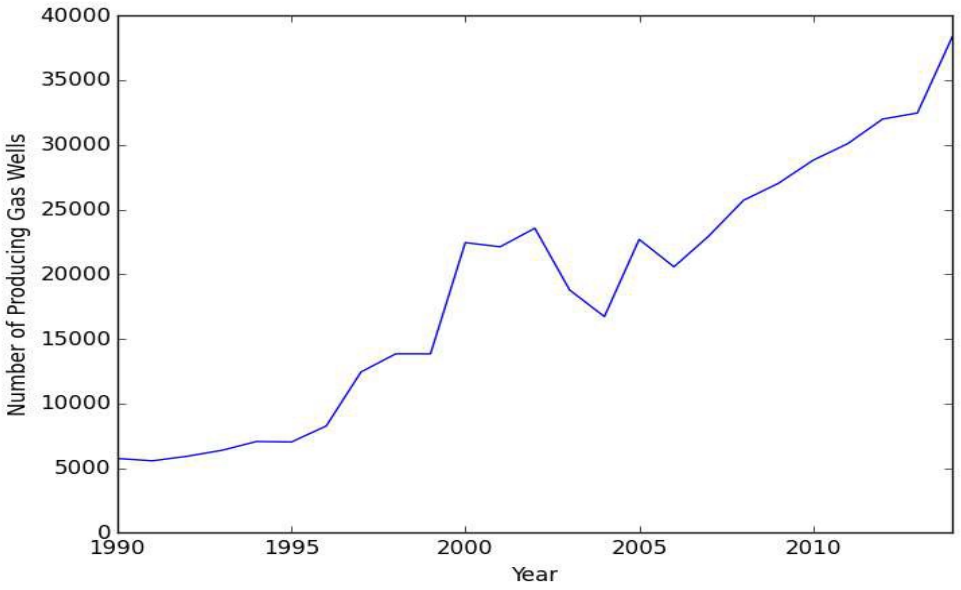

Figure 1.3. Number of producing gas wells in Colorado between 1990 and 2014. This information was obtained from the U.S. Energy Information Administration.

In 2014, approximately 62% of Colorado's 52,556 active oil and gas wells were located in the Denver-Julesburg Basin in Weld County and the Piceance Basin in Garfield County [Weiner, 2014]. Figure 1.4 shows the distribution of active oil and gas wells by county in Colorado in 2014. This plot was made using information provided by the Colorado Oil and Gas Conservation Commission (COGCC) [Weiner, 2014].

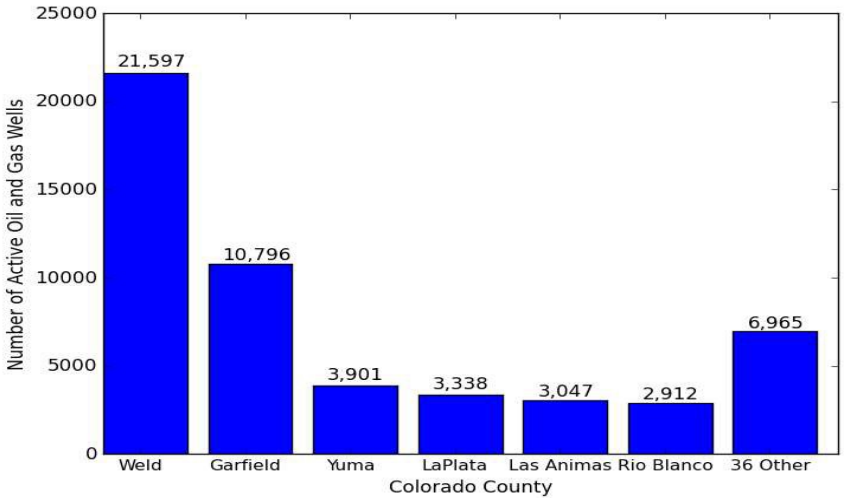

Figure 1.4. Distribution of active oil and gas wells in Colorado in 2014. This information was obtained from the COGCC.

Although technological advances in unconventional natural gas extraction have increased the efficient recovery of important energy resources in the Denver-Julesburg Basin and the Piceance Basin, there are also potentially negative impacts. The expansion of unconventional natural gas extraction has increased concern about the air quality impacts of emissions along the Colorado Front Range and in Garfield County. As a result of the increase in extraction, more emissions of volatile organic compounds (VOCs), greenhouse gases, and subsequent production of secondary air pollutants such as ozone are expected [McKenzie et al., 2012]. Potentially hazardous emissions are possible during the various stages of the natural gas extraction processes, including well assembly, drilling, hydraulic fracturing, flowback, well completion, storage and distribution of natural gas, flaring, gas condensate flashing, and dehydration [Swarthout et al., 2013].

Raw, unprocessed natural gas is approximately 60-90% methane (CH_4) with the remaining portion consisting of various VOCs and nitrogen oxides (NO_x) [Gilman at al., 2013].

CH_4 is a greenhouse gas that is more than 25 times more potent than carbon dioxide over a 100-year period [EPA, 2016a]. Hydrocarbon VOCs are organic chemical compounds consisting of hydrogen and carbon atoms released from both natural and anthropogenic emissions that readily vaporize due to low boiling points and participate in atmospheric photochemical reactions [USGS, 2015]. Hydrocarbon VOCs include alkanes, alkenes, cycloalkanes, and aromatics. These types of VOCs have been shown to be associated with O&NG extraction activities [Gilman et al., 2013; Warneke et al., 2014] and will be the focus of this thesis. Light C_1-C_5 alkanes, are the main constituents of natural gas and gasoline vapors [ARS, 2015]. Heavier alkanes, including C_6-C_{10}, are the main constituents of crude oil [ARS, 2015]. Alkenes are not one of the main constituents of natural gas or crude oil but, are formed when larger alkane molecules oxidize in the atmosphere. Aromatic hydrocarbon compounds are a subset of VOCs that contain a benzene ring or rings as part of their structure. Aromatics are found in gas-fired engine emissions as well as other engine sources associated with O&NG operations [ARS, 2015]. Some VOCs are classified as Hazardous Air Pollutants (HAPs) or air toxics. This group of VOCs includes 187 toxic air pollutants regulated by the Environmental Protection Agency (EPA) [EPA, 2015b]. Benzene, toluene, ethylbenzene, and xylene (BTEX) are classified as HAPs [ARS, 2015].

Recent scientific studies conducted in Colorado and Utah have reported VOC emissions associated with oil and natural gas extraction activities [Gilman et al.,2013; Pétron et al., 2014; Swarthout et al., 2013; Thompson et al., 2014; Warneke et al., 2014]. Gilman et al. [2013] measured a suite of VOCs including propane, benzene, and ethyne in northeastern Colorado to demonstrate the influence of different emission source types on the observed concentrations and to compare the concentrations to those measured in 28 U.S. cities [Baker et al., 2008]. They observed a mean propane mixing ratio of 27 ± 1 ppbv at the Boulder Atmospheric Observatory

(BAO) during the Nitrogen Aerosol Composition and Halogens on a Tall Tower (NACHTT) campaign from February – March 2011, within the range reported by 28 U.S. cities. They estimated that 90% of alkanes, 70% of cycloalkanes, and 20-30% of aromatics, alkenes, and alkynes observed at BAO were from an O&NG source based on the ratio of i-pentane/n-pentane [Gilman et al., 2013]. Swarthout et al. [2013] observed elevated non-methane hydrocarbon (NMHC) mixing ratios; specifically, C_2-C_5 mixing ratios were elevated by an order of magnitude above regional background levels during the same campaign. Pétron et al. [2014] derived emission estimates of propane, n-butane, i-pentane, n-pentane, and benzene from top-down aircraft-based measurements in the heavily drilled Denver-Julesburg Basin in Weld County, CO for two days in May 2012. They determined that the total emissions from all regional sources for those five hydrocarbons were 25.4 ± 8.2 tons/h and attribute all C_3-C_5 emissions to O&NG sources [Pétron et al., 2014]. Thompson et al. [2014] observed elevated NMHC concentrations in the Denver-Julesburg Basin near Wattenberg Gas Field between March-June 2013. They determined that the mean mole fractions of C_2-C_5 alkanes were elevated by a factor of 18-77 compared to the regional background from ambient measurements of NMHCs [Thompson et al., 2014]. During the ground-based Uintah Basin Winter Ozone Study 2012 (UBWOS2012), Warneke et al. [2014] observed mixing ratios of aromatics near 1 ppmv and attributed this to point sources associated with gas well pad operations. Garfield County, CO has been collecting ambient air samples since 2008 at various sites around the county for VOCs associated with oil and natural gas extraction activities. In both 2013 and 2014 the samples consisted of mostly light alkanes (C_1-C_5) with 81% to 89% light alkanes in the 2013 samples and 85% to 87% light alkanes in the 2014 samples showing evidence of O&NG influence [ARS, 2015].

As shown by these previous ambient air studies, the complicated mixture of VOCs emitted from natural gas extraction activities may be of concern and should be investigated because VOC concentrations can reach levels much higher than regional background levels. VOC emissions from oil and natural gas extraction may be harmful because they are associated with degradation of air quality in otherwise rural areas [McKenzie et al., 2012; ARS, 2015]. These activities may raise mean propane concentrations to 27 ppbv, 3-9 times higher than some industrialized cities, and raise mean benzene levels to 0.29 ppbv, within the range of reported urban concentrations [Gilman et al., 2013]. The impact of VOC emissions from natural gas extraction activities is of particular concern in Colorado because the COGCC allows natural gas wells to be located as little as 150 ft from residences [McKenzie et al., 2012]. Although area VOC concentrations in some areas of Colorado may exceed the ranges of industrialized cities, the highest VOC concentrations are expected near O&NG sites and the people living closest to O&NG sites will be exposed to the highest concentrations of primary emissions, including air toxics.

Recent studies have also drawn a connection between VOC emissions from oil and natural gas extraction and ozone formation [e.g. Gilman et al., 2013]. Ozone (O_3) is a secondary pollutant formed by the reaction of VOCs with nitrogen oxides (NO_x) in the presence of sunlight [EPA, 2016b]. An increasing amount of scientific research is concluding that the emission of VOCs and NO_x from oil and natural gas activities is related to high ground-level ozone episodes [e.g. Gilman et al., 2013, Schnell et al., 2009]. Gilman et al. [2013] used VOC and hydroxyl (OH) reactivity as a measure of ozone formation potential and attributed observed high ozone potential to high concentrations of C_2-C_6 alkanes reacting with OH. They estimated on average 55 ± 18% of the VOC-OH reactivity was due to emissions of VOCs from O&NG operations

demonstrating that these emissions were a major source of ozone precursors [Gilman et al., 2013]. Schnell et al. [2009] observed rapid increases in hourly average ozone concentrations from 10 – 30 ppb at night to greater than 140 ppb at solar noon during winter in the rural Upper Green River Basin, Wyoming, which is located near the Jonah-Pinedale Anticline natural gas field. Field et al. [2015] observed frequent high ozone episodes with hourly ozone concentrations greater than 85 ppb in the same area during winter. They also observed a significant decrease in ozone concentrations associated with reductions in VOC concentrations [Field et al. 2015].

1.2 VOC Emission Ratios

The use of emission ratios is a widely used method of determining source composition and allows for the separation of chemistry from meteorology in order to identify source signatures [Koss et al., 2015]. Many studies have used VOC ratios to determine the contribution of O&NG development to regional air pollution. Gilman et al. [2013] used the i-pentane/n-pentane ratio range, obtained from literature reports, of 2.3-3.8 as a source signature for urban emissions [Gentner et al., 2009; McGaughey et al., 2004] and the i-pentane/n-pentane ratio of the Greater Wattenberg oil and gas area in northeastern Colorado (0.86 ± 0.02, $r = 0.97$) to distinguish emission sources at three Colorado locations. They observed i-pentane/n-pentane ratios at BAO tower (0.885 ± 0.002, $r = 0.998$), Fort Collins (0.809 ± 0.008, $r = 0.990$), and Boulder (1.10 ± 0.05, $r = 0.91$) [Gilman et al., 2013] and determined that O&NG operations were the main source of VOCs for Fort Collins and BAO, while both urban and O&NG operations influence emissions in Boulder because the ratio observed there is between the main source ratios [Gilman et al., 2013]. In a similar study conducted by Swarthout et al. [2015] in Pennsylvania in the Marcellus Shale region, the urban i-pentane/n-pentane ratio of Pittsburgh

(1.48) [Baker et al., 2008] was compared to the O&NG i-pentane/n-pentane ratio (0.9) of locations in Pennsylvania with unconventional natural gas development. They determined that samples with an i-pentane/n-pentane ratio of near 0.9 indicated the location was strongly impacted by unconventional natural gas development while a higher ratio indicated more of an influence from urban emissions [Swarthout et al. 2015]. The similar i-pentane/n-pentane ratio observed in Colorado and in Pennsylvania near O&NG development demonstrates the usefulness of ratios to identify primary O&NG source regions. Pétron et al. [2012] observed strong correlations above $r^2 = 0.9$ when comparing C_3H_8 to n-C_4H_{10} and the C_5H_{12} isomers and moderate correlations ($r^2 = 0.66$) between CH_4 and C_3H_8 in an area located near the Wattenberg O&NG field in the Denver-Julesburg Basin. The major emission sources along the Front Range are O&NG operations and urban emissions; therefore, they concluded that oil and gas operations were responsible for elevated alkane levels because the emissions did not correlate well with combustion tracers [Pétron et al., 2012]. Koss et al. [2015] observed strong correlations between benzene and methane emission rates at Horse Pool ground site in the Uintah Basin in 2012 ($r^2 = 0.679$) and 2013 ($r^2 = 0.875$). They extrapolated methane emission rates from benzene emission rates and found that the benzene emission rates were consistent with those calculated from independent aircraft measurements.

1.3 Garfield County

Field measurements discussed in this thesis were conducted in Garfield County, CO. Garfield County is located in the Rocky Mountain Region on the western slope of Colorado. The county experienced an increase in natural gas extraction and production activities between 2000 and 2012 due to the increased use of hydraulic fracturing and horizontal drilling [DrillingEdge Inc., 2015]. Garfield County is located in the Piceance Basin, which straddles the northwestern

section of Colorado and eastern section of Utah. The location of Garfield County and the Piceance Basin are shown in Figure 1.5.

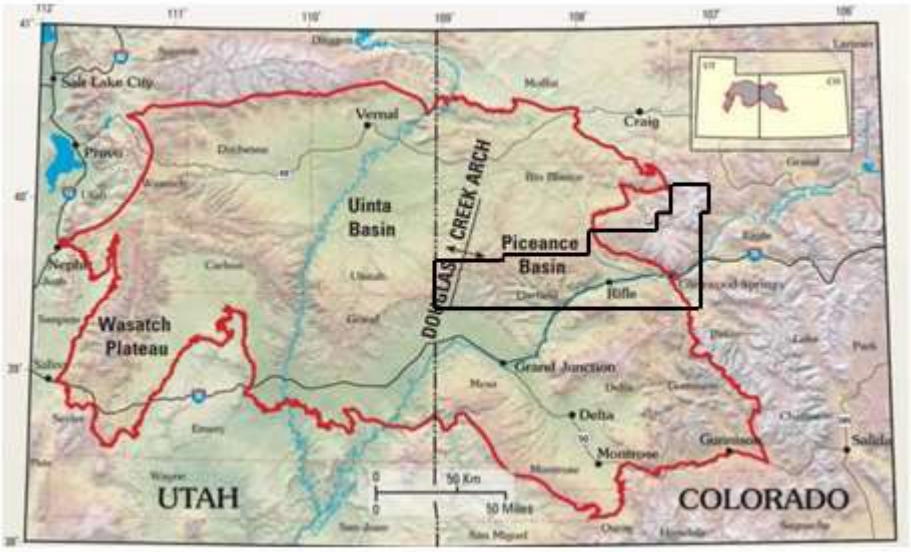

Figure 1.5. Map of Utah and Colorado. The location of Garfield County in western Colorado is outlined in black. The location of the Piceance Basin is outlined in red. The Douglas Creek Arch separates the Uinta Basin from the Piceance Basin [Niobrara News, 2014].

The Piceance Basin is roughly 6,000 square miles wide and includes several layers of underground sedimentary formations. Wells in this region penetrate a tight sands formation called the William's Fork formation, which is the fourth sedimentary layer starting at about 5,000 ft. below the surface [Baytok et al., 2013]. The William's Fork formation is an impermeable or non-porous sedimentary layer rich in natural gas that varies in depth from 5,000 ft. to 12,000 ft. below the surface [Baytok et al., 2013]. The O&NG industry in this region extracts natural gas from this layer in particular because the tight sands formation contains natural gas trapped in "sandstone lenses" ranging from 0.5 to 29.0 ft. in thickness and ranging from 40.1 to 2,791.1 ft. in width sealed by impermeable shale layers [Dennison, 2005]. The tight

sands formation requires special stimulation procedures to extract the natural gas, such as horizontal drilling and hydraulic fracturing [EPA, 2015a].

Before the well development processes can begin a well permit must be submitted and approved by the COGCC [Dennison, 2005]. The O&NG company will also survey the area for road and pad construction during this time. Vertical drilling and preparation of the well pad is the first step in well development, where a rotating pipe with a bit attached to the end is used to begin drilling the borehole. As the pipe enters the ground, more pipe is added at 30 ft. increments [Dennison, 2005]. Drilling mud is then circulated into the ground and back up to the surface to remove drill cuttings and maintain hydrostatic pressure. Evacuation pits are used to store the drilling mud [Dennison, 2005]. Once the piping is in place, three layers of casing are cemented around the piping in the following order: conductor casing to 20-50 ft. in depth, surface casing to 500-2,000 ft. in depth, and production casing to 6,000-9,000 ft. in depth [Dennison, 2005]. These casings are put in place to prevent caving of the well, blowouts, and leakage of various fluids circulated through the well [Dennison, 2005].

Horizontal drilling is a process that involves redirecting a vertically drilled well horizontally through underground rock formations to allow for a much larger area to extract natural gas [EPA, 2015a]. Horizontal drilling used in Garfield County allows for the pockets of natural gas stored in the several sandstone lenses to be identified and extraction potential to increase. In Garfield County, the duration of the drilling stage ranges from 2-7 days per well. Although this well development process maximizes natural gas extraction, it also involves an enormous amount of power and equipment; therefore, there will be emissions of NO_x and VOCs associated with combustion of fuel for the drill rig, generator engines, heaters, and pumps as well as VOC emissions from the drilling waste [Field et al. 2014].

In unconventional reservoirs special stimulation is required to maximize the flow efficiency of the natural gas to the surface after the well is drilled. Hydraulic fracturing is the most commonly used stimulation technique for extraction of natural gas from unconventional reservoirs [Dennison, 2005]. The production casing inserted into the well bore during the drilling stage is perforated in the areas with natural gas in the formation [FracFocus, 2015]. Hydraulic fracturing requires the pumping of large amounts of fluid into underground formations at pressures of more than 10,000 psi until the rock formation can no longer withstand the pressure and the formation begins to crack or fracture [Dennison, 2005]. Emissions of VOCs and NO_x is possible from many sources during the process including the hydraulic fracturing fluid that contains various VOCs, diesel truck exhaust, the equipment used to pump the hydraulic fracturing fluid underground, and the storage of the fracturing fluid that returns to the surface. Fracturing fluid usually contains water, proppants (e.g. sand), and various chemicals [FracFocus, 2015]. Examples of the chemical components of hydraulic fracturing fluid are listed in Table 1.1.

Table 1.1: List of chemicals in hydraulic fracturing fluid. Adapted from FracFocus Chemical Disclosure Registry [2015].

Additive Type	Chemical Type	Purpose
Acid	Hydrochloric Acid	Helps dissolve minerals and initiate cracks
Acid/Corrosion Inhibitor	Isopropanol	Protects casing from corrosion
Biocide	Glutaraldehyde	Eliminates bacteria in the water that cause corrosive byproducts
Base Carrier Fluid	Water	Create fracture geometry and suspend proppant
Breaker	Ammonium Persulfate	Allows a delayed break down of gels
Clay and Shale Stabilization/control	Choline Chloride	Temporary or permanent clay stabilizer to lock down clays in the shale structure
Crosslinker	Petroleum Distillate	Maintains viscosity as temperature increases
Friction Reducer	Polyacrylamide	Reduces friction effects over base water pipe
Gel	Guar Gum	Thickens the water in order to suspend proppant
Iron Control	Citric Acid	Iron chelating agent that helps precipitation of metal oxides
Non-Emulsifier	Lauryl Sulfate	Used to break or separate oil/water mixtures
pH Adjusting Agent/Buffer	Sodium Hydroxide	Maintains the effectiveness of the other additives such as crosslinkers
Propping Agent		Keeps fractures open allowing for hydrocarbon production
Scale Inhibitor	Copolymer of Acrylamide/Sodium Acrylate	Prevent scale in pipe and formation
Surfactant	Lauryl Sulfate	Reduce surface tension of the treatment fluid in formation to improve fluid recovery

Once the formation is adequately cracked, the injection of the fluid ends and the hydraulic fracturing fluid flows back to the surface; this process is called flowback. 10-50% of the hydraulic fracturing fluid flows back to the surface along with wastewater, which is also called produced water. The propping agents remain underground to keep the fractures open to allow natural gas to flow up the well to the surface [FracFocus, 2015]. During flowback, contributions to VOC and NO_x emissions result due to fluid handling and equipment leaks [Field et al., 2014].

1.4 Overview

This thesis project was part of a field study conducted in Garfield County, Colorado from 2013 to 2015 to measure methane, ozone precursors and air toxics associated with natural gas extraction activities. This thesis focuses on characterizing and quantifying different types of VOCs including alkanes, alkenes, and aromatics from whole air canister samples collected downwind from various well pad locations in Garfield County using gas chromatography flame ionization detection (GC-FID). The characterization of VOCs emitted from different natural gas extraction activities can help better identify environmental and health hazards. While measurements of methane emitted from O&NG extraction activities have become more common, very few studies provide direct observations of VOC emissions as these types of measurements are more complex. A particular gap exists regarding VOC emissions for new well development and especially for individual well development activities. VOC emissions from three well development stages are the focus of this thesis: drilling, hydraulic fracturing and flowback as well as combinations of these operation types at locations with simultaneous operations occurring on co-located wells.

VOC concentration measurements using whole air canister samples and real-time methane concentration measurements using a Picarro cavity ring-down analyzer were used to characterize VOC and methane emission rates with the tracer ratio method. Emission rates are more useful than concentration data because emission rates are independent of meteorological conditions and distance from the source. The emission rates of individual VOCs were examined to determine if specific VOC emissions were well correlated with each other and methane emission rates. The relationship between individual VOC emission rates and methane emission rates were also examined through emission ratios for individual stages of well development. By

examining relationships between VOCs and methane emission rates, we can assess whether methane emission rates might be useful surrogates for the emission rates of any individual VOCs for particular activity types. Lastly, emission ratios of source-specific tracer compounds were investigated to determine the source signatures of various O&NG well development operations.

The following Chapter details the methods used for field measurements and GC-FID canister analysis in addition to the methods used for the data analysis to determine emission rates and emission ratios. Chapter 3 presents the results of the field measurements for individual stages of well development including emission rates, emission rate correlations, source signatures and emission ratios. Conclusions are included in Chapter 4 and future work is included in Chapter 5.

CHAPTER 2

METHODS

2.1 Experimental Design

Our field team conducted measurements of VOC emissions for 21 experiments downwind of natural gas well development activities in Garfield County from 2013-2015. The results from 13 of these experiments are discussed in this thesis because the complete data set was not available at the time of analysis. The details of each field experiment are included in Appendix I. Our field team consisted of Dr. Arsineh Hecobian, Dr. Andrea Clements, Kira Shonkwiler, Landan MacDonald, Bradley Wells, Dr. Yuri Desyaterik, Dr. Yong Zhou, and Derek Weber. Kira Shonkwiler had primary responsibility for the tracer release system and the meteorological station. Dr. Andrea Clements had primary responsibility for GC-FID canister analysis and associated chromatogram analysis. Dr. Yong Zhou had primary responsibility for the 5-channel canister analysis. Dr. Arsineh Hecobian had primary responsibility for mobile measurements, data validation, participated in 5-channel chromatogram analysis, and coordinated field measurements. Derek Weber assisted with 5-channel chromatogram analysis and collection of canister samples. Landan MacDonald and Bradley Wells had responsibility for collecting canister samples, and Landan MacDonald performed the extensive analysis on the real-time methane data. I assisted with canister cleaning, chromatogram analysis, canister collection, field set-up, and performed the analysis for VOC data presented here. Table 2.1 summarizes the primary responsibilities for each field team member.

Table 2.1: Primary responsibilities for each field team member.

Field Team Member	Primary Responsibility
Andrea Clements	GC-FID canister analysis, GC-FID chromatogram analysis
Yong Zhou	5-channel GC canister analysis
Arsineh Hecobian	Coordinated field measurements, mobile measurements, data validation, 5-channel chromatogram analysis
Derek Weber	5-channel chromatogram analysis, canister collection
Landan MacDonald	Canister collection, real-time methane data analysis
Bradley Wells	Canister collection
Noel Hilliard	Canister cleaning, GC-FID/5-channel chromatogram analysis, canister collection, VOC data analysis

Figure 2.1 shows a typical field set-up with the equipment used to make measurements on a well pad conducting drilling, fracking, or flowback operations. The experiments were performed using a tracer technique to locate the emission plume downwind of the well pad of interest. A tracer release system was positioned on the well pad to release the tracer gas from a manifold. Downwind of the well pad a meteorological (met) station measured wind, relative humidity, temperature, and pressure. A mobile plume tracker equipped with a Picarro cavity ringdown analyzer (model G2203) to measure CH_4 and the tracer gas was also positioned downwind. Lastly, 1.4 L stainless steel Entech® canisters coated with Silonite® were used to collect whole air samples (WAS). Silonite is a distinctive fused silica layer used to coat the inside of the canisters similar to the inside of a gas chromatograph (GC) column. These canisters are believed to be the most inert canisters available and the best for sampling GC compatible compounds [Entech Instruments Inc., 2015]. Two canisters were positioned on the front of the mobile plume tracker at two heights attached to either a vehicle mounted mast or a tripod. Another canister was deployed on a tripod downwind of the well pad of interest and either closer or further downwind than the mobile plume tracker on a tripod.

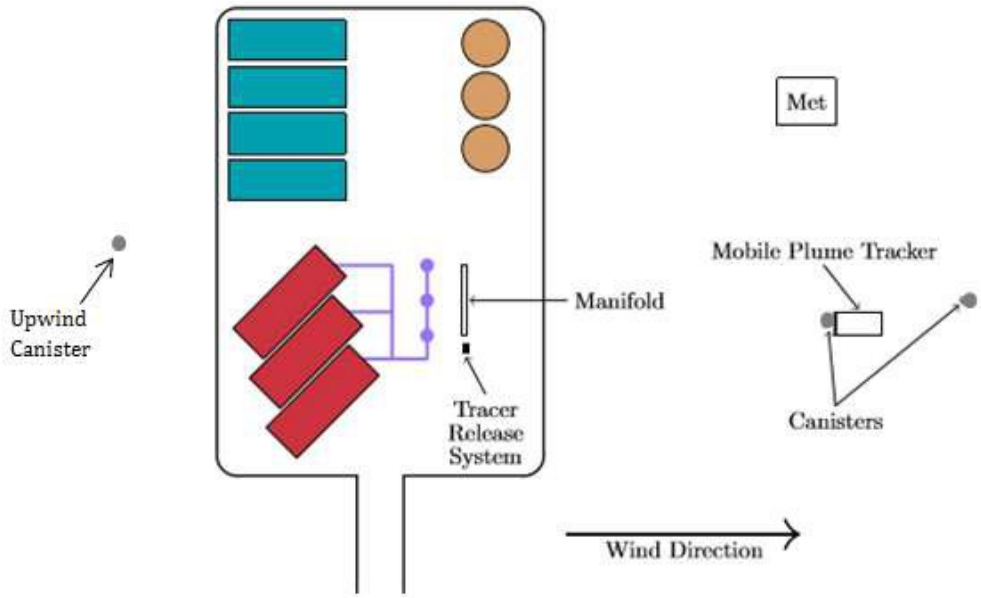

Figure 2.1. Schematic of field work set-up on the well pad. The tracer release system including the distribution manifold located on the well pad [MacDonald, 2015]. The meteorological station, mobile plume tracker and canister triggering systems were located downwind of the well pad to take measurements.

One canister was positioned upwind of the well pad of interest (on a tripod or on the front of the mobile plume tracker attached to a vehicle mounted mast) for each day of sampling to represent the background VOC concentrations. Acetylene was released from the well pad during the collection of the background sample and the Picarro was collecting methane and acetylene to ensure the upwind location of sample collection. The deployed canisters were triggered remotely by a canister triggering system to open for sampling and to close to collect a WAS of the plume emitted from the well pad. This section will give a detailed description of the experimental design used to collect the whole air canister samples in the field.

2.1.1 Canister Preparation

Before each field sampling campaign the canisters were cleaned using an Entech Canister Cleaning System. The system consisted of a molecular drag pump control box (model 3100A), a canister cleaning oven (model 3108), a rough pump, and an ultra-high purity (UHP) nitrogen diluent gas cylinder. Figure 2.2 shows a schematic of the Entech Cleaning System. The canisters were cleaned as follows. First, up to 16 canisters were connected to the manifold. Then, the canister cleaning oven and the system were heated to 80˚C. Then, the canisters underwent eight evacuation/fill cycles consisting of evacuation to 1 x 10^{-2} torr, fill to 18.6 psi with UHP nitrogen diluent that flowed through a humidification chamber because added moisture enhances removal of VOCs from the inside of the canisters, followed by evacuation back to 1 x 10^{-2} torr first using the rough pump and then the molecular drag pump. After the eight cycles of evacuation/fill, the canisters were left under high vacuum for one hour to re-volatilize and remove any remaining

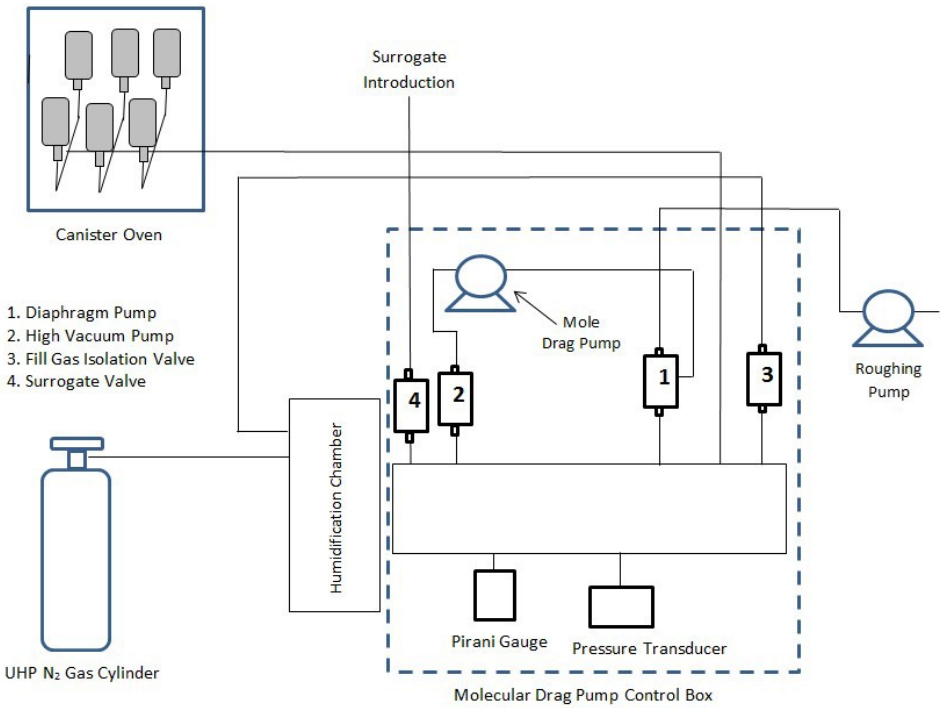

Figure 2.2. Diagram of Entech Canister Cleaning System [Entech Instruments Inc.].

VOCs in the canister. A leak check was also performed by making sure the canisters could reach the 10 mtorr threshold and maintain it once the vacuum was switched off. The total method run time was between 1.5 and 2.5 hours depending on the number and size of canisters being cleaned.

2.1.2 Tracer Release

A tracer technique was used to locate an emission plume downwind of the emission source on the well pad to collect WAS canisters. This technique requires the release of a non-reactive, non-toxic tracer gas co-located with the emission source on the well pad at a known concentration and rate. The location of the plume is then identified by high concentrations of the tracer gas. Downwind of the emission source, samples of the tracer gas and other compounds of interest in the emission plume are collected [Ludwig et al., 1983]. In this field study, acetylene (C_2H_2) was released through a tracer release system as a tracer gas because C_2H_2 is an inert gas that has a low molecular weight, a very low natural background concentration, a very slow atmospheric decomposition time, is readily measured at trace concentration levels, and oil and gas operations are not considered a major source of the gas [Reiche et al., 2014]. The tracer gas was supplied in acetylene cylinders. Acetylene cylinders are filled with a porous-mass filler material saturated with acetone allowing for the acetylene to be stored in the cylinders at a reasonable pressure without risk of explosive decomposition [CGA, 1990]. The acetylene tracer gas was diluted with ambient air by a 3 meter tall tracer release system and released from a 3 meter long perforated manifold at a controlled flow rate. A diagram of the tracer release system is included in Appendix A.

2.1.3 Mobile Measurements

A Chevrolet Tahoe Hybrid mobile plume tracker vehicle equipped with a Picarro instrument was deployed downwind of the tracer release system located on the well pad to locate the plume based on measured acetylene (tracer gas) concentrations. The Picarro instrument measured C_2H_2 (tracer gas) and methane (CH_4) at a frequency of 3 Hz. The Picarro instrument used a Cavity Ringdown Spectroscopy (CRDS) instrument to measure the ambient concentrations of C_2H_2 and CH_4. The system inlet was attached to the front of the Chevrolet Tahoe at a height of 3 meters. Ambient air from the inlet flowed through a 4.62 m teflon tube at a flow rate of 5 L min^{-1} into the Picarro instrument. A detailed description of the Picarro appears in Monster et al. [2014].

2.1.4 Canister Triggering System

Evacuated 1.4 L canisters were deployed for each experiment to collect WAS downwind of the tracer release system located on the well pad co-located with the mobile measurements of CH_4 and C_2H_2 by the mobile plume tracker. Two were positioned on the Picarro inlet mast on the front of the Chevrolet Tahoe at heights of: 2.18 m and 2.92 m or on tripods at heights of 1.83 m and 4.88 m. Another canister was deployed downwind of the well pad of interest and either closer or further downwind than the Tahoe on a tripod at a height of 2 m above the ground. The downwind canister position depended on access and terrain. The deployed canisters were triggered remotely to open for three minutes of sampling and to close to collect a WAS of the plume emitted from the well pad. Figure 2.3 illustrates the canister triggering system on a tripod during canister sampling. The canister triggering system set-up included an antenna, inlet cane, canister triggering system, a sampling canister, and a tripod.

Each deployed canister was attached to a triggering system that was remotely triggered at the same time using a LabVIEW interface on a portable netbook computer located in the Chevrolet Tahoe Hybrid vehicle. The triggering systems were equipped with an Arduino UNO microcontroller controlled valve that opened and closed to collect ambient air in the evacuated canisters during three minutes of sampling. The triggering systems were built and designed by Air Resources Specialists (ARS) Inc. The flow of air into the evacuated canister was controlled by the critical orifice and canisters maintained a slight vacuum after sampling to provide quantitative WAS for analysis. The triggering systems were also equipped with temperature sensors and a GPS. Table 2.2 lists the specific instruments contained in the triggering systems.

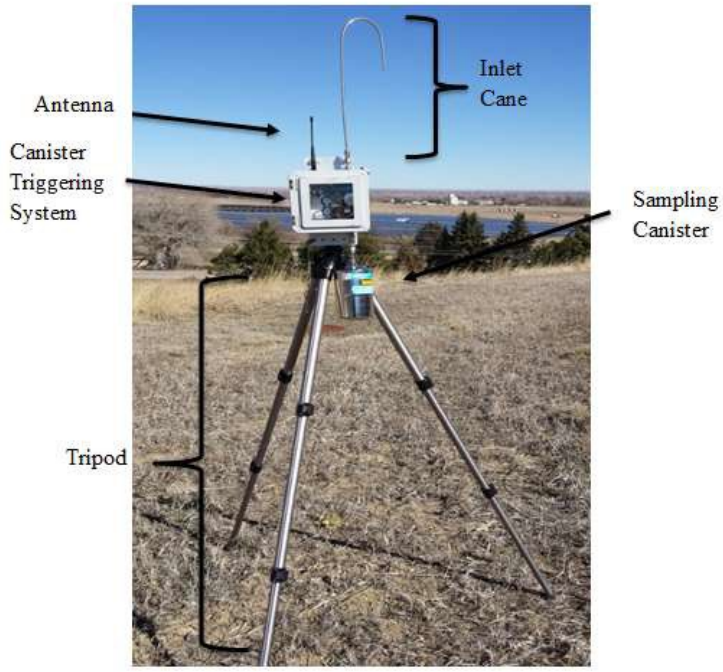

Figure 2.3. Picture of canister triggering system set-up during sampling.

Table 2.2: Instruments contained in the triggering systems.

Instrument	Model Name	Manufacturer
Microcontroller	UNO	Arduino
GPS	PMB-688	Polstar
Temperature Sensor	LM35	Texas Instruments
Wireless Modem	XBee-PRO 900HP	Digi
Pressure Sensor	OEM 0-15 PSIA	Honeywell
Solenoid Valve	S311PF15V2AD5L	GC

2.1.5 Background Canister Collection

A background canister sample was collected upwind of the measurement location at the end of each sampling experiment. The background canister sample was collected by attaching a 1.4 L canister to the front of the Chevrolet Tahoe at a height of 2.92 m above the ground or by using the tripod, which is 2 m above the ground. One background was collected for each experiment because the downwind canister samples were typically collected over a period about 1-2 hours.

2.2 Whole Air Canister Sample Analysis

The WAS canisters collected by our field team were analyzed using two gas chromatography (GC) analytical systems for 48 VOC compounds using the Environmental Protection Agency (EPA) TO-15 method. The chemical formula and relevant sources of the VOCs analyzed are listed in Appendix C. The samples were cryogenically pre-concentrated and paired with GC analytical systems with flame ionization detectors (FID). FID systems are considered advantageous because the detectors are not affected by flow rate, noncombustible gases, or water. The specific pre-concentration procedures and GC methods for each GC analytical system will be discussed later in the chapter.

2.2.1 Hewlett Packard Gas Chromatograph-Flame Ionization Detector System

A Hewlett Packard gas chromatograph-flame ionization detector (GC-FID, model 6890) system was used to analyze 20% of the canisters for 28 VOC compounds. A pre-concentration system (Entech model 7200) was used for Cold Trap Dehydration (CTD) before the sample was injected into the GC column. The GC column and detector information and specific GC method details are listed in Appendix E. Figure 2.4 shows a schematic of the Entech pre-concentration system referred to in the following procedure.

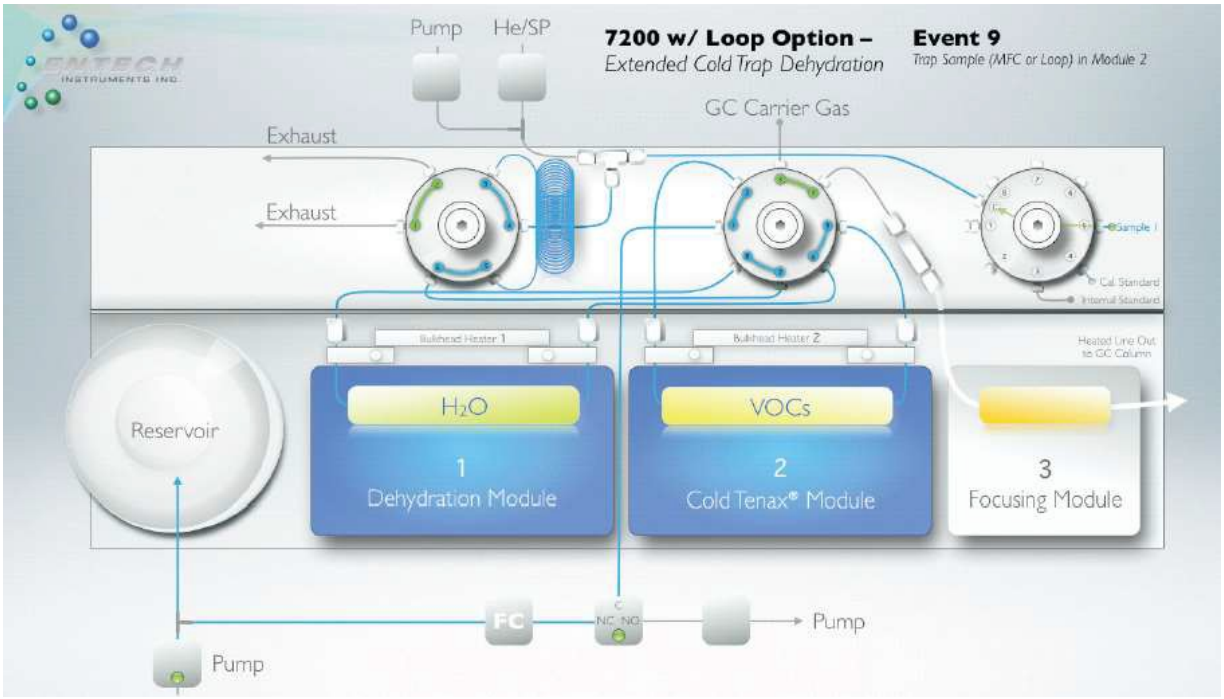

Figure 2.4. Diagram of the Entech pre-concentration system for Cold Trap Dehydration with modules 1-3 identified [Entech Intruments Inc., 2014].

For each canister sample, a 100 cc volume of air from the canister was pre-concentrated for analysis. The Silonite-D coated Dehydration Module 1 (M1) trap was cooled to between -40˚ C to –50˚C in order to remove excess water from the sample. This step also allowed for VOCs at parts per billion (ppb) levels to remain in the gas phase for passage to the Cold Tenax Module

2 (M2) which was also cooled to -40˚C where the VOCs were then trapped onto the Tenax packing. After trapping the correct volume of sample, both modules were purged with ultra-high purity (UHP) helium (carrier gas) at a rate of 25 mL/min to remove remaining air. The M1 trap was heated to -10˚C with UHP helium again. During the transfer from M2 to the Focus Module 3 (M3), M3 was cooled to below – 150˚C and M2 was heated to 230˚C to prepare the VOCs for split-less injection into the GC. Then, M3 was heated and the sample was injected onto the GC column.

After injection onto the column held at an initial temperature of 35˚C for 4 minutes, the GC oven was then heated at a rate of 5˚C/min and held at 190˚C for 40 minutes to allow for separation and evolution of the analytes (VOCs) of interest. The total cycle time for the GC-FID was 75 minutes.

2.2.2 Five-Channel Gas Chromatograph System

A 5-channel gas chromatograph (GC) analytical system was used to analyze 80% of the canisters for 48 VOC compounds. The system consisted of a vacuum manifold line, a stainless steel (30 cm x 0.3175 cm I.D.) cryogenic pre-concentration sample loop packed with 1 mm diameter glass beads, a splitter box, an excess volume can and three GC systems. Figure 2.5 shows a schematic of the 5-channel GC that is referred to in the following procedure. The system contained one GC equipped with a single capillary column and a quadrupole mass spectrometer (GCMS-QP5050A, Shimadzu Corporation) and the other two GCs (GC-17A, Shimadzu Corporation) equipped with two analytical capillary columns with the following detector combinations; two FIDs and one FID with an electron capture detector (ECD) for non-methane hydrocarbon and halocarbon analysis. The VOC analysis discussed in this thesis is from the data analyzed on the GC-FID channels. The 5-channel GC column and detector pairs and specific GC

method details are listed in Appendix E. The analytical system and methodology used for this analysis are similar to those used in Sive [1999], Zhou et al. [2010], and Russo et al. [2010].

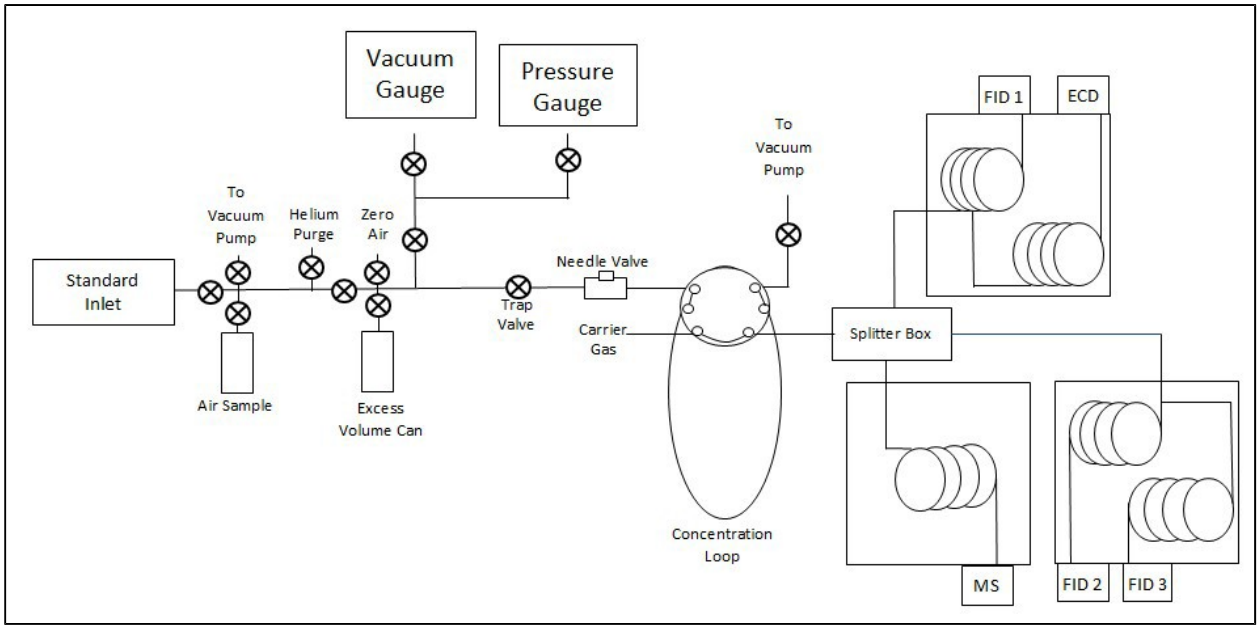

Figure 2.5: Diagram of the vacuum manifold line and the GC instruments used for VOC analysis of canister samples. Diagram adapted from Swarthout [2014].

The sample analyses consisted of uninterrupted sample runs. Before each sample analysis, there was a "warm up" period of ~12 runs in order for the system to equilibrate to the CO_2 and water in the samples. This "warm up" period increased measurement precision and decreased detector drift. In order to establish reproducible split and high measurement precision, a detailed procedure was used and each step was precisely timed. Each sample was split into five sub-streams at a splitter box with each feeding a separate GC column/detector pair. The column's I.D., stationary phase, the oven cooling rate, and the length of the columns determined how the sample was split into each column. The exact timing of each step ensured that the flow was quantitatively split precisely into the five columns and that the results were reproducible.

Canister sample analytes were cryogenically pre-concentrated similar to the previous GC-FID procedure before proceeding into the GC column following this procedure. First, the sample canister was connected to the vacuum line through the sample inlet. Then, the vacuum line and sample inlet were evacuated to 10^{-2} torr range using the vacuum line pump controlled by a vacuum gauge. After evacuation, the sample canister was opened to the vacuum line. Once the sample canister was opened the initial pressure was recorded in the vacuum line and the sample canister (~500 torr). With the switching valve in the "trap" position, a dewar filled with liquid nitrogen was applied to the lower end of the stainless steel pre-concentration loop to cool the loop for two minutes. The dewar was topped off after one minute. After two minutes, the trap valve connecting the vacuum line to the switching valve and pre-concentration loop was then cracked open restricting flow to a rate resulting in a pressure drop of about 1 torr/second. Flow is restricted because if the flow rate is too fast, the loop can become blocked by ice or the air can become throttled, creating condensed oxygen on the pre-concentration loop. The total sampled volume was measured by the pressure difference (ΔP = 100 torr, ~500 torr - ~400 torr). After the sample was trapped in the pre-concentration loop, the valve to the vacuum line was closed. With the dewar filled with liquid nitrogen still applied to the pre-concentration loop, the loop was pumped down for one minute to remove most of the remaining nitrogen and oxygen. The switching valve was then switched from the "trap" position to the "bypass" position in order to isolate the pre-concentration loop. A dewar with approximately 95˚C water replaced the dewar containing liquid nitrogen at the lower end of the pre-concentration loop. This step heats the loop allowing for the trapped analytes to volatilize once again.

The GCs were programmed to cool down in the same order after each sample analysis. During the GC cooling, GC1 would reach its initial temperature after GC2 and GC3 because

GC1 contained an Alumina-PLOT column. After GC1 reached its initial temperature and all of the GCs sat at their initial temperature for 45 seconds, the sample was injected into the column. The sample was injected into the columns by switching the switching valve from the “bypass” position to the “injection” position while the GCs and PCs were started.

While the switching valve was in the “injection” position, helium carrier gas was redirected to move the contents in the sample loop to the splitter box via a 1/16” stainless steel transfer line. A fraction of the flow was directed into each column for separation and detection at the splitter box. Two PCs were used to plot chromatographic traces in real time using CLASS-VP software and GCMS solution software for data acquisition and storage. Once the sample was injected for five minutes, the switching valve was switched from the “injection” position back to the “trap” position. For 10 minutes, the pre-concentration loop was purged with UHP helium (passed through an activated charcoal/molecular sieve trap immersed in liquid nitrogen for higher purity) for four minutes to clean the trap for the next sample and then evacuated to the 1 x 10^{-2} torr range. The trapping process was then repeated for the next sample.

The duration of one complete cycle of trapping, injecting, and chromatographic separation was approximately 33 minutes. The VOCs measured by the 5-channel GC and relevant sources are listed in Appendix C. The remainder of this chapter discusses the VOC analysis from the GC-FID channels.

2.3 Quality Control and Quality Assurance

In order to maintain quality control and assurance during field collection a batch cleaning blank canister was designated after canister cleaning. In order to maintain quality control and assurance during canister analysis the GC analytical systems were both calibrated for each VOC of interest and daily system blanks and calibration checks were performed on the 5-channel GC

analytical system. This section will give a detailed description of the procedures to ensure quality control and assurance.

2.3.1 Batch Cleaning Blank

A batch blank was designated for each batch of canisters cleaned. The batch blank was filled with UHP nitrogen diluent for 4-5 seconds once the other canisters were removed from the canister cleaning oven. Each batch blank canister underwent quality assurance testing on either the HP GC-FID system or the 5-channel GC system. If any of the VOC compounds of interest in the batch blank exceeded a concentration of 0.2 ppbv, the batch blank and all the canisters of the batch were re-cleaned and re-tested for quality assurance. The canisters were stored at room temperature in the laboratory until field sampling within a 2-3 week period.

2.3.2 HP GC-FID and 5-channel GC Blanks

Zero air blank runs were conducted using a zero air generator to remove VOCs from the sample loop. The zero air generator consisted of a pump and a heated catalytic converter (0.5% pd, Al_2O_3). Ambient air was drawn from outside and pumped through the catalytic converter then through the GC analytical system to remove excess VOCs from the sample loop. Three zero runs were performed about every six samples and one zero run was performed between each sample run. A zero run was also performed after running the standard through the system to ensure all VOCs were flushed out of the system.

2.3.3 HP Gas Chromatograph-Flame Ionization Detector System Calibration

The HP GC-FID system was calibrated using a 6 L canister filled with a diluted 1 ppm Linde Gas North America LLC high pressure standard. The diluted standard was made by diluting 40 cc of the 1 ppm standard to 10 ppb with 3960 cc of zero- air. A six-point calibration was used with 2 analyses at each concentration. Appendix D includes calibration statistics for

the HP GC-FID. The following equation was used to calculate the slope of each VOC calibration curve:

$$= \frac{\times}{\times} \quad (2.1)$$

Area is the integrated chromatographic peak area for each VOC. Vol_{samp} is the injection volume for each canister sample in units of cc. The injection volume was 100 cc for every canister sample. Vol_{std} is the injection volume for each calibration in units of cc. Std_{conc} is the concentration of each VOC in the 6 L canister in units of parts per billion (ppb).

2.3.4 Five-Channel Gas Chromatograph Calibration

The 5-channel GC analytical system was calibrated using a Linde Gas North America LLC high-pressure standard. The standard cylinder was diluted and analyzed twice at nine concentration levels for each VOC. Appendix D contains the calibration statistics for the five-channel GC. The following equation was used to calculate the slope of each VOC calibration curve:

$$= \frac{}{\times} \quad (2.2)$$

Slope is the slope of the calibration curve for each VOC. *Area* is the integrated chromatographic peak area for each VOC. DF is the dilution factor for each concentration.

Method precision was estimated as the standard deviation of the peak areas of each VOC of interest during the ambient air standard runs. Five humidified zero air samples filled with UHP nitrogen were generated using an Entech Cleaning System (model 3108) were analyzed on each GC system. Method limits of detection (LOD) for each VOC were calculated for each GC system using the following equation:

$$= \frac{\quad}{\quad} \tag{2.3}$$

$\bar{y}$ is the mean area of the integrated analyte peak for each VOC in the blank samples. **I** is the standard deviation of the integrated analyte peak area for each VOC in the blank samples. *Slope* is the slope of the calibration curve for each VOC. Equation 2.3 incorporates the blanks and the LOD of the discrete samples.

2.4 Data Processing

HP GC-FID, 5-Channel GC, and Picarro data were used to determine VOC emission ratios. In this section, the data selection process will be discussed as well as calculation of VOC emission ratios.

2.4.1 HP GC-FID and Five-Channel GC Canister Data

Shimadzu CLASS-VP software was used for data collection from the 5-channel GC and Agilent MSD ChemStation Data Analysis Software was used for data collection from the GC-FID. The VOC concentration in each sample was determined from the specific VOC peak area obtained from the analysis software and slope of the VOC calibration curve determined as described in Sections 2.3.3 and 2.3.4. The following equation was used for conversion:

$$= \frac{\quad}{\quad} \tag{2.4}$$

2.4.2 VOC Background Correction

If the VOC concentration was below the LOD the VOC concentration was represented by the following equation:

$$Conc \_\_\_\_$$

(2.5)

After the concentration was determined for each VOC, the background VOC concentration was subtracted from each VOC concentration using the following equation:

$$\Delta \quad = \quad - \tag{2.6}$$

ΔVOC_{conc} is the final VOC concentration after background correction. $Conc_{sample}$ is the VOC concentration in each canister sample. $Conc_{bkgd}$ is the VOC concentration in each background canister sample collected upwind of the well pad of interest. If the background was greater than the sample concentration then the canister concentration is represented by Equation 2.7 in the data. This data substitution was applied to all canister samples including background samples.

2.4.3 Data Selection

Not all VOC canister data collected during each experiment were used to calculate emission rates. First, canister data were considered if the C_2H_2 tracer concentrations showed the canister samples were collected inside the plume emitted from the well development operations of interest. The VOC canister data were selected for analysis when the acetylene concentration was above a cutoff value of 3 ppb. The acetylene cutoff was selected by adding the average and two standard deviations of the C_2H_2 background concentrations. The mean C_2H_2 background concentration during sampling days was ~0.9 ppb and the standard deviation of all of the C_2H_2 background concentrations was ~1 ppb. This cutoff value was applied to all canister data collected from the canisters attached to the mobile plume tracker at heights: 2.92 and 2.18, referred to as “Tahoe Up” and “Tahoe Down” and the canister data collected from the canisters placed on a tripod downwind of the well pad of interest denoted “Downwind”.

A second selection criterion was applied to the canister samples co-located with the Picarro instrument. The three-minute averaged Picarro C_2H_2 data were compared separately to the C_2H_2 concentration from canisters attached to the mobile plume tracker at positions: Tahoe

Up and Tahoe Down. The VOC canister data selected from the co-located canisters were included in subsequent analysis of VOC-to-methane ratios if the absolute difference between the canister and Picarro acetylene concentration was less than 70% of the mean of these values. The canister C_2H_2 data were selected based on the following equation:

$$\frac{|\quad\quad|}{\quad\quad} < 0.7 \tag{2.7}$$

Can is the C_2H_2 concentration in the canister. *Picarro* is the three-minute averaged C_2H_2 concentration measured by the Picarro instrument. *Mean* is the average of the C_2H_2 concentration in the canister and the three-minute averaged C_2H_2 concentration measured by the Picarro instrument. Some difference is expected between the canister and the Picarro measured acetylene concentrations because the inlets were not exactly co-located. The purpose of the preceding selection criterion was to eliminate cases where these samplers were sampling drastically different plume concentrations.

Appendix B illustrates how this criterion was used to select the canister data used in this analysis. The above criterion allowed for a comparison between the VOC canister data and Picarro CH_4 data because it ensured that the VOC emissions were collected inside of the same plume as the CH_4 emissions emitted from the operations of interest. Once the relevant C_2H_2 canister data were selected, the corresponding VOC data collected at the corresponding time were used in the subsequent analysis.

2.4.4 Picarro Methane Data

The CH_4 data used for this analysis was selected based on the concentration of C_2H_2 and then averaged over the three minute sampling period for each canister sample [MacDonald, 2015]. C_2H_2 background concentrations were defined as the concentration measured by the

Picarro upwind of the well pad. When the Picarro instrument measured C_2H_2 concentrations above background levels, the CH_4 concentrations were considered in the plume because the tracer gas was being released near the emission source on the well pad. Due to variability in the CH_4 background, an interpolated background was used to represent CH_4 background levels. When C_2H_2 concentrations were detected at background levels (i.e. out of plume), the CH_4 concentrations were also considered out of plume. Since the CH_4 concentration changed as a function of time, the new CH_4 background concentrations were defined as all the periods out of plume. A more detailed description of the CH_4 data processing is included in MacDonald [2015].

2.4.5 VOC Emission Rates and Emission Ratios

VOC emission rates were derived for each measured VOC in the sample canisters taken during the experiments that satisfied previously described screening criteria. CH_4 emission rates were derived using Picarro observations averaged over the three minutes the canisters were collected. The details of the selection process are outlined in Sections 2.4.3. and 2.4.4. The tracer ratio method was used to derive emission rates for each VOC using the following equation:

$$= \frac{[\quad]}{[\quad]} \times \qquad (2.8)$$

Q_{voc} is the emission rate of each VOC in units of g s^{-1}. [VOC] is the mixing ratio of a VOC in ppb. $[C_2H_2]$ is the mixing ratio of the tracer gas in units of ppb. Q_{C2H2} is the release rate of the tracer gas in L min^{-1}. The unit conversion from L min^{-1} to g s^{-1} is described in Appendix F. The emission rates for CH_4 were calculated using the same equation replacing [VOC] with $[CH_4]$. Each VOC concentration and methane averaged concentration was background corrected. The tracer ratio method assumes:

- The tracer gas is released at a known rate
- The tracer gas and the VOC emission source are co-located

- The effect of turbulent processes transporting the tracer and the emission plume are the same
- There is no chemical transformation of the tracer or the emission plume

The main advantages of the tracer ratio method are that the entire emission plume does not need to be measured and local meteorology is not needed to estimate the VOC emission rates.

The CH_4 emission rates and VOC emission rates were used to derive the emission ratios discussed in this thesis. The emission ratios were used to characterize and quantify emissions during various stages of natural gas well development. The only canisters used in this analysis (comparison with CH_4) were the canisters co-located with the Picarro instrument because the VOCs are being compared to the CH_4 that was measured by the Picarro instrument. The following equation was used to calculate the emission ratio of each VOC to CH_4:

—— = (2.9)

Q_{voc} is the emission rate of each VOC in units of g s^{-1}. Q_{CH4} is the emission rate of methane in units of g s^{-1}.

CHAPTER 3

RESULTS

3.1 Emission Rates

VOC emissions and methane were measured downwind of well development operations in Garfield County in 21 experiments. Results from 13 of these experiments are presented here. The concentrations of 48 VOCs from WAS canisters, including acetylene were collected downwind and upwind (background sample) of well pads and measured by GC. Methane concentrations were measured downwind of well pads by a Picarro instrument and averaged over periods of canister sampling. The VOC and methane data were processed and screened using the methods described in Section 2.4. Emission rates were determined for 48 VOCs and CH_4 using the tracer ratio method for drilling, fracking, and flowback. This section will present select individual VOC and CH_4 emission rates, source signatures, and select VOC emission rate correlations for each well-development operation.

3.1.1 VOC Emissions from Drilling

Figure 3.1 shows VOC emission rate distributions determined from 31 canister measurements collected during drilling operations. Select alkanes, aromatics, and alkenes are included and grouped separately. Alkanes (C_2-C_{10}) are included because these VOCs are main constituents of natural gas and crude oil [ARS, 2015]. Alkenes (C_2-C_3) are included; these VOCs are formed when larger molecules oxidize in the atmosphere [ARS, 2015]. Aromatics (BTEX) are included; aromatics may be emitted directly from gas and oil deposits and/or from combustion processes such as engines associated with O&NG operations [ARS, 2015]. In Figure 3.1 the red line represents the median, the box depicts the interquartile range and the whiskers

represent the 5th and 95th percentiles of the emission rates, with points beyond these limits represented by plus symbols. The outliers are represented by a cross. The y-axis is plotted with a log-scale since the observed emission rates span several orders of magnitude. Emission rate distributions for the full suite of VOCs measured during drilling operations are included in Appendix F. Table 3.1 tabulates some of the results shown in Figure 3.1.

The C_2, C_3, nC_4, C_9, and C_{10} alkanes show a fairly tight emission rate distribution spanning an order of magnitude or less. This may suggest that these individual VOCs are being emitted from a single source that does not vary considerably in strength during drilling.

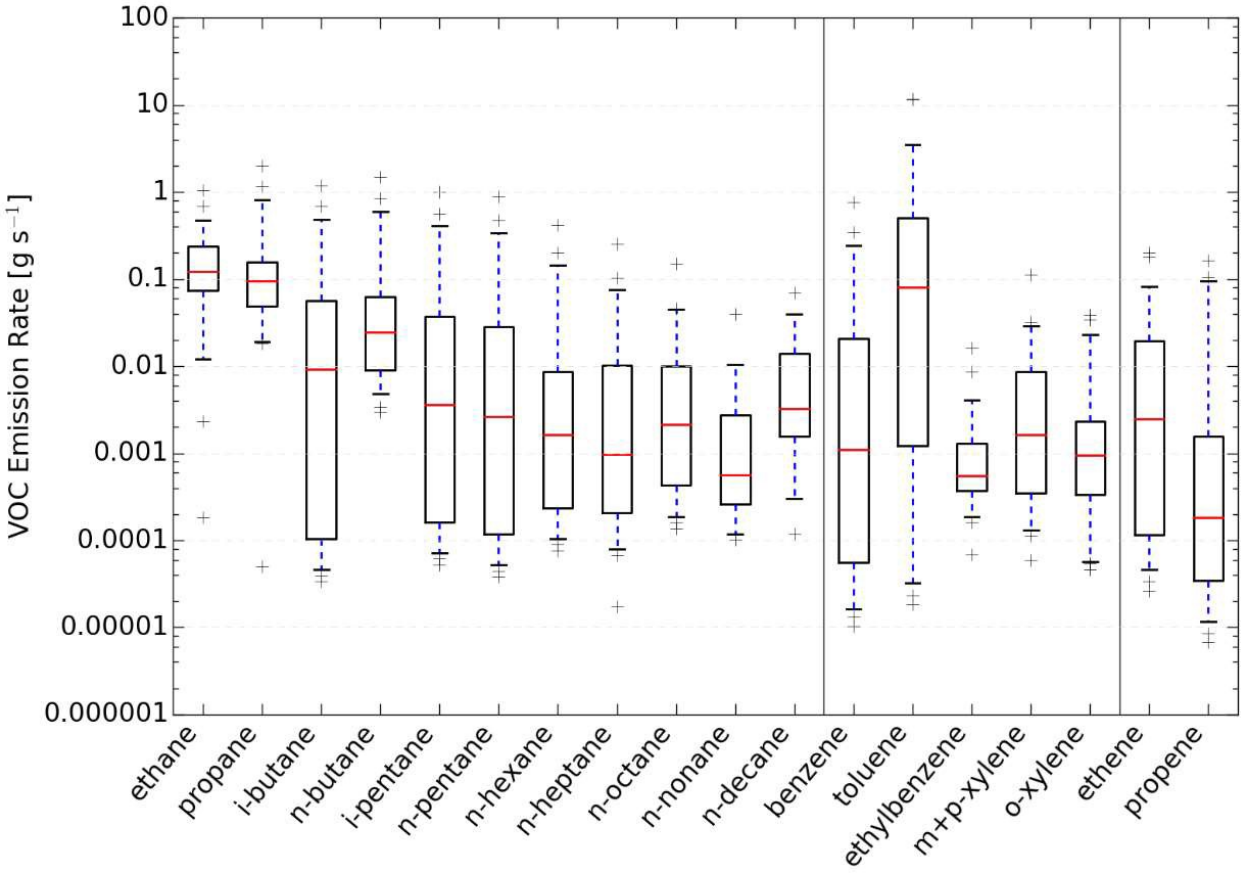

Figure 3.1. Select VOC emission rate distributions during drilling operations.

Ethane emissions are largest among alkanes, closely followed by propane. Both compounds are important components of natural gas emissions and are usually emitted from the same sources [Vinciguerra et al., 2015; Pétron et al., 2014]. Heavier alkanes, such as C_9-C_{10} alkanes, are likely emitted from combustion sources present during drilling operations, such as combustion including vehicle and generator exhaust [Graedel et al., 1986]. i-Pentane and n-pentane have wide emission rate distributions spanning at least two orders of magnitude suggesting that they may be emitted from multiple and/or variable sources during drilling operations. i-Pentane and n-pentane are both present in gasoline, vehicle exhaust, and natural gas, which could contribute to variable emission rates [Gilman et al., 2013; Howard et al., 1993].

Benzene, toluene, and alkene emission rate distributions span 2-3 orders of magnitude suggesting that these VOCs are emitted from various and/or variable strength sources during drilling operations. Benzene and toluene may be emitted from a variety of sources with inconsistent emission rates during drilling operations, including exposed drilling mud, truck traffic at the site, and combustion of fuel for the drill rig, generator engines, heaters, and pumps [Field et al., 2014]. The greater abundance of toluene emissions relative to benzene is consistent with important contributions from a combustion source. Small amounts of alkenes are present in natural gas emissions and motor gasoline, which are sources that would have vastly different emission rates [Sanchez, 2008; Intratec, 2012]. Other BTEX compounds have tighter emission rate distributions, varying by less than an order of magnitude, with ethylbenzene having the tightest emission rate distribution. Ethylbenzene is a major component of diesel fuel [Graedel et al., 1986]; its tighter emission rate distribution suggests that diesel engines operating during drilling may provide a fairly steady source.

Table 3.1. VOC emission rates for drilling operations calculated using the tracer ratio method. 31 canister samples were collected during drilling operations. Med is the median.

VOCs	Mean [g/s]	Med [g/s]	5^{th} %ile [g/s]	25^{th} %ile [g/s]	75^{th} %ile [g/s]	95^{th} %ile [g/s]
ethane	0.193	0.121	0.008	0.074	0.236	0.574
propane	0.232	0.094	0.019	0.049	0.156	0.977
i-butane	0.104	0.009	4.3E-05	0.0001	0.056	0.575
n-butane	0.134	0.025	0.004	0.009	0.063	0.711
i-pentane	0.084	0.004	6.7E-05	0.0002	0.037	0.478
n-pentane	0.071	0.003	4.9E-05	0.0001	0.028	0.399
n-hexane	0.031	0.002	9.8E-05	0.0002	0.009	0.169
n-heptane	0.018	0.0009	7.4E-05	0.0002	0.010	0.088
n-octane	0.013	0.002	0.0002	0.0004	0.010	0.045
n-nonane	0.004	0.0006	0.0001	0.0003	0.003	0.010
n-decane	0.011	0.003	0.0003	0.002	0.014	0.039
benzene	0.056	0.001	1.5E-05	5.6E-05	0.021	0.289
toluene	1.24	0.081	2.8E-05	0.001	0.501	7.11
ethylbenzene	0.002	0.0006	0.0002	0.0004	0.001	0.006
m+p-xylene	0.009	0.002	0.0001	0.0003	0.009	0.030
o-xylene	0.005	0.001	5.6E-05	0.0003	0.002	0.028
ethene	0.022	0.002	4.1E-05	0.0001	0.019	0.128
propene	0.014	0.0002	1.04E-05	3.4E-05	0.002	0.100

3.1.2 VOC Emissions from Fracking

Figure 3.2 shows emission rate distributions of VOCs determined from 26 canister samples collected during fracking operations. The VOC emission rate distributions for the full suite of VOCs measured are in Appendix F. Table 3.2 tabulates some of the results shown in Figure 3.2. Ethane and propane are once again among the most abundant alkane emissions, but relatively large emission rates are also observed for C_6-C_{10} alkanes. C_2-C_5 alkanes except iC_4 show a wide emission rate distribution spanning at least 2 orders of magnitude, suggesting that these VOCs are being emitted from multiple and/or variable strength sources present during fracking operations.

Lighter alkanes (C_2-C_5) are primarily emitted from natural gas, but C_4-C_5 can also be emitted from combustion sources including evaporation/combustion of fossil fuel and engine exhaust emitted during fracking operations. C_6-C_{10} alkanes show more consistent emission rates, but there is still a fairly wide distribution spanning at least an order of magnitude. BTEX and alkene emission rates also show a wide distribution spanning at least an order of magnitude. These results suggest that heavier alkanes (C_6-C_{10}), BTEX, and alkenes are emitted from sources with variable emission rates. The abundance of larger alkane and BTEX emissions suggests that combustion sources are likely important contributions to emissions observed during fracking.

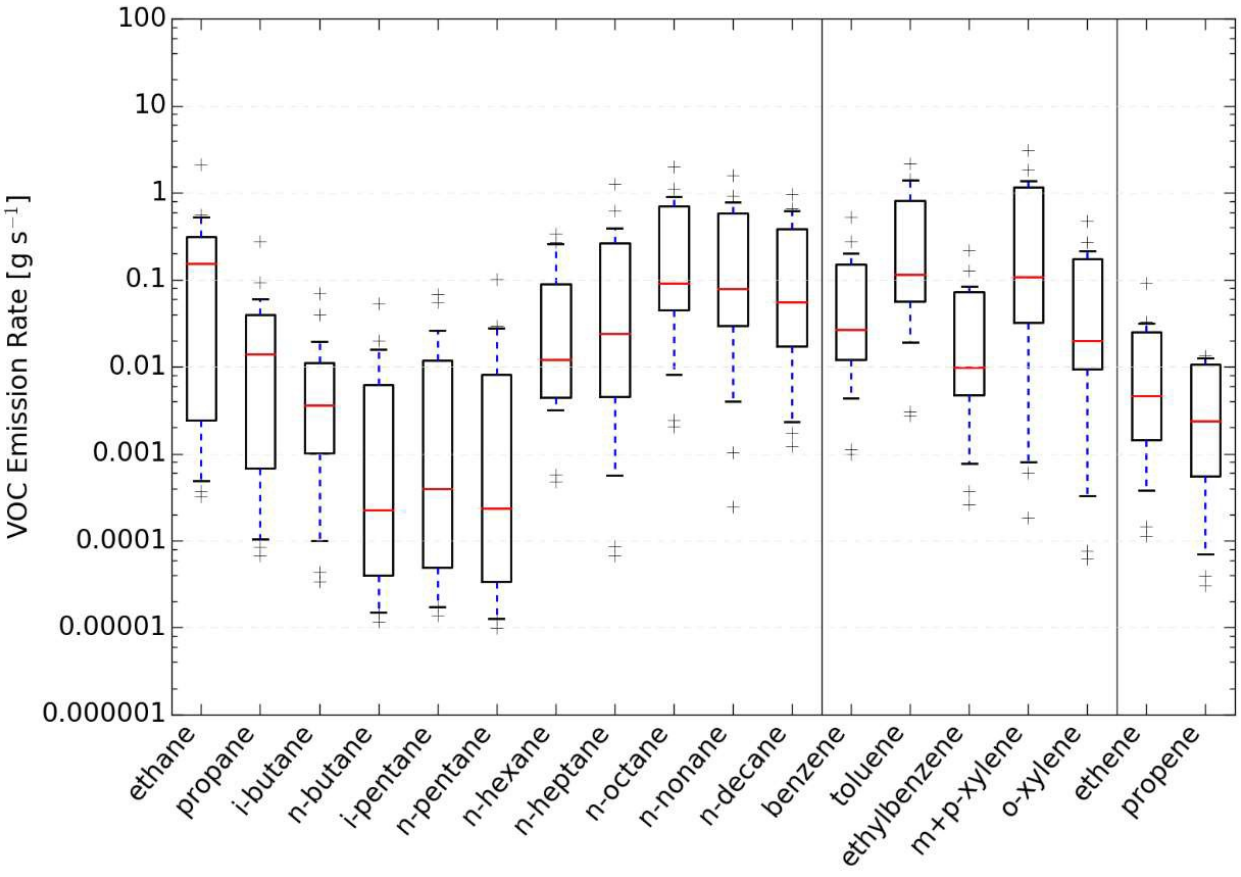

Figure 3.2. Select VOC emission rate distributions during fracking operations.

Table 3.2. VOC emission rates for fracking operations calculated using the tracer ratio method. 26 canister samples were collected during fracking operations. Med is the median.

VOCs	Mean [g/s]	Med [g/s]	5th %ile [g/s]	25th %ile [g/s]	75th %ile [g/s]	95th %ile [g/s]
ethane	0.246	0.155	0.0004	0.002	0.312	0.549
propane	0.032	0.014	9.0E-05	0.0007	0.039	0.085
i-butane	0.009	0.004	5.7E-05	0.001	0.011	0.035
n-butane	0.005	0.0002	1.5E-05	3.9E-05	0.006	0.019
i-pentane	0.009	0.0004	1.8E-05	4.9E-05	0.012	0.048
n-pentane	0.009	0.0002	1.3E-05	3.4E-05	0.008	0.029
n-hexane	0.063	0.012	0.001	0.004	0.089	0.265
n-heptane	0.155	0.024	0.002	0.005	0.267	0.565
n-octane	0.351	0.091	0.004	0.045	0.704	1.06
n-nonane	0.290	0.079	0.002	0.029	0.579	0.879
n-decane	0.203	0.056	0.002	0.017	0.382	0.655
benzene	0.087	0.0265	0.002	0.012	0.149	0.256
toluene	0.469	0.116	0.007	0.057	0.816	1.42
ethylbenzene	0.037	0.009	0.0005	0.005	0.072	0.116
m+p-xylene	0.523	0.107	0.0006	0.032	1.16	1.72
o-xylene	0.084	0.020	0.0001	0.009	0.175	0.254
ethene	0.014	0.005	0.0002	0.001	0.025	0.033
propene	0.005	0.002	4.7E-05	0.0006	0.011	0.013

3.1.3 VOC Emissions from Flowback

Figure 3.3 shows emission rate distributions determined from 54 canister samples collected during flowback operations. The VOC emission rate distributions for the full suite of VOCs measured during flowback operations are included in Appendix F. The results shown in Figure 3.3 are tabulated in Table 3.3.

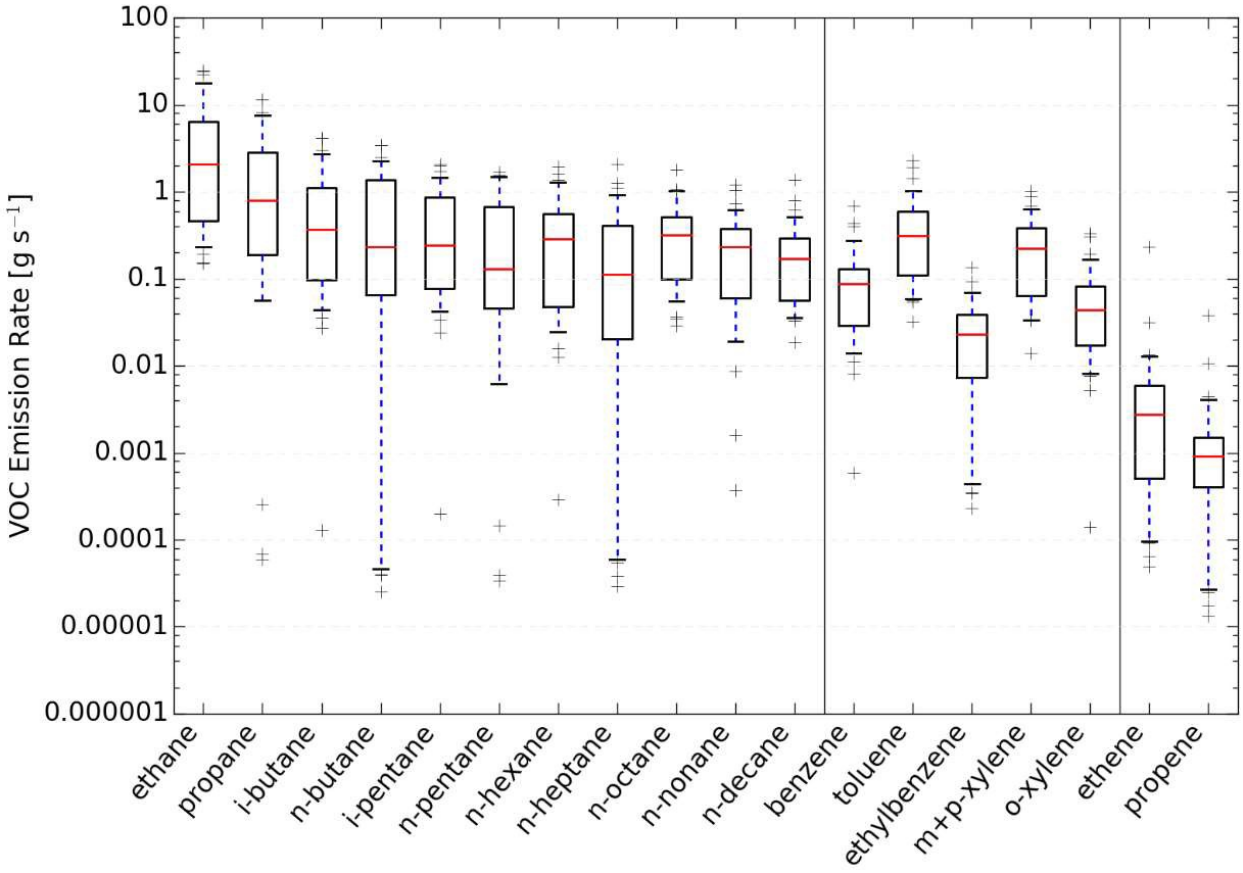

Figure 3.3. Select VOC emission rate distributions during flowback operations.

Alkane emissions during flowback are highest for ethane and decrease for larger compounds. Most of the VOCs depicted in Figure 3.2 show fairly tight emission distributions, suggesting a dominant source with fairly steady emission rates. During well flowback active combustion sources are typically not present on site, suggesting that volatilization from flowback liquids are the main emission source of lighter alkanes (C_2-C_5), heavier alkanes (C_6-C_{10}) and BTEX. Propene has a tight distribution of less than one order of magnitude while ethene has a wider distribution. Small amounts of alkenes can be emitted from flowback fluid because alkenes are present in hydraulic fracturing fluid and in natural gas [Thakur et al., 2016; Sanchez et al., 2008].

Table 3.3. VOC emission rates for flowback operations calculated using the tracer ratio method. 54 canister samples were collected during flowback operations. Med is the median.

VOCs	Mean [g/s]	Med [g/s]	5th %ile [g/s]	25th %ile [g/s]	75th %ile [g/s]	95th %ile [g/s]
ethane	5.07	2.08	0.220	0.467	6.47	19.3
propane	2.06	0.794	0.037	0.191	2.85	7.79
i-butane	0.785	0.371	0.041	0.097	1.12	2.82
n-butane	0.708	0.233	4.4E-05	0.066	1.38	2.33
i-pentane	0.511	0.244	0.039	0.078	0.864	1.56
n-pentane	0.404	0.130	0.004	0.046	0.675	1.49
n-hexane	0.387	0.289	0.022	0.048	0.564	1.31
n-heptane	0.284	0.112	5.8E-05	0.020	0.408	0.995
n-octane	0.383	0.318	0.049	0.099	0.512	1.02
n-nonane	0.268	0.234	0.016	0.061	0.379	0.659
n-decane	0.224	0.169	0.036	0.057	0.292	0.552
benzene	0.111	0.087	0.013	0.029	0.130	0.319
toluene	0.437	0.315	0.058	0.110	0.594	1.16
ethylbenzene	0.027	0.023	0.0004	0.007	0.039	0.070
m+p-xylene	0.256	0.222	0.034	0.064	0.382	0.653
o-xylene	0.064	0.044	0.008	0.017	0.083	0.176
ethene	0.008	0.003	9.5E-05	0.0005	0.006	0.013
propene	0.002	0.0009	2.6E-05	0.0004	0.002	0.004

3.1.4 VOC Emission Rate Comparison by Operation Type

The mean emission rates for drilling, fracking and flowback of select VOCs in Garfield County are compared to emission rates from in Pétron et al. [2014] and Swarthout et al. [2013] in Figure 3.4. The error bars in Figure 3.4 represent the 5th and 95th percentiles of VOC emissions for each operation type. The mean emission rates for all alkanes (up to C_7) are higher during flowback compared to the other operations. Since lighter alkanes (C_2-C_5) are main components of natural gas, this result suggests that natural gas is being emitted at highest rates during flowback operations followed by drilling and fracking operations. Natural gas emissions might be expected to occur at lower rates during fracking because hydraulic fracturing fluid is being pumped “downhole” into the well. The mean emission rates of heavier alkanes (C_6-C_{10})

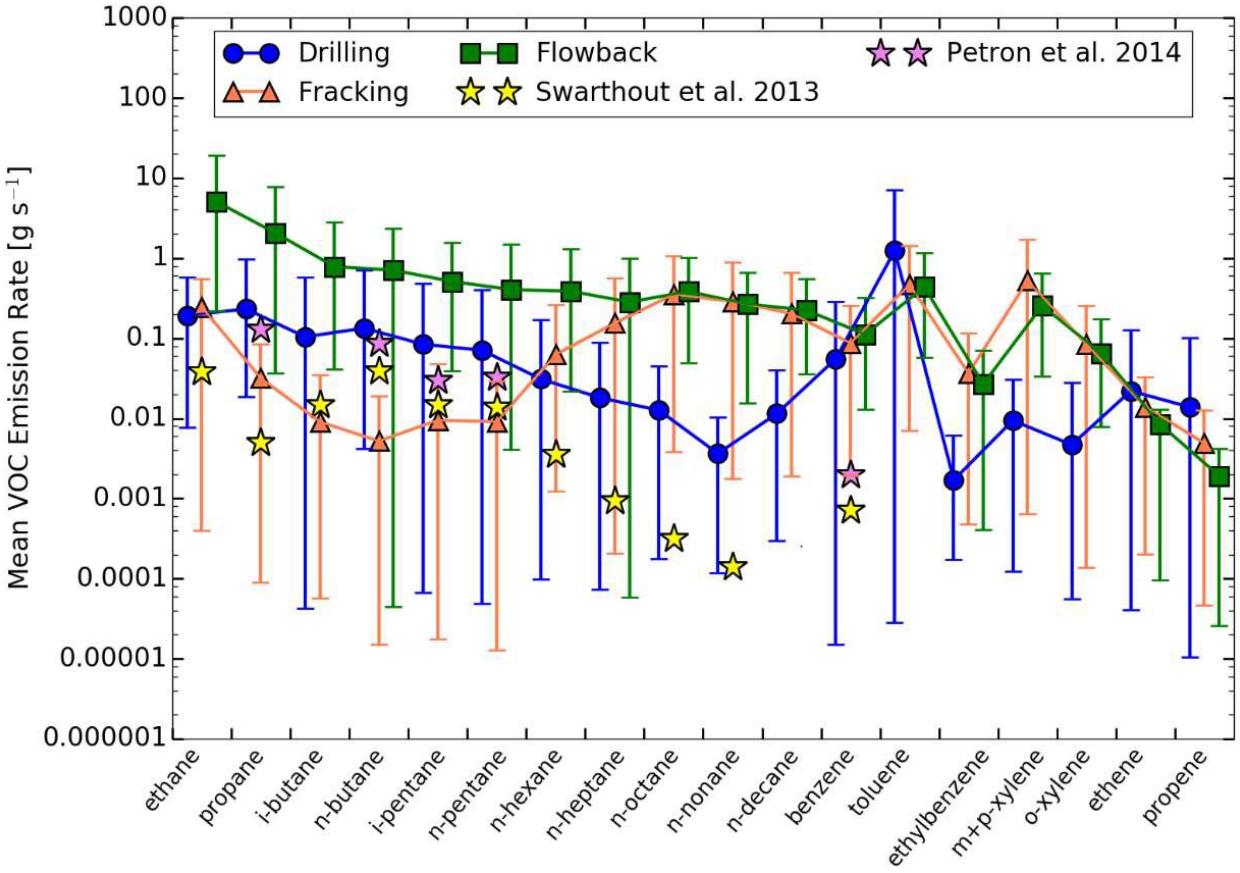

Figure 3.4. Mean VOC emission rate by operation type. The error bars represent the 5th and 95th percentiles of the VOC emission rates.

are elevated compared to lighter alkanes (C_2-C_5) during fracking operations. This result suggests strong influence of combustion-related sources and fluid handling to VOC emissions rather than direct natural gas emissions during fracking. During fracking operations, large trucks, engines, and generators use a great deal of power to pump hydraulic fracturing fluid into the well at high pressures resulting in emissions of heavier VOCs from exhaust. Mean benzene emission rates are fairly similar for all three operations.

Previous studies in Colorado have estimated emission rates for various VOCs emitted from O&NG operations, although specific information about emissions during new well development is extremely limited. Table 3.4 summarizes the mean emission rates for this study

during well development operations and compares them to other similar studies by Pétron et al. [2014] and Swarthout et al. [2013] in the Denver Julesburg Basin. Unlike the Piceance Basin in Garfield County, the Denver-Julesburg Basin contains many sedimentary layers of sandstone and shale containing natural gas co-produced with oil called "wet gas" [Pétron et al., 2014]. Pétron et al. [2014] estimated emission rates of propane, n-butane, i-pentane, n-pentane, and benzene using discrete flask air samples collected on aircraft in the planetary boundary layer for Weld County, CO in 2012. Here, the number of producing wells in Weld County (~25,000), as reported by the COGCC in 2012, were used to convert the basin-wide emission rates presented by Pétron et al. [2014] to emission rates from each well, these results are shown in Table 3.4. The average emission rate per production well in Weld County for C_4 is one order of magnitude lower than C_4 emission rates during drilling and flowback operations in Garfield County, but one order of magnitude greater than emission rates during fracking. Benzene emission rates per producing well in Weld County were lower than the emission rates observed in Garfield County during drilling, fracking, and flowback. While the benzene emission rates during well drilling and completion are higher than for production, the time duration of new well development is of course much shorter than a well's many year production lifetime. Propane, i-pentane, and n-pentane emission rates per Weld County producing well are the same order of magnitude as Garfield County drilling operations, larger by one order of magnitude for fracking operations, and smaller by one order of magnitude than flowback operations.

Swarthout et al. [2013] estimated the emission rates of a suite of VOCs at the BAO tower in 2011 and extrapolated regional emission rates for Weld County. Here, the number of producing wells in Weld County (~24,000), as reported by the COGCC in 2011, were used to convert the county-wide emission rates presented by Swarthout et al. [2013] to emission rates

from each well, these results are shown in Table 3.4. The extrapolated regional emission rates for C_2-C_4, C_6-C_9, and benzene in Weld County were much smaller by 1-3 orders of magnitude overall compared to Garfield County and the largest difference was with heavier alkanes (C_6-C_9) and benzene emission rates. Heavier alkane (C_6-C_{10}) emission rates for Garfield County are much higher by at least one order of magnitude compared to Swarthout et al. [2013]. The emission rates observed for pentane isomers by Swarthout et al. [2013] were on the same order of magnitude as the pentane emission rates observed in Garfield County during drilling operations. This suggests that pentane emission rates from producing wells are comparable to a well during drilling operations.

Mean toluene emission rates are elevated compared to the other BTEX compounds for all operation types in Garfield County. Toluene is emitted from a variety of sources such as combustion of fuel for the drill rig, generator engines, heaters, and pumps [Field et al., 2014]. Mean toluene emission rates are noticeably high during drilling operations compared to the other VOCs. Toluene is used as a solvent in drilling fluid [Brown, 2007; Broni-Bediako et al., 2010]. Mean xylene emission rates are higher during fracking and flowback operations compared to drilling operations. Xylenes are present in hydraulic fracturing fluid and flowback fluid and they are considered an effective solvent and acidizing agent for removing organic materials from the well [Fisher et al., 2013].

Mean alkene emission rates are higher during drilling and fracking operations compared to flowback. Alkenes are emitted from combustion sources so this result is consistent with combustion sources and vehicle exhaust emissions comprising major sources during drilling and fracking operations [Jobson et al., 2004].

Table 3.4. Comparison of mean VOC emission rates in Garfield County (GC) with similar studies.

VOCs	Drilling GC [g s^{-1}]	Fracking GC [g s^{-1}]	Flowback GC [g s^{-1}]	Weld County Pétron et al. [2014] [g s^{-1}]	Weld County Swarthout et al [2013] [g s^{-1}]
ethane	0.193	0.246	5.07	-	0.038
propane	0.232	0.032	2.06	0.131	0.005
i-butane	0.104	0.009	0.785	-	0.015
n-butane	0.134	0.005	0.708	0.086	0.039
i-pentane	0.084	0.009	0.511	0.030	0.015
n-pentane	0.071	0.009	0.404	0.033	0.014
n-hexane	0.031	0.063	0.387	-	0.0036
n-heptane	0.018	0.155	0.284	-	9.4E-04
n-octane	0.013	0.351	0.383	-	3.2E-04
n-nonane	0.004	0.290	0.268	-	1.4E-04
n-decane	0.011	0.203	0.224	-	-
benzene	0.056	0.087	0.111	0.002	7.2E-04
toluene	1.24	0.469	0.437	-	-
ethylbenzene	0.002	0.037	0.027	-	-
m+p-xylene	0.009	0.523	0.256	-	-
o-xylene	0.005	0.084	0.064	-	-
ethene	0.022	0.014	0.008	-	-
propene	0.014	0.005	0.002	-	-

3.1.5 Methane Emission Rates

Figure 3.5 shows emission rate distributions for methane during all operation types including individual operations and combination operations. The combination operation means drilling, fracking, and/or flowback operations were occurring simultaneously on co-located wells. The emission rates were determined using the tracer ratio method for Picarro methane and acetylene measurements made during canister collection periods.

The red line represents the median, the box depicts the interquartile range and the whiskers represent the 5^{th} and 95^{th} percentiles of the emission rates, with points beyond these limits represented by plus symbols. The y-axis is plotted with a log-scale since the observed

methane emission rates span several orders of magnitude. The methane emission rates shown in Figure 3.5 are tabulated in Table 3.5.

The methane emission rates during flowback operations exhibited the greatest median value and a fairly wide emission rate distribution. During flowback operations, methane emissions mostly reflect emission of methane from flowback fluid recovered from the well that includes natural gas dissolved or incorporated into the fluid and stored in containers [Allen et al.,

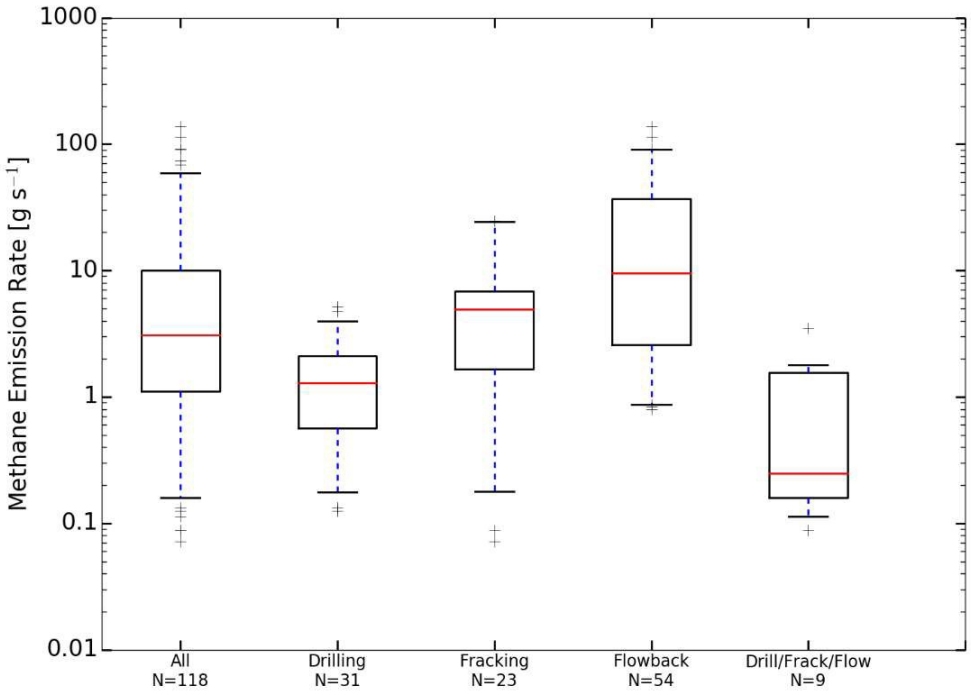

Figure 3.5. Methane emission rate distributions by individual operation types and for one combination operation. N is the number of sample periods.

2013]. Flowback rates vary over time and recovery of dissolved gases can vary depending on operator and subcontractor equipment and practices. The methane emission rate distributions during drilling and fracking operations span less than an order of magnitude suggesting that methane is emitted at fairly consistent rates during these operation types.

Table 3.5. Methane emission rates for each operation type. Med is the median.

Operation Type	Mean [g/s]	Med [g/s]	25th %ile [g/s]	75th %ile [g/s]
All	13.5	3.09	1.11	9.99
Drilling	1.57	1.29	0.564	2.09
Fracking	6.78	4.90	1.67	6.82
Flowback	25.6	9.57	2.57	36.9
Drill/Frack/Flow	0.88	0.247	0.159	1.56

Various studies have estimated the emission rate of methane from various stages of the production and transport of natural gas. The following studies estimated methane emission rates for stages other than the operation types discussed in this thesis, but these can provide context for the methane emission rates shown in Figure 3.5. Roscioli et al. [2015] estimated methane emission rates from gathering facilities and natural gas processing plants. They found an average methane emission rate of 12.2 ± 2.3 g s^{-1} for gathering facilities and 35.6 ± 18.3 g s^{-1} for natural gas processing plants [Roscioli et al., 2015]. The methane emission rates shown in Figure 3.5 during flowback operations for individual wells are on the same order of magnitude as the methane emission rates measured by Roscioli et al. [2015] at gathering facilities which process gas from multiple wells. Subramanian et al. [2015] measured methane emission rates from natural gas compressor stations in the transmission and storage sector. Methane emission rates spanned over two orders of magnitude from 0.54 g s^{-1} to 281.6 g s^{-1}.

This range overlaps much of the range shown in Figure 3.5, suggesting that the methane emission rates observed at natural gas compressor stations are roughly comparable to a single well during well development. Koss et al. [2015] estimated methane emission rates from O&NG extraction activities ranging from 0.7 g s^{-1} $well^{-1}$ to 1.5 g s^{-1} in the Uintah Basin, which are lower than Garfield County methane emission rates associated with new well development. Based on the results of this study and studies discussed above, wells in well development stage emit more methane at higher rates and over shorter time scales than wells in the production phase.

3.1.6 VOC Emission Rate Correlations

Correlations between individual VOC emission rates were analyzed to identify major sources and determine the strength of the relationship between individual VOC emission rates during drilling, fracking, and flowback operations. Figure 3.6 shows a correlation matrix of emission rates for select VOCs during drilling operations. Select alkanes, aromatics, and alkenes are included and grouped separately. A correlation matrix of emission rates for the full suite of VOCs for drilling operations is shown in Appendix G. Emission rates of C_2-C_9 alkanes are highly correlated ($r^2 > 0.87$) with each other during drilling operations, suggesting that they are emitted from the similar sources. Light alkanes (C_2-C_5) are mostly sourced from natural gas on the well pad and can be incorporated in drilling fluid [Allen et al. 2013]. While heavier alkanes (C_6-C_9) are emitted from drilling fluid and combustion-related sources on the well pad [Warneke et al., 2014; Swarthout et al., 2013; Thompson et al., 2014]. Emission rates of C_8-C_{10} alkanes are fairly well correlated with BTEX ($r^2 > 0.71$) specifically C_9-C_{10} ($r^2 > 0.81$).

Heavier alkanes and BTEX are present in small amounts in natural gas, but are likely sourced mainly from combustion sources on the well pad such as combustion of fuel for the drill rig, diesel engines, vehicle exhaust and generators [Field et al., 2014]. BTEX emission rates are moderately correlated ($r^2 > 0.73$) with each other during drilling operations. BTEX are released

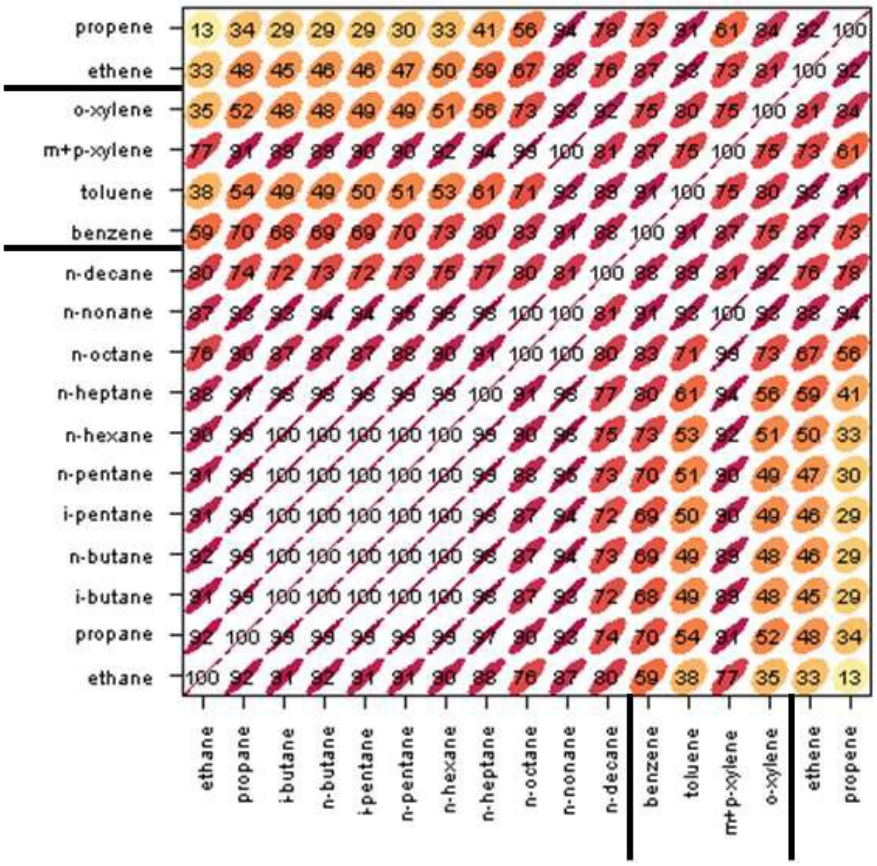

Figure 3.6. Correlation matrix of emission rates for select VOCs during drilling operations.

from drilling fluid [Broni-Bediako et al., 2010] and present in petroleum byproducts such as natural gas and gasoline [Rich et al., 2014]. Alkene emission rates are not well correlated with C_2-C_8 alkanes (r^2 = 0.13-0.67), but are more correlated with BTEX ($r^2 > 0.73$). Heavy alkanes

(C_9-C_{10}) and alkenes are both emitted from similar sources on the well pad during drilling operations such as diesel, gasoline, and vehicle exhaust [Graedel et al., 1986; Intratec, 2012].

Figure 3.7 shows a correlation matrix of emission rates for select VOCs during fracking

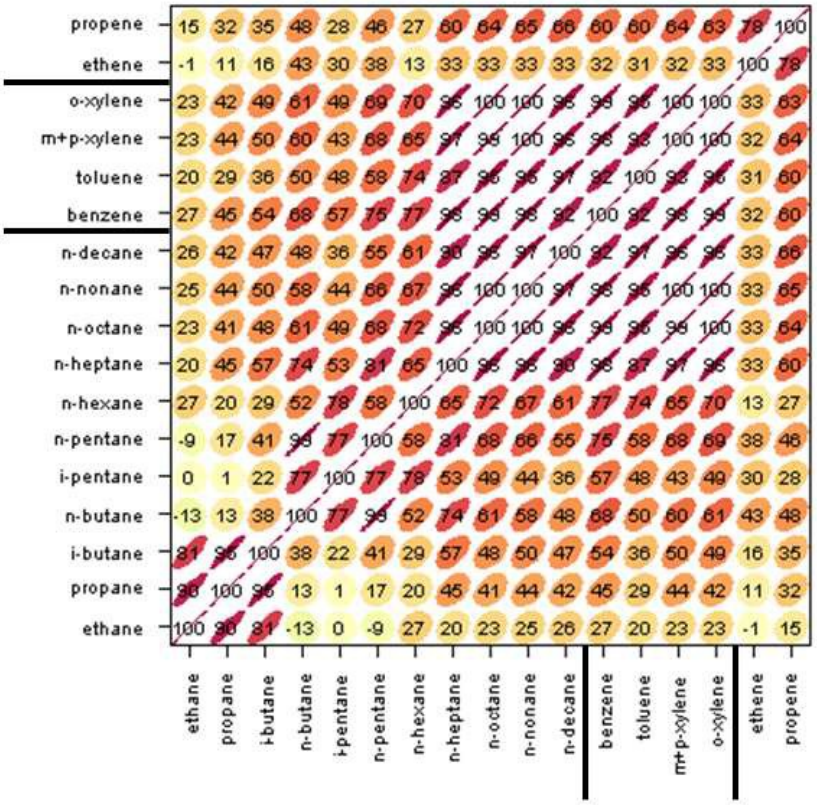

Figure 3.7. Correlation matrix of emission rates for select VOCs during fracking operations.

operations. A correlation matrix of emission rates for the full suite of VOCs for fracking operations is shown in Appendix G. C_2-iC_4 alkanes are well correlated with each other (r^2 > 0.81), but not with nC_4-C_{10} during fracking operations. Lighter alkanes (C_2-C_4) are primarily emitted from natural gas while heavier alkanes are also emitted from combustion sources or hydraulic fracturing fluid. Heavier alkanes (C_7-C_{10}) are highly correlated with each other and BTEX compounds (r^2 > 0.84). Heavy alkanes and BTEX compounds may be partially emitted from hydraulic fracturing fluid, but also partially sourced from similar combustion and gasoline

related sources such as evaporation and combustion of fossil fuels, gasoline vapor, vehicle exhaust and diesel engines [Lee et al., 2006; Howard 1993]. Combustion sources especially engines and generators emit heavier VOCs during fracking operations in order to pump hydraulic fracturing fluid into the well at high pressures.

Figure 3.8 shows a correlation matrix of emission rates for select VOCs during flowback operations. A correlation matrix of emission rates for the full suite of VOCs is shown in

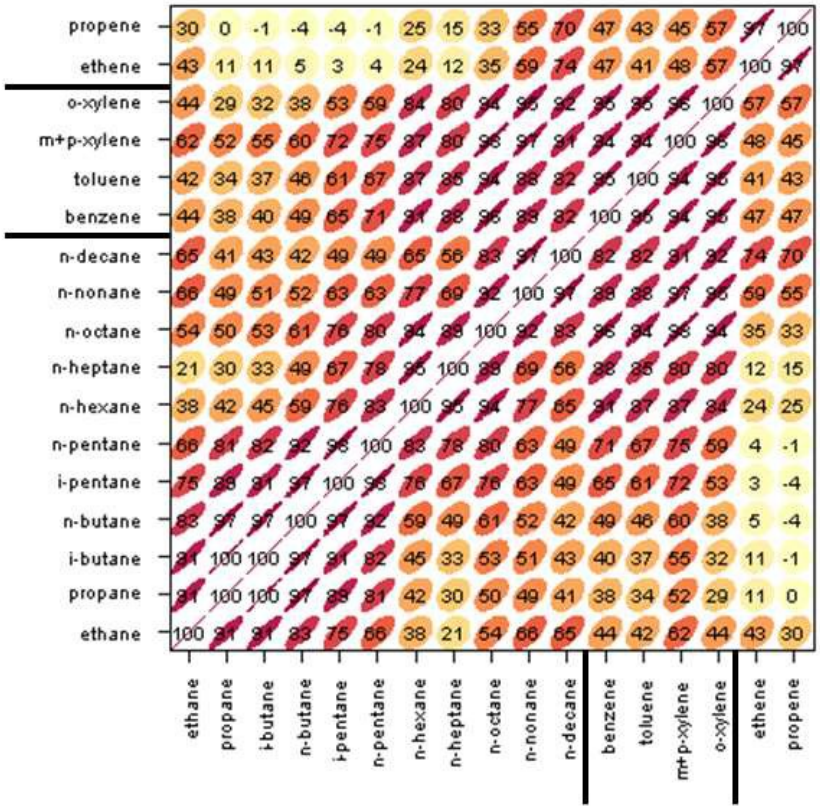

Figure 3.8. Correlation matrix of emission rates for select VOCs during flowback operations.

Appendix G. C_2-C_5 alkanes are well correlated with each other ($r^2 > 0.75$), consistent with a natural gas source volatilized from flowback fluids, but not very well correlated with heavier alkanes (C_6-C_{10}) or BTEX compounds. Heavier alkanes are well correlated with each other ($r^2 >$

0.83) and BTEX compounds during flowback operations. Natural gas containing lighter alkanes is released from the well. Heavier alkanes and BTEX are also probably emitted from flowback fluid instead of combustion sources during flowback operations [Field et al., 2015]. Their weaker correlation with light alkane emissions may be the result of different removal efficiencies in vapor recovery systems used in green completions.

3.1.7 VOC to Methane Emission Rate Correlation

Correlations between VOC emission rates and methane emission rates were investigated to assess whether methane emission rates might be useful surrogates for the emission rates of any individual VOCs for particular operation types. The existence of such correlations would be useful because methane is much easier and faster to monitor near O&NG operations and consequently, much more frequently measured. Figure 3.9 compares the correlation of VOC emission rates with methane emission rates for select VOCs by operation type. Select alkanes, aromatics, and alkenes are included and grouped separately. Ethane emission rates are highly correlated ($r^2 > 0.8$) with methane emission rates for all operation types, suggesting that methane and ethane have a common source and methane emission rates may be a useful surrogate for ethane emission rates. Ethane is a tracer of fugitive natural gas emissions and a main constituent of natural gas [Vinciguerra et al., 2015; Thompson et al., 2013]. The correlation coefficient for C_3-C_9 emission rates to methane emission rates is similar ($r^2 \approx 0.4$). During drilling operations, drilling mud containing heavier alkanes (C_6-C_{10}) and natural gas containing lighter alkanes is released from the well [Thompson et al., 2014; Broni-Bediako et al., 2010]. The correlation coefficient is probably lower for C_3-C_9 because these alkanes can be emitted from other non-methane sources during drilling operations such as combustion. C_4-C_6 alkane emission rates and methane emission rates are negatively correlated for fracking operations. This result suggests that

these VOCs and methane are likely emitted from different sources during this operation type; clearly methane emission rates are not useful surrogates for these VOC emission rates during fracking operations.

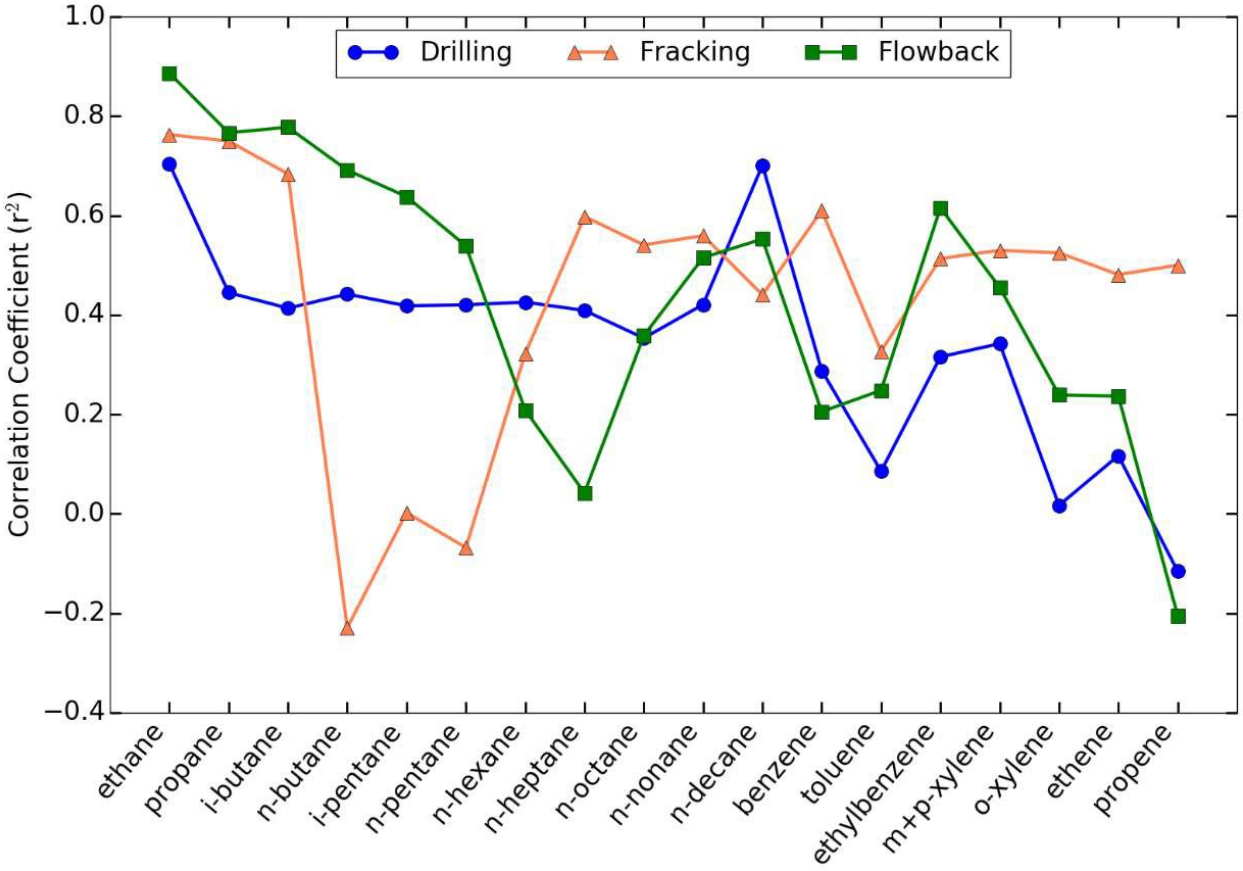

Figure 3.9. Comparison of the correlation coefficient of VOC emission rates with methane emission rates for selected VOCs by operations type.

Sources such as vehicle exhaust from trucks and generators are not necessarily co-located with methane sources on the well pad. During fracking and flowback operations, fluid/gas handling, processing, and combustion are emission sources of heavier alkanes, therefore the heavier VOCs would not be as strongly correlated with methane as the lighter VOCs [Warneke et al., 2014]. Methane emission rates are not well correlated with emission rates of benzene, toluene, xylenes and alkenes. Although, benzene, toluene and xylenes are used in hydraulic

fracturing fluid which is present during fracking and flowback operations, benzene, toluene, xylenes and alkenes are also associated with other sources on the well pad that may not necessarily emit methane such as vehicle exhaust, combustion, gasoline evaporation, and diesel engines [Borbon et al, 2001; Khoder, 2007; Ho et al., 2004]. Ethylbenzene and m+p-xylene have the highest correlation ($r^2 \approx 0.5$-0.6) with methane compared to the other BTEX compounds during flowback operations. Very few combustion sources are present during flowback operations, but ethylbenzene and m+p-xylene are major component of diesel [Graedel et al., 1986]. These results suggests overall that methane emission rates are not particularly useful surrogates for BTEX emission rates during new well drilling and completions.

3.1.8 VOC to Propane Emission Rate Correlations

Figure 3.10 compares the correlations of VOC emission rates with propane emission rates for select VOCs by operation type, because propane is a byproduct of natural gas production. Select alkanes, aromatics, and alkenes are included and grouped separately. C_2-C_8 emission rates during drilling operations and C_2-C_4 emission rates during flowback operations are highly correlated ($r^2 > 0.8$) with propane emission rates. The high correlation between C_2-C_9 and propane ($r^2 > 0.8$) during drilling suggests that these VOCs are being emitted from similar sources. During drilling operations, drilling mud containing heavier alkanes (C_6-C_{10}) returns to the surface releasing natural gas and lighter alkanes including propane. The correlation coefficients for C_4-C_{10}, BTEX, and alkene to propane emission rates are low during fracking ($r^2 < 0.5$) and C_6-C_{10}, BTEX, and alkene to propane are low during flowback ($r^2 < 0.5$) unlike for drilling operations. This suggests that during fracking and flowback operations, heavier VOCs are being emitted at higher rates from similar sources other than propane sources such as hydraulic fracturing fluid, solvents, combustion of diesel engines, vehicle exhaust, and gasoline

vapor [Graedel, 1978; Howard 1993]. The correlation coefficients for C_5-C_{10} and BTEX to propane emissions are higher during drilling operations compared to the other operation types.

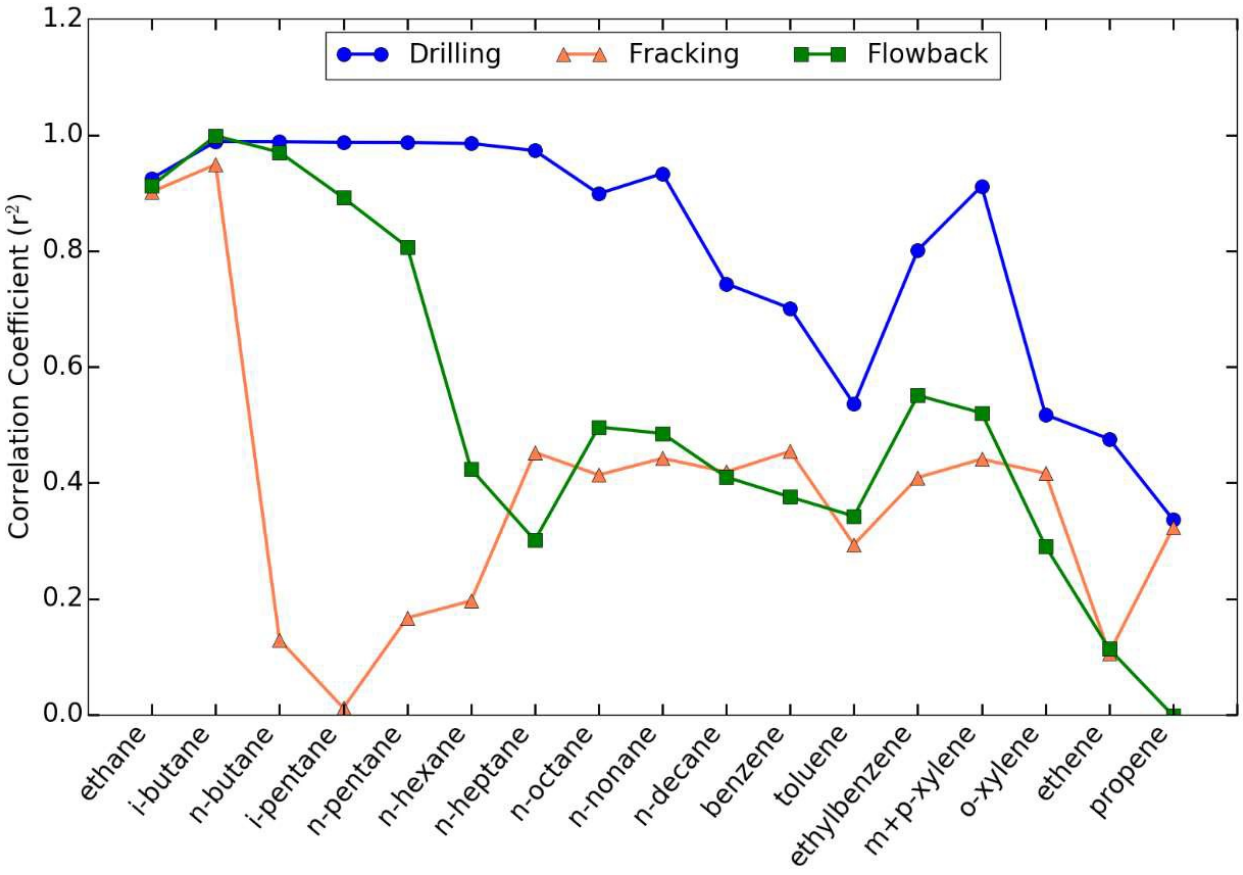

Figure 3.10. Comparison of the correlation coefficient of VOC emission rates with propane emission rates for selected VOCs by operations type.

3.1.9 Source Signatures

Concentration ratios of source-specific tracer compounds were investigated to determine the source signatures of various O&NG well development operations. The i-pentane to n-pentane ratio (iC_5/nC_5) and the i-butane to n-butane ratio (iC_4/nC_4) were determined using a least squares linear regression. These ratios were investigated because these ratios have unique natural gas and vehicular exhaust source signatures. The concentration ratios are not affected by air mass mixing

and dilution therefore these ratios are unaffected by boundary layer changes or the distance from the emission source [Gilman et al., 2013].

In Figure 3.11, the observed iC_5/nC_5 ratio for all operation types is shown. "All Operations" ($m = 1.04 \pm 0.013$, $r^2 = 0.994$) includes data collected from all sites conducting drilling ($m = 1.19 \pm 0.007$, $r^2 = 0.999$), fracking ($m = 0.635 \pm 0.030$, $r^2 = 0.989$), and flowback ($m = 1.02 \pm 0.017$, $r^2 = 0.994$) combined. The data used in this plot were selected based on the criteria outlined in Section 2.4. Drilling and flowback operations have the highest iC_5/nC_5 ratio of 1.19 and 1.02. iC_5/nC_5 ratio values from other studies for natural gas sources range from 0.86 to 1.0 [Gilman et al., 2013; Swarthout et al., 2013; Thompson et al., 2013]. Higher iC_5/nC_5 ratios occur when there is increased fuel evaporation and vehicle exhaust because i-pentane is a more common component of gasoline than n-pentane [Thompson et al., 2014, Swarthout et al., 2013]. The observed iC_5/nC_5 ratio during drilling operations is higher than the literature values for natural gas because drilling operations require an enormous amount of power to drill the well and move fluids through the well and are accompanied by combustion of fuel for the drill rig, generator engines, heaters, and pumps as well as emissions from drilling waste [Field et al., 2014]. The observed iC_5/nC_5 ratio of 1.02 during flowback operations is within the range of the literature values reported for natural gas. During flowback operations major emissions from power generation sources are not present, but natural gas is released during this stage and flows up the well to the surface with flowback fluid [FracFocus, 2015]. The observed iC_5/nC_5 ratio of 0.635 during fracking operations is not within the natural gas range of other studies where emissions were influenced by O&NG activities. The "All Operations" iC_5/nC_5 ratio of 1.04 is also within the range of literature values reported for natural gas suggesting strong natural gas signature during these well development operation types.

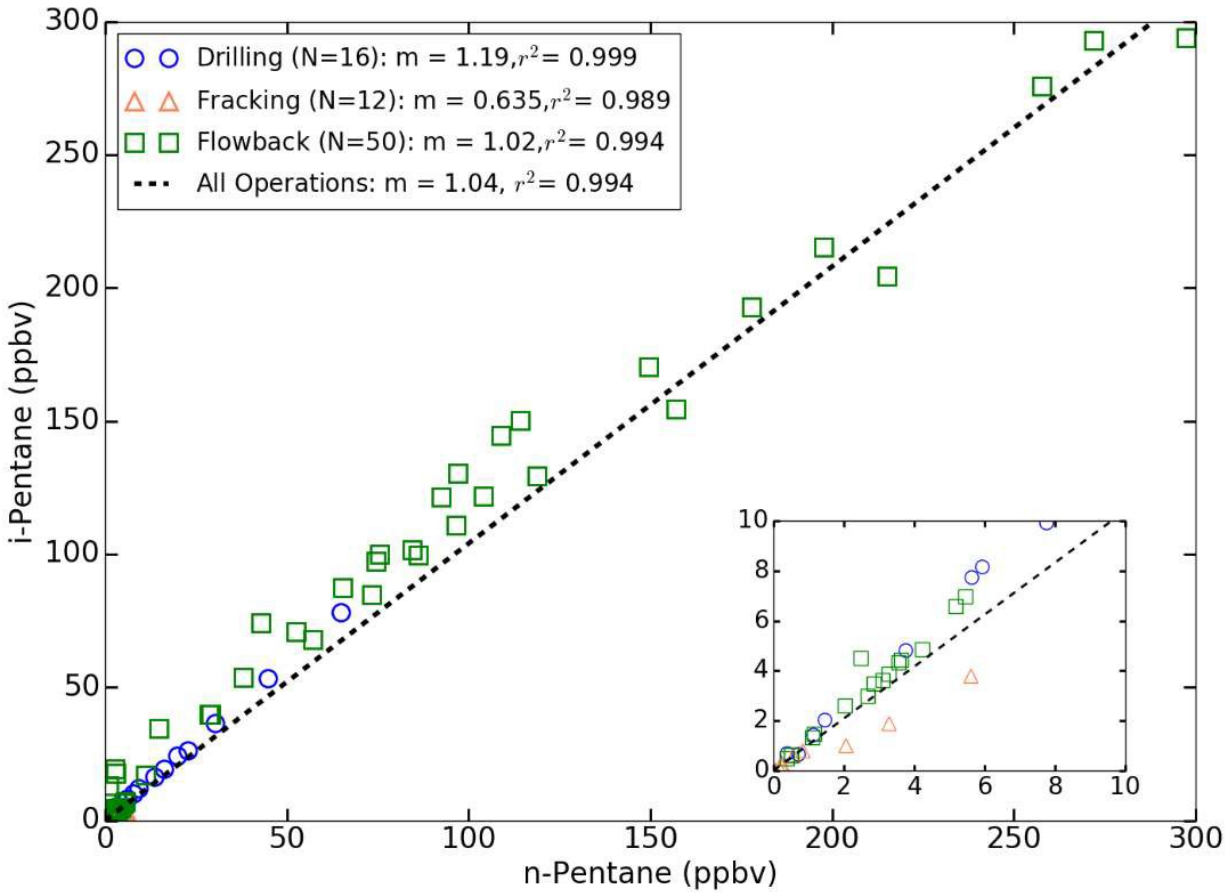

Figure 3.11. Correlation plot of i-pentane vs. n-pentane for drilling, fracking, and flowback operations in Garfield County. The dashed line includes data from the three operation types.

In Figure 3.12, the observed iC_5/nC_5 ratio from Garfield County for individual operation types is compared to several O&NG and urban studies. Characteristic iC_5/nC_5 ratios from relevant studies are represented by dashed lines. The observed iC_5/nC_5 ratio from Garfield County for individual operation types is compared to the characteristic natural gas iC_5/nC_5 ratio of 0.86 from samples collected at Wattenberg Gas Field [Gilman et al., 2013] and a characteristic vehicular exhaust iC_5/nC_5 ratio of 2.95 [Broderick et al., 2002]. An iC_5/nC_5 ratio of 0.74 was observed during a CSU study in North Dakota near O&NG sites in the Bakken oil patch in 2014 [Hecobian, pers. Commun, 2016]. Swarthout et al. [2013] reported an iC_5/nC_5 ratio of 1.0 during

the NACHTT campaign at BAO, which is located on the southwestern section of Wattenberg Gas Field. Thompson et al. [2013] reported an iC_5/nC_5 ratio of 0.965 in the Erie/Longmont area on the southwestern edge of Wattenberg Gas Field in Colorado. The similarities between the iC_5/nC_5 ratio of 1.04 observed in Garfield County and the various studies conducted in the Northern Front Range indicate that natural gas is a major source of light alkane emissions during new well drilling and completions in Garfield County. The observed iC_5/nC_5 ratio in Garfield County is much smaller than the iC_5/nC_5 ratios observed at urban sites. Russo et al. [2010] observed an iC_5/nC_5 ratio of 2.2 in New Hampshire at the AIRMAP Observatory, an area influenced by industrial and urban emissions. Gilman et al. [2013] reported an iC_5/nC_5 ratio of 2.41 in Pasadena, CA from measurements taken during the CalNex (California Nexus) campaign.

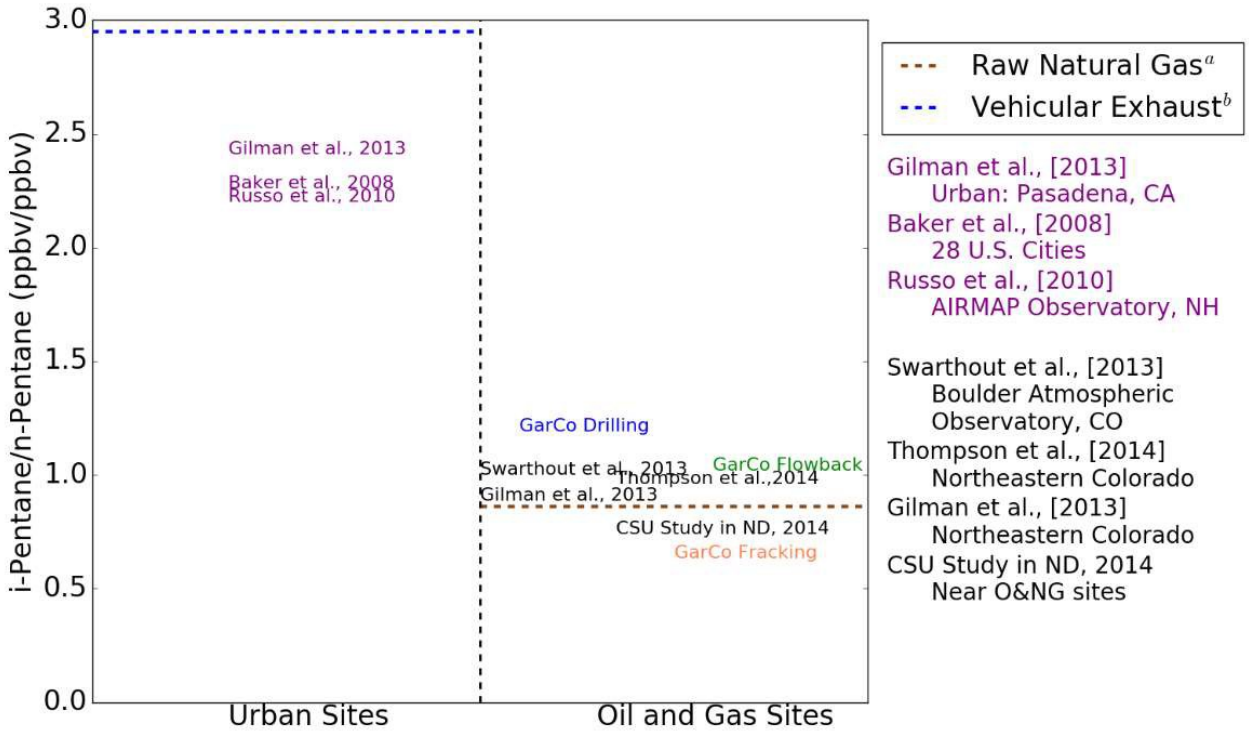

Figure 3.12. Comparison of i-pentane/n-pentane ratios from Garfield County for individual operation types with relevant studies. [a]Gilman et al. [2013], [b]Broderick et al. [2002]

Figure 3.13 shows the iC_4/nC_4 ratio for each operation type. "All Operations" (m = 1.07 ± 0.035, r^2 = 0.961) includes data from all sites conducting drilling (m = 1.24 ± 0.010, r^2 = 0.999), fracking (m = 1.02 ± 0.134, r^2 = 0.930), and flowback (m = 1.07 ± 0.053, r^2 = 0.949) combined. The data used in this plot were selected based on the criteria outlined in Section 2.4. The iC_4/nC_4 ratios for "All Operations" and the individual operation types are greater than 1. Literature iC_4/nC_4 ratio values for natural gas range from ~0.6 to > 1. Literature iC_4/nC_4 ratio values for exhaust/vehicular exhaust range from ~0.2-0.3 [Jobson et al., 2004; Simpson et al., 2013; Russo et al., 2013]. The iC_4/nC_4 ratios for all of the individual operation types are influenced by natural gas.

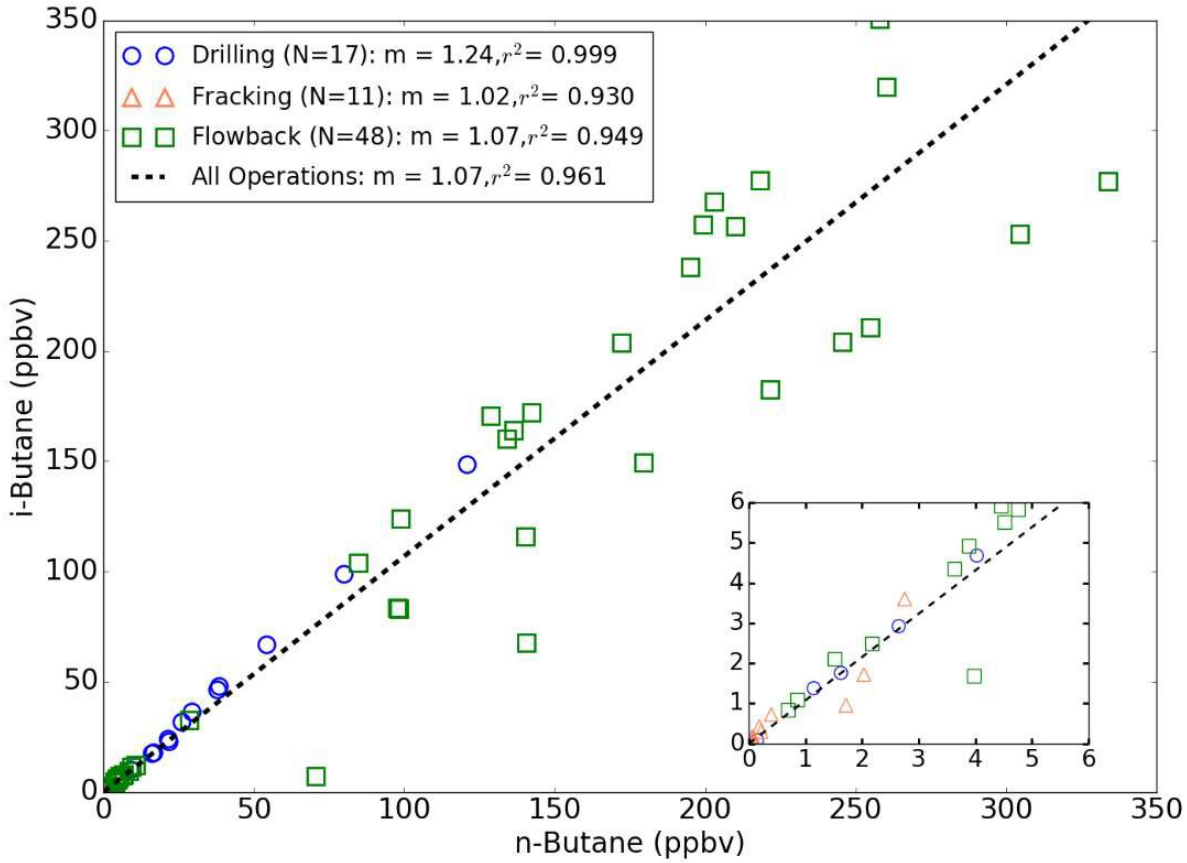

Figure 3.13. Correlation plot of i-butane vs. n-butane for drilling, fracking, flowback operations in Garfield County. The dashed line includes data from the three operations types. N is the number of canister samples. m is the slope.

In Figure 3.14, the observed iC_4/nC_4 ratios in Garfield County for individual operation types is compared to several O&NG and urban studies, the characteristic liquefied petroleum gas (LPG) iC_4/nC_4 ratio of 0.46, the characteristic natural gas iC_4/nC_4 ratio range of ~0.6-1.0, and the characteristic urban/vehicular exhaust iC_4/nC_4 ratio range of ~0.2-0.3 [Simpson et al., 2013; Russo et al., 2010]. The observed iC_4/nC_4 ratios in Garfield County are within the characteristic natural gas range for all operation types. Rich et al. [2014] found an iC_4/nC_4 ratio of 1.33 in the Barnett Shale region, which is similar to the iC_4/nC_4 ratios found in this study for drilling, fracking, and flowback operations. Thompson et al. [2014] and Gilman et al. [2013] found an iC_4/nC_4 ratio of 0.43 in the Denver-Julesburg Basin closer to LPG. Russo et al. [2010] found an iC_4/nC_4 ratio of 0.5 at the AIRMAP Observatory in New Hampshire, a location influenced by

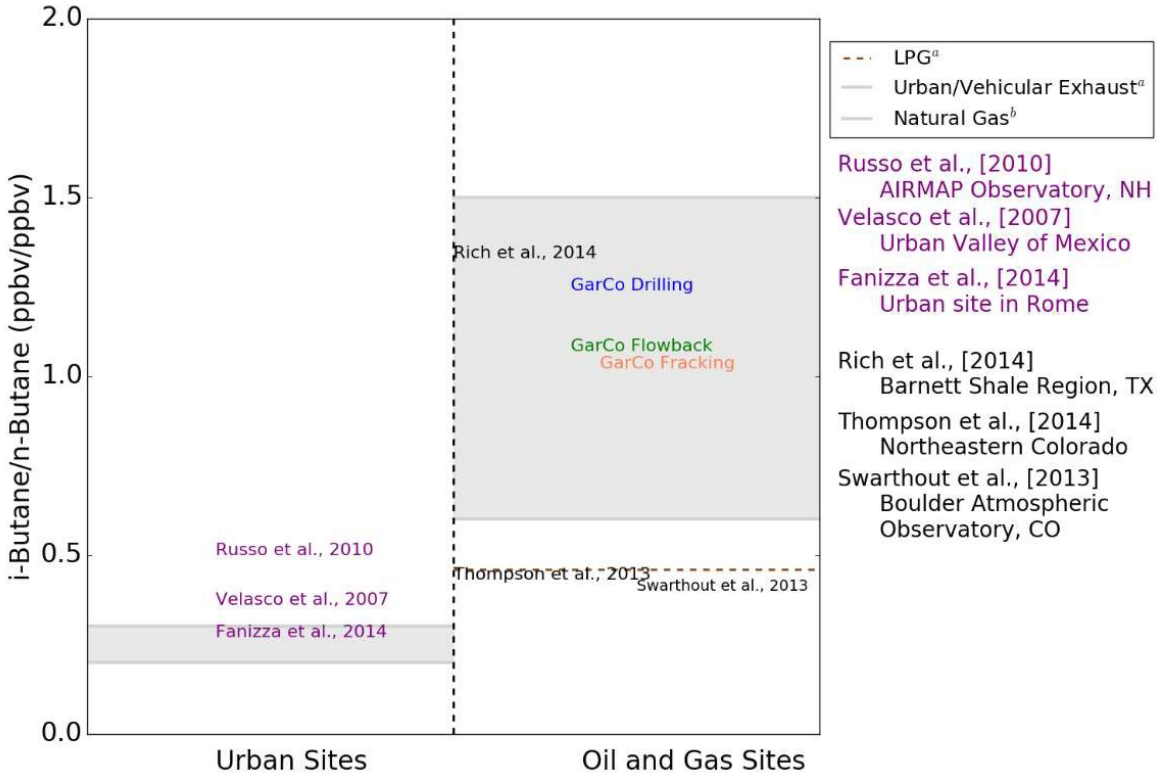

Figure 3.14. Comparison of i-butane/n-butane ratios from Garfield County for individual operation types with relevant studies. [a]Russo et al., [2010], [b]Simpson et al., [2013]

urban and industrial emissions. Fanizza et al. [2014] found an iC_4/nC_4 ratio of 0.28 at an urban site in Rome. Velasco et al. [2007] found an iC_4/nC_4 ratio of 0.37 at an urban site in the Valley of Mexico.

In Figure 3.15, the observed benzene/toluene (C_6H_6/C_7H_8) ratio is compared for each operation type. The data used in this plot were selected based on the criteria outlined in Section 2.4.

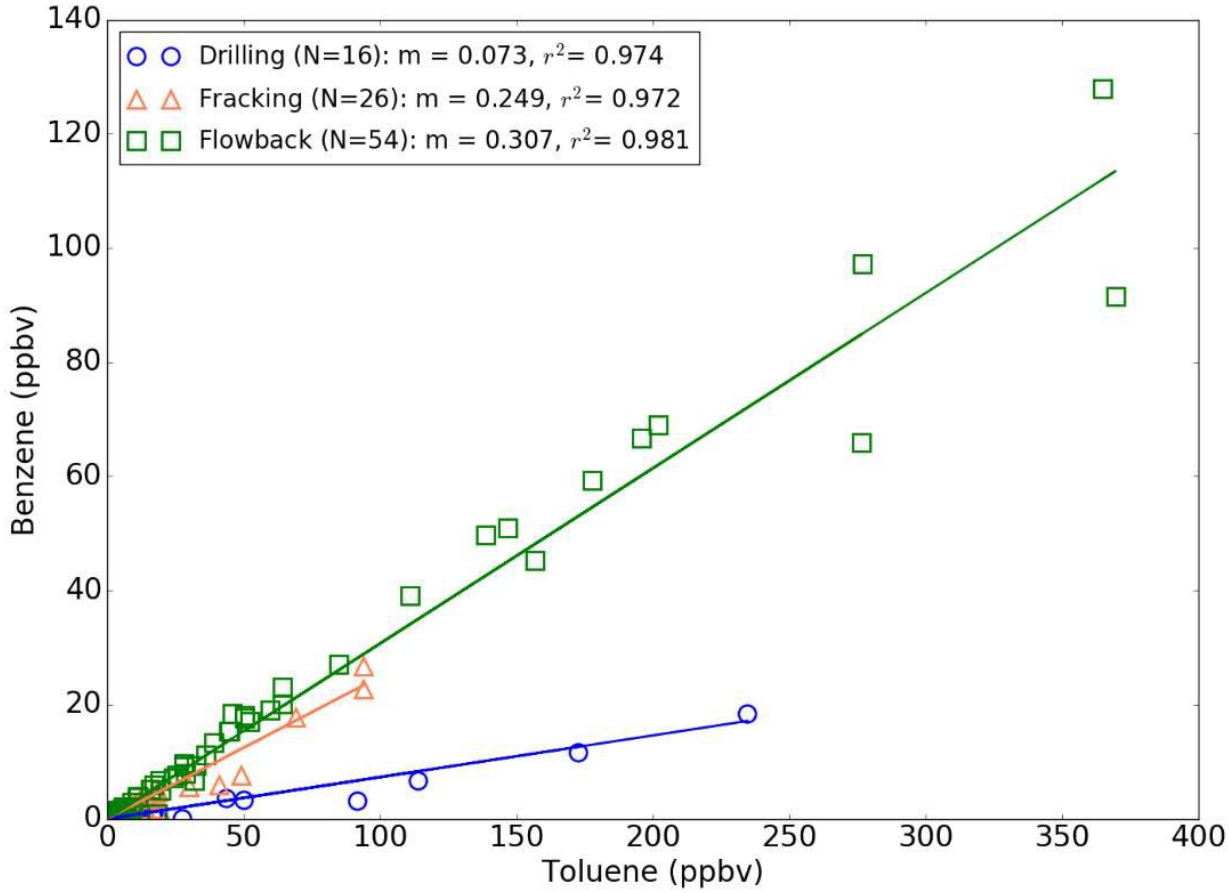

Figure 3.15. Comparison of C_6H_6/C_7H_8 ratios by operation type. N is the number of canister samples and m is the slope.

Benzene and toluene are frequently found in petroleum byproducts such as natural gas and gasoline [Rich et al., 2014]. All operation types show a tight correlation between benzene and toluene suggesting that benzene and toluene are emitted from the same sources during

individual operation types. The lowest C_6H_6/C_7H_8 ratio of 0.073 was observed during drilling operations indicating that the observed toluene mixing ratios were much higher than benzene mixing ratios. This suggests that although benzene and toluene are both combustion tracers, toluene may have other significant sources other than combustion on the well pad during drilling operations. Toluene is present as a solvent in drilling fluid and an acidizing agent for removing organics from the well [Fisher et al., 2013]. The average urban concentrations are 175 ppb and 572 for benzene and toluene, respectively [Baker et al., 2008]. Baker et al. [2008] found a C_6H_6/C_7H_8 ratio of 0.306 from 28 U.S. cities, which is similar to the C_6H_6/C_7H_8 ratio of 0.307 found during drilling operations in Garfield County.

3.2 Emission Rate Ratios

Emission rate (ER) ratios were derived from the VOC emission rates and CH_4 emission rates derived for each stage of well development: drilling, fracking, and flowback in Garfield County. The emission rate ratios were used to determine if methane emission rates would be useful surrogates for individual VOC emission rates during various stages of natural gas well development. The emission rate ratios were derived by dividing the VOC emission rates determined from the canisters co-located with the Picarro instrument by the average methane emission rates (from the Picarro) over the three minutes of canister sampling. The selection criterion for the VOC data and the CH_4 data for this section were processed and screened using the methods described in Section 2.4. The equation used to derive the emission rate ratios is outlined in Section 2.4. This section will present select individual VOC-to-methane emission rate ratios for each well development operation.

3.2.1 Drilling VOC Emission Rate Ratios

Figure 3.16 shows VOC-to-methane emission rate ratio distributions determined from 14 canister samples co-located with the Picarro instrument during drilling operations. Select alkanes, aromatics, and alkenes are included and grouped separately. In Figure 3.16, the red line represents the median, the box depicts the interquartile range and the whiskers represent the 5th and 95th percentiles of the emission rate ratios, with points beyond these limits represented by plus symbols. The y-axis is plotted with a log-scale since the observed emission rate ratios span several orders of magnitude. Emission rate ratio distributions for the full suite of VOCs measured during drilling operations are in Appendix H. Table 3.6 tabulates some of the results shown in Figure 3.16.

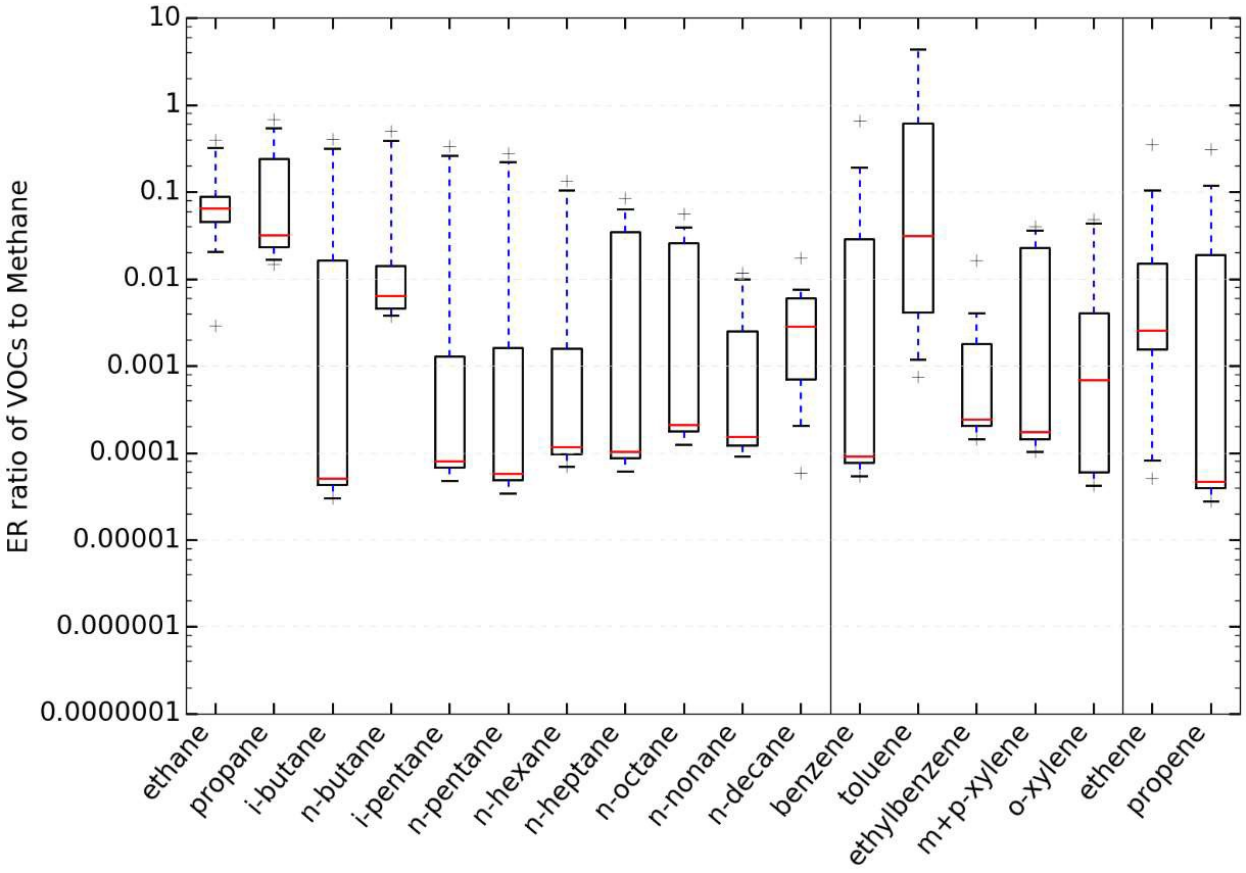

Figure 3.16. Select emission rate ratio of VOCs to methane distributions during drilling operations.

Ethane and n-butane have tight emission rate ratio distributions spanning much less than an order of magnitude. iC_4 and C_5-C_{10} have larger emission rate ratio distributions spanning more than one order of magnitude suggesting that emissions of VOCs other than light alkanes from natural gas are not significant consistent sources during drilling operations. BTEX compounds also have wide emission rate ratio distributions spanning two or more orders of magnitude except ethylbenzene, which has an emission rate distribution spanning about one order of magnitude. BTEX, heavier alkanes, and i-butane are primarily emitted from combustion related sources during drilling operations, therefore the emission rates of these VOCs would vary compared to methane emission rates.

Table 3.6. VOC-to-methane emission rate ratios for drilling operations. 14 samples co-located with the Picarro instrument collected during drilling operations were used for this analysis. Med is the median.

VOCs	Mean [g/s]	Med [g/s]	5th %ile [g/s]	25th %ile [g/s]	75th %ile [g/s]	95th %ile [g/s]
ethane	0.110	0.065	0.014	0.045	0.088	0.348
propane	0.180	0.032	0.016	0.024	0.239	0.590
i-butane	0.075	5.1E-05	3.0E-05	4.3E-05	0.016	0.347
n-butane	0.096	0.006	0.004	0.005	0.014	0.429
i-pentane	0.061	8.0E-05	4.8E-05	6.7E-05	0.001	0.286
n-pentane	0.052	5.8E-05	3.5E-05	4.9E-05	0.002	0.241
n-hexane	0.024	0.0001	6.9E-05	9.8E-05	0.002	0.115
n-heptane	0.017	0.0001	6.1E-05	8.7E-05	0.035	0.071
n-octane	0.013	0.0002	0.0001	0.0002	0.026	0.045
n-nonane	0.003	0.0002	9.2E-05	0.0001	0.002	0.011
n-decane	0.004	0.003	0.0001	0.0007	0.006	0.013
benzene	0.071	9.1E-05	5.4E-05	7.7E-05	0.029	0.356
toluene	2.19	0.031	0.001	0.004	0.621	10.6
ethylbenzene	0.002	0.0002	0.0001	0.0002	0.002	0.008
m+p-xylene	0.011	0.0002	0.0001	0.0001	0.023	0.037
o-xylene	0.008	0.0007	4.2E-05	5.9E-05	0.004	0.046
ethene	0.039	0.003	7.2E-05	0.002	0.015	0.189
propene	0.035	4.7E-05	2.8E-05	3.9E-05	0.019	0.187

Propene has an emission rate ratio distribution spanning 3 orders of magnitude while ethene has a distribution spanning about one order of magnitude. Propene can be emitted from combustion related sources such as motor gasoline [Intratec, 2012] while ethene is a component of natural gas emissions [Sanchez et al., 2008].

3.2.2 Fracking VOC Emission Rate Ratios

Figure 3.17 shows VOC-to-methane emission rate ratio distributions determined from 13 canister samples co-located with the Picarro instrument during fracking operations. The emission rate ratio distributions for the full suite of VOCs during fracking operations are in Appendix H. Table 3.7 tabulates some of the results shown in Figure 3.17. C_2-iC_4 and C_6-C_{10} show emission rate ratio distributions spanning one order of magnitude or less during fracking operations.

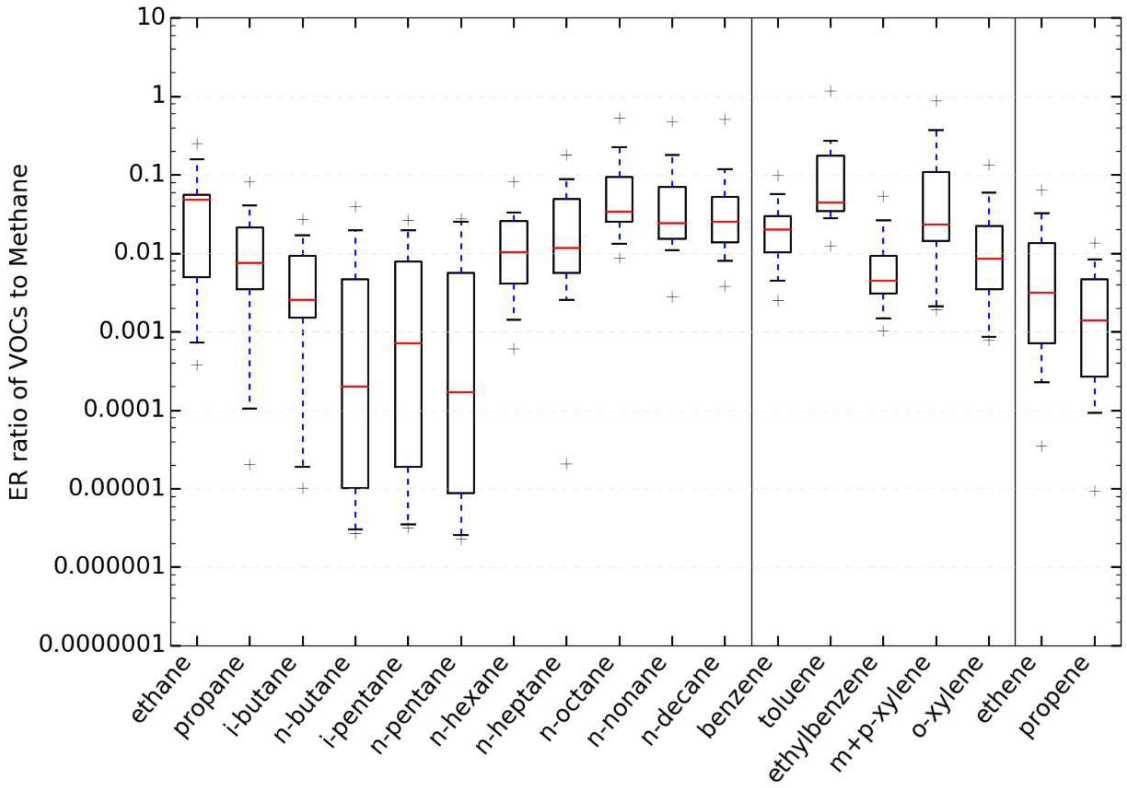

Figure 3.17. Select emission rate ratios of VOCs to methane during fracking operations.

Heavier alkanes (C_6-C_{10}) are present in hydraulic fracturing fluid and natural gas condensate [Warneke et al., 2014]. n-Butane, i-pentane, and n-pentane show wide distributions spanning 3 orders of magnitude suggesting inconsistent emission rate ratios when comparing to methane. BTEX compounds also show tight distributions spanning one order of magnitude or less. Alkene emission rate ratios span a little over one order of magnitude.

Table 3.7. VOC-to-methane emission rate ratios for fracking operations. 13 samples co-located with the Picarro instrument collected during fracking operations were used for this analysis. Med is the median.

VOCs	Mean [g/s]	Med [g/s]	5th %ile [g/s]	25th %ile [g/s]	75th %ile [g/s]	95th %ile [g/s]
ethane	0.058	0.049	0.0006	0.005	0.055	0.187
propane	0.016	0.008	7.9E-05	0.003	0.021	0.053
i-butane	0.006	0.003	1.6E-05	0.002	0.009	0.020
n-butane	0.005	0.0002	2.9E-06	1.03E-05	0.005	0.026
i-pentane	0.006	0.0007	3.4E-06	1.9E-05	0.008	0.021
n-pentane	0.005	0.0002	2.5E-06	8.7E-06	0.006	0.026
n-hexane	0.017	0.010	0.001	0.004	0.026	0.048
n-heptane	0.033	0.012	0.002	0.006	0.049	0.116
n-octane	0.096	0.034	0.012	0.025	0.094	0.319
n-nonane	0.075	0.024	0.009	0.015	0.069	0.270
n-decane	0.066	0.025	0.007	0.014	0.053	0.237
benzene	0.026	0.020	0.004	0.010	0.030	0.069
toluene	0.169	0.044	0.023	0.035	0.176	0.547
ethylbenzene	0.009	0.004	0.001	0.003	0.009	0.035
m+p-xylene	0.127	0.023	0.002	0.014	0.109	0.523
o-xylene	0.022	0.009	0.0008	0.003	0.022	0.082
ethene	0.011	0.003	0.0002	0.0007	0.013	0.042
propene	0.003	0.001	6.7E-05	0.0003	0.005	0.009

Flowback VOC Emission Rate Ratios 3.2.3

Figure 3.18 shows VOC-to-methane emission rate ratio distributions determined from 30 canister samples co-located with the Picarro instrument during flowback operations. The emission rate ratio distributions of the full suite of VOCs are in Appendix H. Table 3.8 tabulates

some of the results shown in Figure 3.18. C_2-C_{10} emission rate ratios and BTEX compounds show tight distributions spanning one order of magnitude or less.

This result suggests emissions during flowback operations are influenced by both natural gas emissions containing lighter alkanes (C_2-C_5) and flowback fluid containing heavier alkanes (C_6-C_{10}) and BTEX. Ethene shows a tight emission rate ratio distribution spanning less than an order of magnitude suggesting natural gas influence, while propene has a wider distribution.

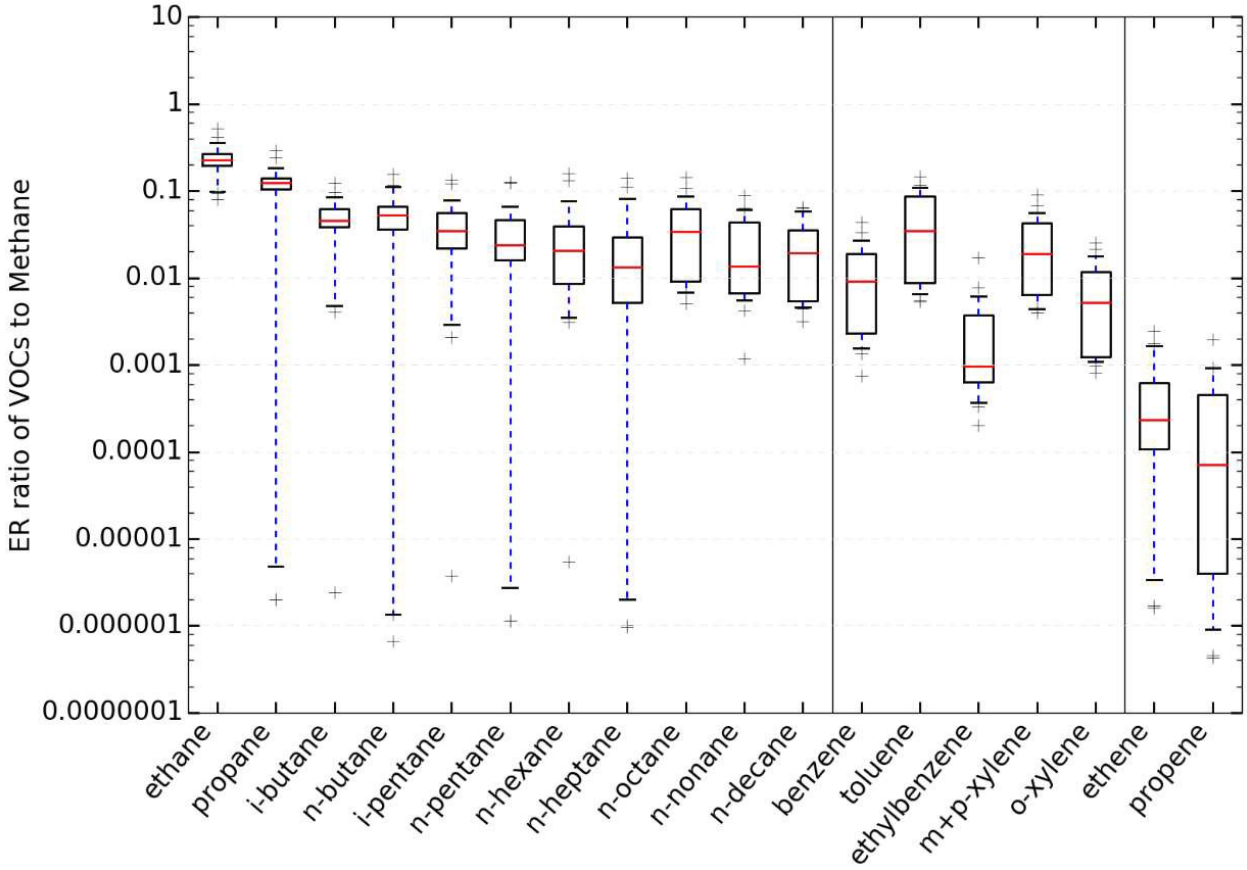

Figure 3.18. Select ER ratios of VOCs to methane during flowback operations.

Table 3.8. VOC-to-methane emission rate ratios for flowback operations. 30 samples co-located with the Picarro instrument were collected during flowback operations were used for this analysis. Med is the median.

VOCs	Mean [g/s]	Med [g/s]	5th %ile [g/s]	25th %ile [g/s]	75th %ile [g/s]	95th %ile [g/s]
ethane	0.235	0.227	0.096	0.194	0.269	0.387
propane	0.118	0.124	3.3E-06	0.104	0.140	0.216
i-butane	0.047	0.046	0.004	0.039	0.062	0.092
n-butane	0.052	0.053	1.3E-06	0.036	0.066	0.114
i-pentane	0.041	0.035	0.002	0.022	0.056	0.102
n-pentane	0.033	0.024	1.9E-06	0.016	0.047	0.097
n-hexane	0.033	0.020	0.003	0.009	0.039	0.107
n-heptane	0.027	0.013	1.5E-06	0.005	0.029	0.098
n-octane	0.039	0.034	0.007	0.009	0.062	0.098
n-nonane	0.026	0.014	0.005	0.007	0.043	0.062
n-decane	0.023	0.019	0.005	0.005	0.035	0.062
benzene	0.012	0.009	0.001	0.002	0.019	0.030
toluene	0.048	0.034	0.006	0.009	0.087	0.112
ethylbenzene	0.003	0.0009	0.003	0.0006	0.004	0.007
m+p-xylene	0.027	0.019	0.004	0.006	0.042	0.062
o-xylene	0.007	0.005	0.001	0.001	0.012	0.198
ethene	0.0005	0.0002	2.5E-06	0.0002	0.0007	0.002
propene	0.0003	7.08E-05	6.6E-07	4.0E-06	0.0005	0.0009

3.2.4 Emission Rate Ratios Comparison by Operation Type

The mean VOC-to-methane emission rate (ER) ratios for drilling, fracking, and flowback of select VOCs in Garfield County are compared to Rich et al. [2014] and Warneke et al. [2014] in Figure 3.19. The error bars in Figure 3.19 represent the 5th and 95th percentiles of VOC-to-methane emission rate ratios for each operation type.

The highest mean emission rate ratio was toluene during drilling operations when the toluene emission rate was greater than the CH_4 emission rate. Toluene and benzene are both combustion tracers, but toluene can also be present in drilling fluid as a solvent [EPA, 1994; Broni-Bediako et al., 2010]. C_2-C_7 emission rate ratios are similar during drilling and fracking operations. C_2-C_5 mean emission rate ratios during fracking operations are much lower than

those during drilling and flowback operations. C_8-C_{10} mean emission rate ratios during fracking and flowback operations are higher than during drilling operations. Fluid handling and storage may contribute to higher heavier alkane emissions during fracking and flowback operations. Propene emission rate ratios differ greatly across operation types. Higher relative propene emissions during drilling and fracking are consistent with fuel and/or combustion [Intratec, 2012].

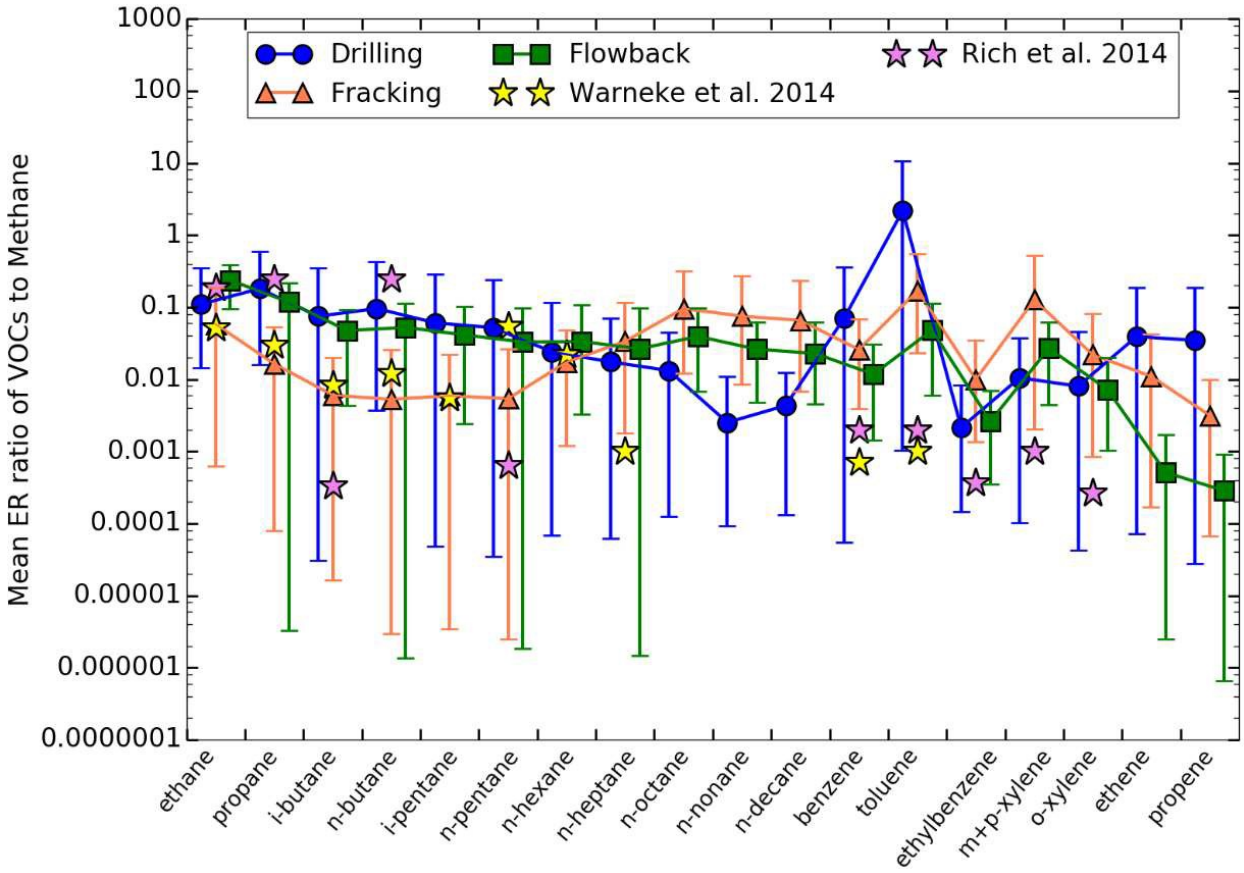

Figure 3.19. Mean emission rate ratios for select VOCs to methane by operation type.

Studies in the Denver Julesburg Basin, Uintah Basin, and the Barnett Shale have characterized emissions of methane and VOCs. Table 3.9 summarizes the mean emission rate ratios for this study during well development operations in Garfield County and compares them

to studies by Warneke et al. [2014] in the Utintah Basin and Rich et al. [2014] in the Barnett Shale. VOC to methane emission ratios differ by basin due to natural gas composition, but this comparison is provided to put the VOC to methane emission ratios in this study into context. Pétron et al. [2012] measured methane and various non-methane hydrocarbons near BAO tower during 2007 to 2009. They observed a C_3H_8/CH_4 emission ratio ranging from 0.079 to 0.105, which overlaps the mean emission rate ratio range observed in Garfield County (0.016-0.180) for the three operation types. The similarity in emission ratios is interesting given that mostly "wet gas" is produced in the Denver Julesburg Basin [Pétron et al., 2014].

Warneke et al. [2014] measured VOC emissions from individual gas and oil wells and other point sources in the Uintah Basin in 2012. Mean heptane, benzene, and toluene emission ratios for all Garfield County operation types reported here are higher by at least one order of magnitude compared to Warneke et al. [2014]. Rich et al. [2014] measured VOC emissions associated with shale gas development and production in the Barnett Shale Region from 2008-2010. Mean iC_4, nC_5, and BTEX ratios in Garfield County are higher by at least two orders of magnitude.

Table 3.9. Comparison of mean VOC-to-methane emission ratios in Garfield County (GC) with other studies.

VOCs	Drilling GC	Fracking GC	Flowback GC	Utintah Basin Warneke et al. [2014]	Barnett Shale Rich et al. [2014]
ethane	0.110	0.058	0.235	0.052	0.189
propane	0.180	0.016	0.118	0.029	0.248
i-butane	0.075	0.006	0.047	0.008	3.29E-04
n-butane	0.096	0.005	0.052	0.012	0.025
i-pentane	0.061	0.006	0.041	0.006	-
n-pentane	0.052	0.005	0.033	0.006	6.44E-04
n-hexane	0.024	0.017	0.033	0.022	-
n-heptane	0.017	0.033	0.027	0.001	-
n-octane	0.013	0.096	0.039	-	-
n-nonane	0.003	0.075	0.026	-	-
n-decane	0.004	0.066	0.023	-	-
benzene	0.071	0.026	0.012	0.0007	0.002
toluene	2.19	0.169	0.048	0.001	0.002
ethylbenzene	0.002	0.009	0.003	-	3.69E-04
m+p-xylene	0.011	0.127	0.027	-	0.001
o-xylene	0.008	0.022	0.007	-	2.66E-04
ethene	0.039	0.011	0.0005	-	-
propene	0.035	0.003	0.0003	-	-

CHAPTER 4

CONCLUSIONS

The widespread use of unconventional natural gas extraction technologies has allowed for significant growth of the natural gas industry in Colorado in the last decade. Garfield County is located in the Piceance Basin in Colorado where natural gas wells penetrate a tight sand formation rich in natural gas, called the William's Fork formation. In order to increase extraction potential of natural gas trapped in several sandstone lenses, horizontal drilling is used. Hydraulic fracturing is used as a stimulation technique to maximize the flow and efficiency of natural gas transport to the surface from unconventional reservoirs. Approximately 10-50% of hydraulic fracturing fluid flows back to the surface.

Our field team collected samples in Garfield County between 2013-2015 to measure methane, ozone precursors, and air toxics associated with natural gas extraction activities. Very few prior studies have provided direct observations of VOC emissions from individual well development activities. Emission rates of 48 VOCs and methane were determined for three well development operations: drilling, hydraulic fracturing (fracking), and flowback for a subset of samples collected. In general, methane and VOCs are released at the highest rates during flowback operations. We found that methane had mean emission rates of 1.57, 6.78, and 25.6 $g\ s^{-1}$ for drilling, hydraulic fracturing, and flowback operations respectively, while toluene had mean emission rates of 1.24, 0.469, and 0.437 $g\ s^{-1}$ for these operations.

Overall, the per-well emission rates of several key VOCs for well development operations in Garfield County were higher than other studies that estimated emission rates from production activities. Per-well benzene emission rates during well development operations in

Garfield County are much higher compared to other studies of production emissions and there are currently no studies to compare toluene emission rates.

Speciated VOC concentrations and emission rates are much less commonly measured than methane concentrations and emission rates, in part due to the greater measurement complexity. Methane emission rates may be useful surrogates for lighter VOC (C_2-C_4 alkane) emission rates for some operation types. For example, C_2-C_3 and methane are emitted from the same sources during fracking operations; propane, butane, and methane appear to be mostly emitted from the same sources during flowback; and ethane and methane appear to be emitted from the same sources for all operation types. Heavier VOCs including C_5-C_{10} alkanes, BTEX, and alkenes are generally not well correlated with methane for any of the well development operation types indicating that methane emission rates are not good predictors of emission rates for these VOCs.

Drilling and fracking emissions appear to be largely influenced by emissions from combustion, while flowback emissions appear to be largely influenced by the release of natural gas and other substances from the well. This study provides important advances regarding direct observations of a wide range of VOCs and quantifying VOC emission rates from individual well development operations.

CHAPTER 5

FUTURE WORK

This study provides important advances regarding direct observations of a wide range of VOC emissions from new well development and especially for individual well development operations, but there is still much to investigate with the dataset collected in Garfield County. The full dataset was not used in this thesis. The full dataset includes six more experiments. The analysis of the full dataset will provide more comprehensive results. Beyond the Garfield County study there is also a strong need to examine emissions of speciated VOCs from well development in other regions, especially those with different gas compositions. Changes in emission control practices, especially for flowback operations, also call for continued investigation of VOC emissions to ascertain the success of these new practices.

We found toluene to be emitted at much higher rates than benzene during all well development operations, even though these VOCs are both combustion tracers. The enhancement of toluene emissions to benzene was large enough to suggest that there are toluene sources on the pad other than combustion sources. More investigation is needed into the major sources of toluene for individual well development operations.

REFERENCES

Air Resource Specialist (ARS). (2015). Garfield County: 2014 Air Quality Monitoring Summary. (2015, June 30). Retrieved from Garfield County Air Quality Management: http://www.garfield-county.com/air-quality/documents/airquality/2014-GARCO-air-monitoring.pdf

Allen, D. T., Torres, V. M., Thomas, J., Sullivan, D. W., Harrison, M., Hendler, A., Herndon, S. C., Kolb, C. E., Fraser, M. P. Hill, A. D., Lamb, B. K., Miskimins, J., Sawyer, R. F., Seinfeld, J. H. (2013). Measurements of methane emissions at natural gas production sites in United States. PNAS, 110(44), 17768-17773. doi:10.1073/pnas.1304880110

American Petroleum Institute (API). (2015). Facts About Shale Gas. Retrieved from http://www.api.org/Policy-and-Issues/Policy-Items/Exploration/Facts_About_Shale_Gas

Australian Government: Department of the Environment. (2014, May 28). n-Hexane: Sources of Emissions. Retrieved from National Pollutant Inventory: http://www.npi.gov.au/resource/n-hexane-sources-emissions

Baker, A. K., Beyersdorf, A. J., Doezema, L. A., Katzenstein, A., Meinardi, S., Simpson, I. J., Blake, D. R., Sherwood Rowland, F. (2008). Measurements of nonmethane hydrocarbons in 28 United States cities. Atmospheric Environment, 42(1), 170-182. doi:doi:10.1016/j.atmosenv.2007.09.007

Baytok, S., & Pranter, M. J. (2013). Fault and fracture distribution within a tight-gas sandstone reservoir: Mesaverde Group, Mamm Creek Field, Piceance Basin, Colorado, USA. Petroleum Geoscience, 19, 203-222. doi:10.1144/petgeo2011-093

Berezin, I. V., Denisov, E. T., & Emanuel, N. M. (1966). The Oxidation of Cyclohexane. Oxford: Pergamon Press Ltd.

Borbon, A., Fontaine, H., Veillerot, M., Locoge, N., Galloo, J. C., & Guillermo, R. (2001). An investigation into the traffic-related fraction of isoprene at an urban location. Atmospheric Environment, 35, 3749-3760. doi:10.1016/S1352-2310(01)00170-4

Broderick, B. M., & Marnane, I. S. (2002). A comparison of the C_2-C_9 hydrocarbon compositions of vehicle fuels and urban air in Dublin, Ireland. Atmospheric Environment, 36(6), 975-986. doi:10.1016/S1352-2310(01)00472-1

Broni-Bediako, E., & Amorin, R. (2010). Effects of drilling fluid exposure to oil and gas workers presented with major areas of exposure and exposure indicators. Research Journal of Applied Sciences: Engineering and Technology, 2(8), 710-719.

Brown, V. J. (2007). Industry Issues: Putting Heat on Gas. Environmental Health Perspectives, 115(2), A76.

Colorado Oil & Gas Commission (COGCC). (2016). COGCC Production Data. Retrieved from Colorado Oil & Gas Commission.

Compressed Gas Association (CGA). (1990). Acetylene. In Handbook of Compressed Gases (pp. 213-215). New York: Chapman & Hall.

Daguat, P., Ristori, A., Bakali, E., & Cathonnet, M. (2002). Experimental and kinetic modeling study of the oxidation of n-propylbenzene. Fuel, 81, 173-184. doi:10.1016/S0016-2361(01)00139-9

Dennison, D. (2005). Drilling 101: Drilling a natural gas well and natural gas production in the Piceance Basin. Retrieved from Garfield County- Oil & Gas: http://www.garfield-county.com/oil-gas/documents/drilling_101.pdf

DrillingEdge Inc. (2015). Oil and Gas Production By Year in Garfield County, CO. Retrieved from Garfield County, CO Permits, Production, Wells, & Operators: http://www.drillingedge.com/colorado/garfield-county

U.S. Energy Information Administration (EIA). (2014) U.S. Energy Information Adminstration - Independent Statistics & Analysis. Retrieved from http://www.eia.gov/state/analysis.cfm?sid=CO

U.S. Energy Information Administration (EIA). (2015) U.S. Energy Information Adminstration - Independent Statistics & Analysis. Retrieved from http://www.eia.gov/state/analysis.cfm?sid=CO

Entech Instruments Inc. (2014). Users Manual Version 2.0: Entech Model 7200 Preconcentrator.

Entech Instruments Inc. (n.d.). Operators Manual Version 1.0, Smart Lab Based Canister Cleaning System: Model 3100A.

Entech Instruments Inc. (2015). Comparing SUMMA Canisters and Silonite Canisters for Air Monitoring. What's Best? Retrieved from SUMMA Canisters and How They Differ From Silonite Canisters and Other TO-15 Canisters: http://www.entechinst.com/document-library/air-monitoring-research/summa-canisters-differ-silonite-canisters-15-canisters/

U.S. Environmental Protection Agency (EPA). (1994). Locating and Estimating Air Emissions from Sources of Xylene. (Office of Air Quality Standards, Ed.) Retrieved from Locating and Estimating Sources of Xylene: http://www3.epa.gov/ttnchie1/le/xylene.pdf

U.S. Environmental Protection Agency (EPA). (2015a). The Process of Hydraulic Fracturing. Retrieved from http://www2.epa.gov/hydraulicfracturing/process-hydraulic-fracturing.

U.S. Environmental Protection Agency (EPA). (2015b). What are Hazardous Air Pollutants? Retrieved from https://www.epa.gov/haps/what-are-hazardous-air-pollutants.

U.S. Environmental Protection Agency (EPA). (2015c). Cumene. Retrieved from https://www3.epa.gov/airtoxics/hlthef/cumene.html.

U.S. Environmental Protection Agency (EPA). (2016a). Overview of Greenhouse Gases. Retrieved from Methane Emissions: Climate Change: http://www3.epa.gov/climatechange/ghgemissions/gases/ch4.html

U.S. Environmental Protection Agency (EPA). (2016b). Ozone Pollution. https://www.epa.gov/ozone-pollution

Fanizza, C., Incoronato, F., Baiguera, S., Schiro, R., & Brocco, D. (2014). Volatile organic compound levels at one site in Rome urban air. Atmospheric Pollution Research, 5(2), 303-314. doi:10.5094/APR.2014.036

Field, R. A., Soltis, J., & Murphy, S. (2014). Air quality concern of conventional oil and natural gas production. Environmental Science: Processes & Impacts, 16, 954-969. doi:10.1039/C4EM00081A

Field, R. A., Soltis, J., McCarthy, M. C., Murphy, S., & Montague, D. C. (2015). Influence of oil and gas field operations on spatial and temporal distributions of atmospheric non-methane hydrocarbons and their effect on ozone formation in winter. Atmospheric Chemistry and Physics, 15(6), 3527-3542. doi:10.5194/acp-15-3527-2015

Fisher, K. (2013). Terpenes Replacing BTEX in Oil Field. Retrieved from The American Oil & Gas Reporter: http://www.aogr.com/magazine/editors-choice/terpenes-replacing-btex-in-oil-field

FracFocus. (2015). FracFocus: Chemical Disclosure Registry. Retrieved from https://fracfocus.org/

Gentner, D. R., Harley, R. A., Miller, A. M., & Goldstein, A. H. (2009). Diurnal and seasonal variability of gasoline-related volatile organic compound emissions in Riverside, California. Environmental Science & Technology, 43(12), 4247-4252. doi:10.1021/es9006228

U.S. Geological Survey (USGS). (2015). Environmental Health-Toxic Substances: Volatile Organic Compounds (VOCs) Definition Page. Retrieved from http://toxics.usgs.gov/definitions/vocs.html

Gilman, J. B., Lerner, B. M., Kuster, W. C., & de Gouw, J. A. (2013). Source signature of volatile organic compounds from natural gas operations in northeastern Colorado. Environmental Science & Technology, 47(3), 1297-1305. doi:10.1021/es304119a

Graedel, T. E. (1978). Chemical Compounds in the Atmosphere. New York, New York: Academic Press Inc.

Graedel, T. E., Hawkins, D. T., & Claxton, L. D. (1986). Atmospheric Chemical Compounds: Sources, Occurence, and Bioassay. Orlando, Florida: Academic Press Inc.

GuoYi, H., Jian, L., ZhiSheng, L., Xia, L., QingWu, S., & ChengHua, M. (2008). Preliminary study on the orgin identification of natural gas by the parameters of light hydrocarbon. Science in China Series D: Earth Sciences, 51, 131-139. doi:10.1007/s11430-008-5017-x

Ho, K. F., Lee, S. C., Guo, H., & Tsai, W. Y. (2004). Seasonal and diurnal variations of volatile organic compounds (VOCs) in the atmosphere of Hong Kong. Science of the Total Environment, 322, 155-166. doi:10.1016/j.scitotenv.2003.10.004

Howard, P. H. (1989). Large Production and Priority Pollutants: Handbook of Environmental Fate and Exposure Data for Organic Chemicals (Vol. I). Boca Raton, Florida: CRC Press LLC.

Howard, P. H. (1993). Solvents 2: Handbook of Environmental Fate and Exposure Data for Organic Chemicals (Vol. IV). Chelsea, Michigan: Lewis Publishers.

Howard, P. H. (1997). Solvents 3: Handbook of Environmental Fate and Exposure Data for Organic Chemicals (Vol. V). Boca Raton, Florida: CRC Press Inc.

Intratec Solutions Inc. (2012). Intratec Report #TEC003A. Technology Economics Program: Propylene Production Via Propane Dehydrogenation . United States of America: Intratec Solutions LLC.

Jaffe, M. (2012). Like Wyoming, Utah finds high wintertime ozone pollution near oil, gas wells. The Denver Post. Retrieved from http://www.denverpost.com/ci_20042330

Jobson, B. T., Berkowitz, C. M., Kuster, W. C., Goldan, P. D., Williams, E. J., Fesenfeld, F. C., Apel, E. C., Karl, T., Lonneman, W. A., & Riemer, D. (2004). Hydrocarbon source signatures in Houston, Texas: Influence of petrochemical industry. Journal of Geophysical Research: Atmospheres, 109(D24). doi:10.1029/2004JD004887

Khoder, M. I. (2007). Ambient levels of volatile organic compounds in the atmosphere of Greater Cairo. Atmospheric Environment, 41, 554-566. doi:10.1016/j.atmosenv.2006.08.051

Koss, A. R., de Gouw, J., Warneke, C., Gilman, J. B., Lerner, B. M., Graus, M., Yuan, B., Edwards, P., Brown, S. S., Wild, R.; Roberts, J. M., Bates, T. S., Quinn, P. K. (2015). Photochemical aging of volatile organic compounds associated with oil and natural gas extraction in the Utintah Basin, UT, during a wintertime ozone formation event. Atmospheric Chemistry and Physics, 15, 5727-5741. doi:10.5194/acp-15-5727-2015

Lee, B. H., Munger, J. W., Wofsy, S. C., & Goldstein, A. H. (2006). Anthropogenic emissions of nonmethane hydrocarbons in the northeastern United States: Measured seasonal variations from 1992-1996 and 1999-2001. Journal of Geophysical Research: Atmospheres, 111(D20). doi:10.1029/2005JD006172

Lugwig, F. L., Liston, E. M., & Salas, L. J. (1983). Tracer techniques for estimating emissions from inaccessible ground level source. Atmospheric Environment, 17(11), 2167-2172.

MacDonald, L. (2015). Estimating emission rates of volatile organic compounds from oil and gas operations in the Piceance Basin, MS Thesis. Colorado State University.

McGaughey, G. R., Desai, N. R., Allen, D. T., Seila, R. L., Lonneman, W. A., Fraser, M. P., Harley, R. A., Pollack, A. K., Ivy, J. M.,Price, J. H. (2004). Analysis of motor vehicle emissions in the Houston tunnel during the Texas Air Quality Study 2000. Atmospheric Environment, 38(20), 3363-3372. doi:10.1016/j.atmosenv.2004.03.006

McKenzie, L. M., Witter, R. Z., Newman, L. S., & Adgate, J. L. (2012). Human health risk assessment of air emissions from development of unconventional natural gas resources. Science of the Total Environment(424), 79-87. doi:10.1016/j.scitotenv.2012.02.08

Miller, L., Xiaohong, X., Grgicak-Mannon, A., Brook, J., & Wheeler, A. (2012). Multi-season, multi-year concentrations and correlations amongst the BTEX group of VOCs in an urbanized industrial city. Atmospheric Environment, 61, 305-315. doi:10.1016/j.atmosenv.2012.07.041

Monster, J. G., Samuelsson, J., Kjeldsen, P., Rella, C. W., & Scheutz, C. (2014). Quanitifying methane emission from fugitive sources by combining tracer release and downwind measurements - A sensitivity analysis based on multiple field surveys. Waste Management, 34(8), 1416-1428. doi:10.1016/j.wasman.2014.03.025

Niobrara News (2014). WPX Energy Advancing Their Piceance Basin Niobrara Exploration Efforts. Retrieved from Niobrara News: Niobrara Shale Oil Play: http://www.niobraranews.net/drilling/wpx-energy-advancing-piceance-basin-niobrara-exploration-efforts/

Pétron, G., Frost, G., Miller, B. R., Hirsch, A. I., Montza, S. A., Karion, A., Trainer, M., Sweeney, C., Andrews, A. E., Miller, L., Kofler, J., Bar-llan, A., Dlugokencky, E. J., Patrick, L., Moore Jr, C. T., Ryerson, T. B., Sisso, C., Kolodzey, W., Lang, P. M.,

Conwat, T., Novelli, P., Masarie, K., Hall, B., Guenther, D., Miller, J., Welsh, D., Wolfe, D., Neff, W., & Tans, P. (2012). Hydrocarbon emissions characterization in the Colorado Front Range. Journal of Geophysical Research, 117(D4), 2156-2202. doi:10.1029/2011JD016360

Pétron, G., Karion, A., Sweeney, C., Miller, B. R., Montzka, S. A., Frost, G. J., Trainer, M., Tans, P., Andrews, A., Kofler, J., Helmig, D., Guenther, D., Dlugokencky, E., Lang, P., Newberger, T., Wolter, S., Hall, B., Novelli, P., Brewer, A., Conley, S., Hardesty, M., Banta, R., White, A., Noone, D., Wolfe, D., & Schell, R. (2014). A new look at methane and nonmethane hydrocarnon emissions from oil and natural gas operations in the Colorado Denver-Julesburg Basin. Journal of Geophysical Research, 119(11), 6836-6852. doi:10.1002/2013JD021272

Reiche, N., Westerkamp, T., Lau, S., Borsdorf, H., Dietrich P., & Schütze C. (2014). Comparative study to evaluate three ground-based optical remote sensing techniques under field conditions by a gas tracer experiment. Environ Earth Sci, 72, 1435-1441. doi: 0.1007/s12665-014-3312-8

Rich, A., Grover, J. P., & Sattler, M. L. (2014). An exploratory study of air emissions associated with shale gas development and production in the Barnett Shale. Journal of the Air& Waste Management Association, 64(1), 61-72. doi:10.1080/10962247.2013.832713

Roscioli, J. R., Yacovitch, T. I., Floerchinger, C., Mitchell, A. L., Tkacik, D. S., Subramanian, R., Martinez, D. M., Vaughn, T. L., Williams, L., Zimmerle, D.; Robinson, A. L., Herndon, S. C., & Marchese, A. J. (2015). Measurements of methane emissions from natural gas gathering facilities and processing plants: measurement methods. Atmospheric Measurement Techniques, 2017-2035. doi:10.5194/amt-8-2017-2015

Russo, R. S., Zhou, Y., White, M. L., Mao, H., Talbot, R., & Sive, B. C. (2010). Multi-year (2004-2008) record of nonmethane hydrocarbons and halocarbons in New England: seasonal variations and regional sources. Atmospheric Chemistry and Physics, 10(10), 4909-4929. doi:10.5194/acp-10-4909-2010

Sanchez, M., Karnae, S., & John, K. (2008). Source characterization of volatile organic compounds affecting the air quality in a urban area of South Texas. International Journal of Environmental Research and Public Health, 5(3), 130-138. doi:10.3390/ijerph5030130

Schauer, J. J., Kleeman, M. J., Cass, G. R., & Simoneit, B. R. (2002). Measurement of emissions from air pollution sources. 5. C1-C32 organic compounds from gasoline-powered motor vehicles. Environmental Science & Technology, 36(6), 1169-1180. doi:10.1021/es0108077

Schnell, R. S., Oltmans, S. J., Neely, R. R., Endres, M. S., Molenar, J. V., & White, A. B. (2009). Rapid photchemical production at high concentrations in a rural site during winter. Nature Geoscience, 2, 120-122. doi:10.1038/ngeo415

Simpson, I. J., Marrero, J. E., Batterman, S., Meinardi, S., Barletta, B., & Blake, D. R. (2013). Air quality in the Industrial Heartland of Alberta, Canada and potential impacts on human health. Atmospheric Environment, 81, 702-709. doi:10.1016/j.atmosenv.2013.09.017

Sive, B. C. (1999). Atmospheric nonmethane hydrocarbons: Analytical methods and estimated hydroxyl radical concentrations, PhD Dissertation. University of California, Irvine.

Subramanian, R., Williams, L. L., Vaughn, T. L., Zimmerle, D., Roscioli, J. R., Herndon, S. C., Yacovitvch, T. I., Floerchinger, C., Tkacik, D. S., Mitchell, A. L., Sullivan, M. R., Dallmann, T. R., & Robinson, A. L. (2015). Methan emissions from natural gas compressor stations in the transmission and storage sector: Measurements and coparisons with the EPA greenhouse reporting program protocol. Environmental Science & Technology. doi:10.1021/es5060258

Swarthout, R. F. (2014). Volatile organic compounds emissions from unconventional natural gas production: Source signatures and air quality impacts, PhD Dissertation. University of New Hampshire.

Swarthout, R. F., Russo, R. S., Zhou, Y., Hart, A. H., & Sive, B. C. (2013). Volatile organic compound distributions during the NACHTT campaign at the Boulder Atmospheric Observatory: Influence of urban and natural gas sources. Journal of Geophysical Research: Amospheres, 118(18), 10,614-10,637. doi:10.1002/jgrd.50722

Swarthout, R. F., Russo, R. S., Zhou, Y., Miller, B. M., Mitchell, B., Horsman, E., Lipsky, E., McCabe, D. C., Baum, E., & Sive, B. C. (2015). Impact of Marcellus Shale natural gas development in Southwest Pennsylvania on volatile organic compound emissions and regional air quality. Environmental Science & Technology, 49(5), 3175-3184. doi:10.1021/es504315f

Thakur, V. K., & Thakur, M. K. (2016). Handbook of Sustainable Polymers: Processing and Applications. Boca Raton, FL: Taylor & Francis Group.

Thompson, C. R., Hueber, J., & Helmig, D. (2014). Influence of oil and gas emissions on ambient non-methane hydrocarbons in residential areas of Northeastern Colorado. Elementa Science of the Anthropocene, 2. doi:10.12952/journal.elementa.000035#sthash.fakeJ33g.dpuf

Velasco, E., Lamb, B., Westberg, H., Allwine, E., Sosa, G., Arriaga-Colina, J. L., Jobson, B. T., Alexander, M. L., Prazeller, P., Knighton, W. B., Rodgers, T. M., Grutter, M., Herndon, S. C., Kolb, C. E., Zavala, M., deFoy, B., Volkamer, R., Molina, L. T., & Molina, M. J.

(2007). Distribution, magnitudes, reactivities, ratios and diurnal patterns of volatile organic compounds in the Valley of Mexico during the MCMA 2002 & 2003 field campaigns. Atmospheric Chemistry and Physics, 7, 329-353.

Vinciguerra, T., Yao, S., Dadzie, J., Chittams, A., Deskins, T., Ehrman, S., & Dickerson, R. R. (2015). Regional air quality impacts of hydraulic fracturing and shale natural gas activity: Evidence from abient VOC observations. Atmospheric Environment, 110, 144-150. doi:doi:10.1016/j.atmosenv.2015.03.056

Warneke, C., Geiger, F., Edwards, P. M., Dube, W., Petron, G., Kofler, J., Zahn, A.; Brown, S. S., Graus, M., Gilman, J. B., Lerner, B. M., Peischl, J., Ryerson, T. B., de Gouw, J. A., & Roberts, J. M. (2014). Volatile organic compound emissions from the oil and natural gas industry in the Utintah Basin, Utah: oil and gas well pad emissions compared to ambient air composition. Atmospheric Chemistry and Physics, 14, 10977-10988. doi:10.5194/acp-14-10977-2014

Weiner, C. (2014). Oil and Gas Development in Colorado - 10.639. Retrieved from Colorado State University Extension - Oil and Gas Development in Colorado: http://extension.colostate.edu/docs/pubs/consumer/10639.pdf

Weissermel, K., & Hans-Jurgen, A. (2003). Industrial Organic Chemistry (Vol. IV). Weinheim: Wiley-VCH Verlag GmbH & Co.

Western Energy Alliance (WEA). (2015). Oil and Natural Gas: Why Western Oil & Natural Gas? Retrieved from http://www.westernenergyalliance.org/why-western-oil-natural-gas

Zhou, Y., Shively, D., Mao, H., Russo, R. S., Pape, B., Mower, R. N., Talbot, R., & Sive, B. C. (2010). Air toxic emissions from snowmobiles in Yellowstone National Park. Environmental Science and Technology, 44(1), 222-228. doi:10.1021/es9018578

APPENDIX A

TRACER RELEASE SYSTEM

In order to perform the tracer ratio method in the field, we had to release a tracer gas from a tracer release system co-located with the emission source of VOCs on the well pad. The tracer gas (acetylene) was released at a controlled release rate that was used to calculate the emission rates of the other VOCs discussed in this thesis. Figure A.1. shows a schematic of the tracer release system. Once acetylene is diluted with ambient air by the tracer release system, it is released from a perforated manifold. The manifold is shown in Figure A.2.

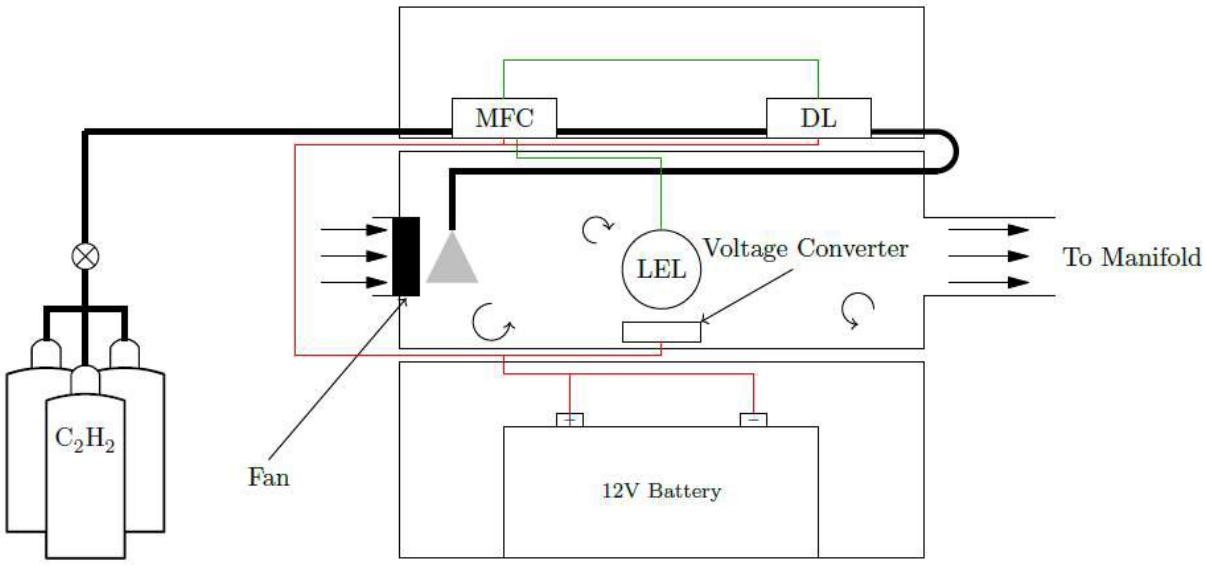

Figure A.1. Schematic of the tracer release system from MacDonald [2015]. Acetylene tanks are attached to a Mass Flow Controller (MFC). Acetylene flowed into a mixing box with a Lower Explosive Limit (LEL) detector. The acetylene is then directed to a manifold (Figure A.2.). A Data Logger (DL) powered by a 12 V battery is used to collect data.

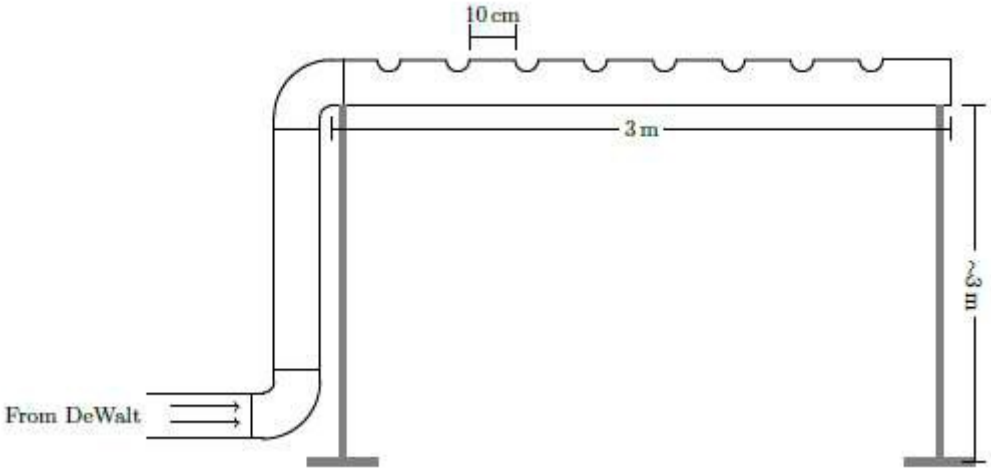

Figure A.2. Schematic of the perforated manifold [MacDonald, 2015]

APPENDIX B

COMPARE CANISTER ACETYLENE TO PICARRO ACETYLENE

The acetylene measured by the Picarro instrument was used as a tracer for methane emissions and the acetylene measured in the canisters was a tracer for VOC emissions. For the VOC-to-methane ratios and correlations only canisters co-located with the Picarro instrument were used. Figure B.1. shows all the concentrations of acetylene measured by the GC plotted against all the concentrations of acetylene measured by the Picarro instrument. A 1:1 dashed line is plotted in black. Each dot represents the acetylene concentration measured by the Picarro instrument averaged over the three minute canister sampling period and the acetylene measured in the corresponding canister sample. This comparison was applied to all co-located canisters, which are called “Tahoe Up” and “Tahoe Down.” The coral line represents the slope of the canisters positioned “Tahoe Up” and the green line represents the slope of the canisters positioned “Tahoe Down.” The specific location of these canisters with respect to the Picarro instrument is discussed in Section 2.1.

This comparison was used to select the VOC data used in the VOC-to-methane ratios and correlations. The VOC canister data were included in the analysis of VOC-to-methane ratios and correlations if the absolute difference between the canister acetylene and Picarro acetylene was less than 70% of the mean of these values. Some difference is expected between the canister and the Picarro measured acetylene concentrations because the inlets were not exactly co-located, but the purpose of this selection criterion was to eliminate cases when the samplers were sampling drastically different plume concentrations. Figure B.2. shows the canisters used for the analysis of VOC-to-methane ratios and correlations after data selection.

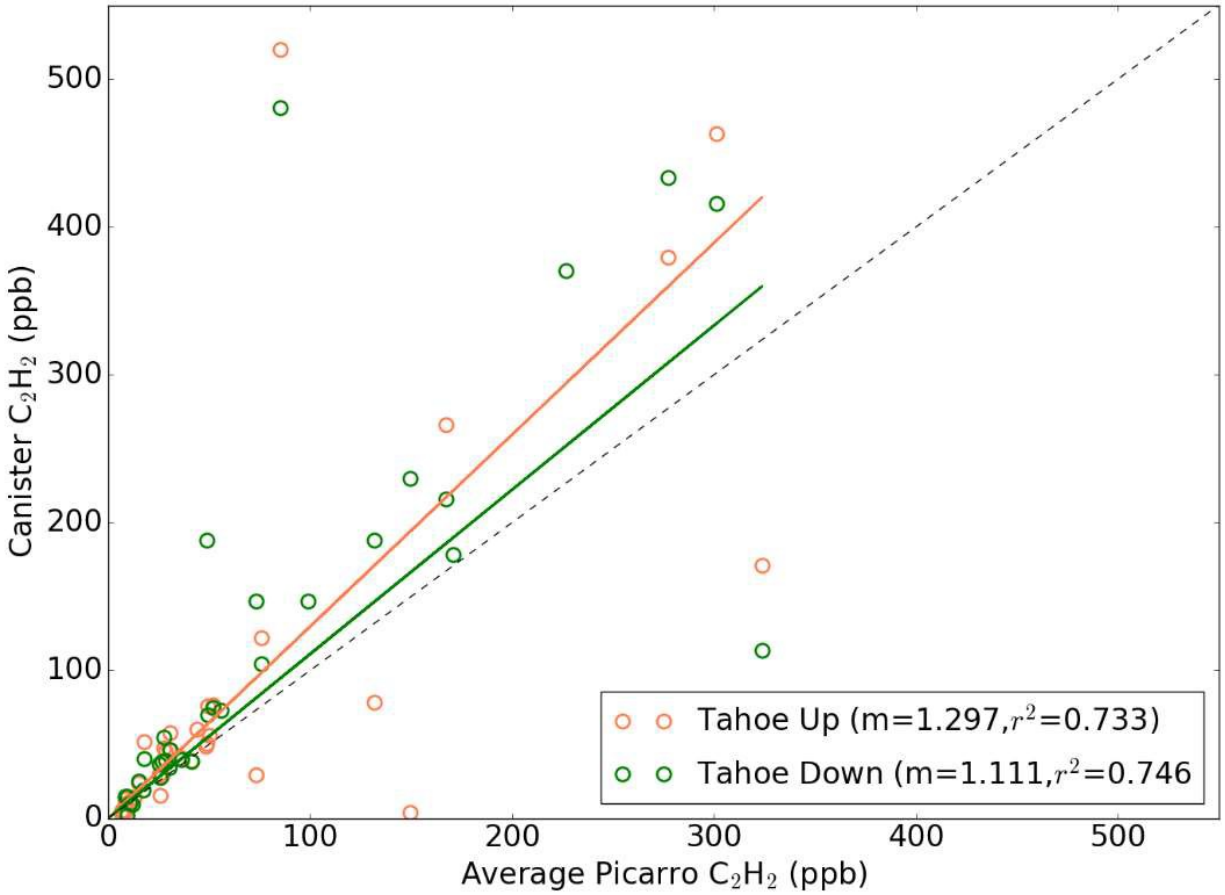

Figure B.1. Comparison of the acetylene concentrations measured in the canisters by the GC with the acetylene concentrations measured by the Picarro instrument before data selection. The acetylene concentrations measured by the Picarro instrument are averaged over the three minute canister sampling period.

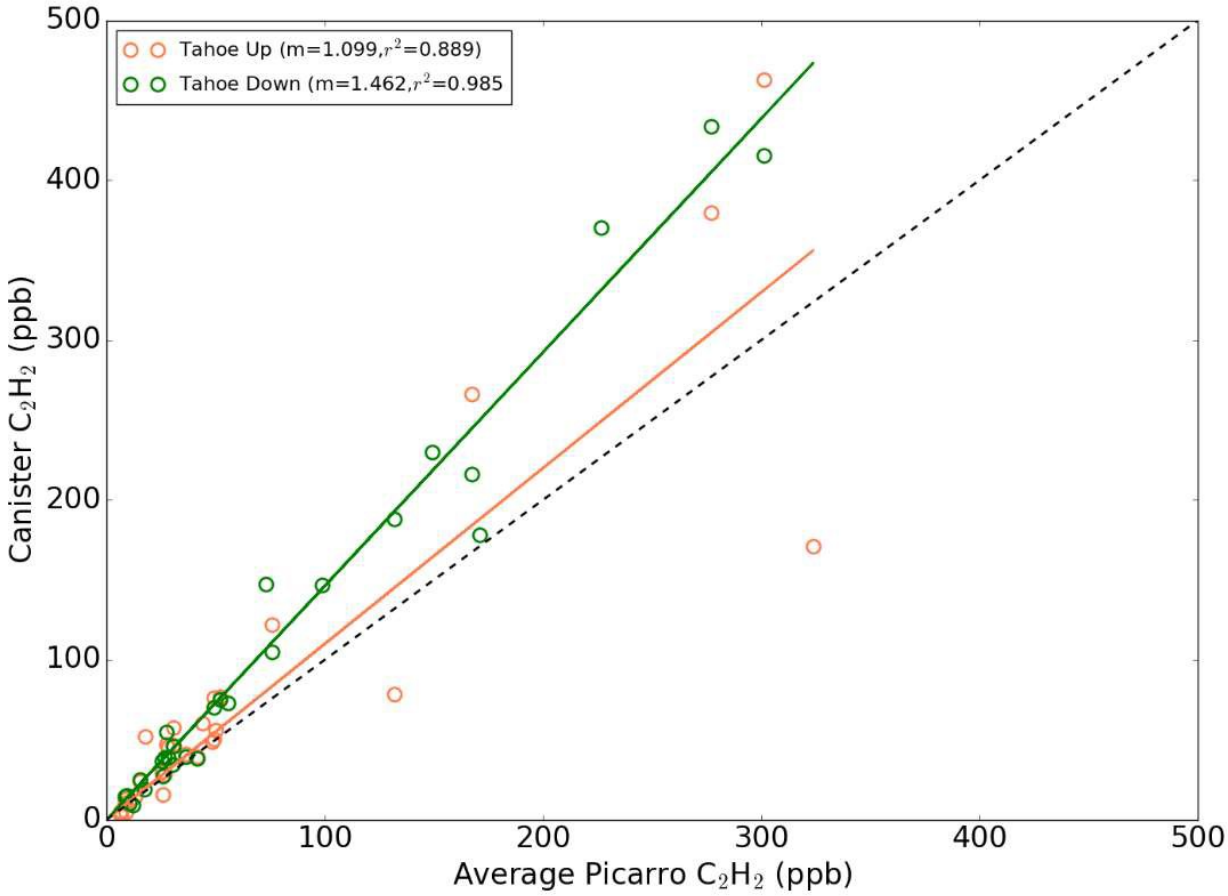

Figure B.2. Comparison of the acetylene concentrations measured in the canisters by the GC with the acetylene concentrations measured by the Picarro instrument after data selection. The acetylene concentrations measured by the Picarro instrument are averaged over the three minute canister sampling period.

APPENDIX C

VOC INFORMATION

Tables C.1. – C.3. includes the chemical formula and relevant sources for the VOCs measured on the GC analytical systems.

Table C.1. List of alkane compounds measured by the GC analytical systems. The chemical formula and sources are also listed.

VOC	Chemical Formula	Sources
ethane	C_2H_6	Main constituent of natural gas [Thompson et al., 2014].
propane	C_3H_8	Oil and natural gas production. Natural gas processing and crude oil refinement [Thompson et al., 2014].
i-butane	C_4H_{10}	Blending component with petroleum and natural gas [EIA, 2014]. Evaporation and combustion of fossil fuels [Lee et al., 2006].
n-butane		Blending component with petroleum and natural gas [EIA, 2014]. Natural gas and automobiles [Thompson et al., 2014]. Evaporation and combustion of fossil fuels [Lee et al., 2006].
i-pentane	C_5H_{12}	Vehicle exhaust. Oil and natural gas emissions [Gilman et al., 2013]
n-pentane		Combustion of gasoline and diesel fueled engines [Howard, 1993].
n-hexane	C_6H_{14}	Refining of crude oil. Diesel, gasoline vapor, natural gas, petroleum manufacturing [Graedel, 1978]
n-heptane	C_7H_{16}	Vehicle exhaust, gasoline vapor, natural gas, solvent, petroleum manufacturing [Graedel, 1978]
n-octane	C_8H_{18}	Major component of gasoline and vehicle emissions [Schauer et al., 2002]
n-nonane	C_9H_{20}	Vehicle emissions, biomass/coal combustion, diesel, gasoline vapor, petroleum manufacturing [Graedel et al., 1986].
n-decane	$C_{10}H_{22}$	Paraffin fraction of crude oil and natural gas [Howard, 1993]. Flare emissions [Sanchez et al., 2008]
2,4-dimethylpentane	C_7H_{16}	Vehicle emissions and gasoline vapor [Graedel, 1978]

2,3-dimethylpentane	C_7H_{16}	Vehicle emissions, gasoline vapor, and natural gas [Graedel, 1978]
2,2,4-trimethylpentane	C_8H_{18}	Vehicle emissions, gasoline vapor, and natural gas [Graedel, 1978]
2,3,4-trimethylpentane		Vehicle emissions and gasoline vapor [Graedel, 1978]
2-methylhexane	C_7H_{16}	Vehicle emissions [Graedel, 1978]
3-methylhexane		Vehicle emissions, gasoline vapor, natural gas [Graedel, 1978]
2-methylheptane	C_8H_{18}	Vehicle emissions, gasoline vapor, natural gas, petroleum manufacturing [Graedel et al., 1986]
3-methylheptane		Vehicle emissions, gasoline vapor [Graedel et al., 1986]
cyclohexane	C_6H_{12}	Component of crude oil [Berezin et al., 1966]. Natural gas emissions [Sanchez et al., 2008]
methylcyclohexane	C_7H_{14}	Component of natural gas [GuoYi et al., 2008]
cyclopentane	C_5H_{10}	Natural gas, petroleum manufacturing, gasoline vapor, and vehicle emissions [Graedel, 1978]

Table C.2. List of alkene compounds measured on the GC analytical systems. The chemical formula and sources are listed.

VOC	Chemical Formula	Sources
ethene	C_2H_4	Natural gas emissions [Sanchez et al., 2008]. Petroleum combustion [Borbon et al., 2001].
propene	C_3H_6	Refinery processes, liquefied petroleum gas, motor gasoline [Intratec, 2012]
t-2-butene	C_4H_8	Byproducts of refining motor fuel and cracking processes of butane or gas oil for gasoline production [Weissermel, 2003]
1-butene		Byproducts of refining motor fuel and cracking processes of butane or gas oil for gasoline production [Weissermel, 2003]
i-butene		Byproducts of refining motor fuel and cracking processes of butane or gas oil for gasoline production [Weissermel, 2003]
c-2-butene		Byproducts of refining motor fuel and cracking processes of butane or gas oil for gasoline production [Weissermel, 2003]
isoprene	C_5H_8	Vehicle exhausts. Petroleum fueled and diesel car exhausts [Borbon et al., 2001]
t-2-pentene	C_5H_{10}	Flare emissions [Sanchez et al., 2008]
1-pentene		Flare emissions [Sanchez et al., 2008]
cis-2-pentene		Flare emissions [Sanchez et al, 2008]

Table C.3. List of aromatic compounds measured on the GC analytical systems. The chemical formula and sources are listed

VOC	Chemical Formula	Sources
benzene	C_6H_6	Gasoline and automobile exhaust [Khoder et al., 2007]
toluene	C_7H_8	Crude oil from gasoline production [EPA, 1994]. Gasoline evaporation [Ho et al., 2004]
ethylbenzene	C_8H_{10}	Vehicle exhaust [Miller et al., 2012]. Diesel gasoline vapor [Graedel et al., 1986]

m+p-xylene	C_8H_{10}	Vehicle exhaust [Khoder et al., 2006]. Gasoline vapors [Graedel et al., 1986]
o-xylene		Petroleum and constituent of smoke from many combustion sources [EPA ,1994]
styrene	C_8H_8	Automobile exhaust, stack emissions from waste incineration [Howard, 1989]
n-propylbenzene	C_9H_{12}	Engine combustion fuel evaporation, diesel fuel, and kerosene [Daguat et al., 2002]
isopropylbenzene		Constituent of crude oil, petroleum refining, evaporation of petroleum products [EPA, 2015c]
1,3,5-trimethylbenzene		Traffic emissions and fuel evaporation [Khoder et al., 2007]. Flare emissions [Sanchez et al., 2008]
1,2,3-trimethylbenzene		Traffic emissions and fuel evaporation [Khoder et al., 2007]
1,2,4-trimethylbenzene		Traffic emissions and fuel evaporation [Ho et al., 2004]
1,3-diethylbenzene	$C_{10}H_{14}$	Component of gasoline, combustion engines, wastewater from oil refineries [Howard, 1997]
1,4-diethylbenzene		Component of gasoline, combustion engines, wastewater from oil refineries [Howard, 1997]
2-ethyltoluene	C_9H_{12}	Automobile emissions and gasoline vapor [Graedel et al.,1986]
3-ethyltoluene		Automobile emissions and gasoline vapor [Graedel et al., 1986]
4-ethyltoluene		Automobile emissions and gasoline vapors [Graedel et al., 1986]

APPENDIX D

GC ANALYTICAL SYSTEMS CALIBRATION STATISTICS

Tables D.1. D.3. include calibration statistics for the VOCs measured on the five channel system. Tables D.4.-D.6. include calibration statistics for the VOCs measured on the GC-FID system.

Table D.1. Calibration statistics for alkane and cycloalkane compounds measured on five-channel GC.

VOC	Calibration r^2	LOD (ppb)	Slope of Calibration Curve (Area/ppb)	Standard range (ppbv)
ethane	0.999	0.105	137	0.4-3362
propane	0.999	0.020	1294	0.4-3203
i-butane	0.999	0.008	1682	0.4-3171
n-butane	0.999	0.010	1691	0.4-3140
cyclopentane	0.999	0.009	2097	0.4-3171
i-pentane	0.999	0.009	2110	0.4-3171
n-pentane	0.998	0.007	2039	0.4-3108
2,4-dimethylpentane	0.992	0.004	4049	0.4-3330
2,3-dimethylpentane	0.998	0.013	1049	0.4-3362
2,2,4-trimethylpentane	0.998	0.018	1196	0.4-3298
2,3,4-trimethylpentane	0.999	0.009	1174	0.4-3299
n-hexane	0.999	0.012	2467	0.4-3267
2-methylhexane	0.999	0.010	1079	0.4-3299
3-methylhexane	0.999	0.014	1064	0.4-3299
n-heptane	0.995	0.009	3164	0.4-3299
2-methylheptane	0.999	0.022	1165	0.4-3299
3-methylheptane	0.999	0.016	1177	0.4-3267
n-octane	0.999	0.016	1115	0.4-3299
n-nonane	0.999	0.010	1165	0.4-3235
n-decane	0.999	0.011	1131	0.4-3299
cyclohexane	0.999	0.015	895	0.4-3330
methylcyclohexane	0.999	0.019	1058	0.4-3299

Table D.2. Calibration statistics for alkene compounds and acetylene measured on five-channel GC.

VOC	Calibration r^2	LOD (ppbv)	Slope of Calibration Curve	Standard range (ppbv)
ethene	0.999	0.053	945	0.4-3362
propene	0.999	0.009	1179	0.4-3203
t-2-butene	0.999	0.018	1662	0.4-3108
1-butene	0.998	0.013	1651	0.4-3104
c-2-butene	0.999	0.022	1756	0.4-3362
isoprene	0.998	0.012	2202	0.4-3171
t-2-pentene	0.996	0.014	1809	0.4-3203
1-pentene	0.998	0.023	1909	0.4-3076
cis-2-pentene	0.998	0.012	1917	0.4-3330
acetylene	0.999	0.013	1186	0.4-3362

Table D.3. Calibration statistics for aromatic compounds measured on five-channel GC.

VOC	Calibration r^2	LOD (ppbv)	Slope of Calibration Curve	Standard range (ppbv)
benzene	0.999	0.010	903	0.4-3266
1,3,5-trimethylbenzene	0.999	0.012	1091	0.4-3235
1,2,3-trimethylbenzene	0.996	0.012	1074	0.4-3140
1,2,4-trimethylbenzene	0.997	0.0124	1077	0.4-3171
ethylbenzene	0.999	0.019	1066	0.4-3266
1,3-diethylbenzene	0.998	0.027	1136	0.4-3140
1,4-diethylbenzene	0.998	0.013	1133	0.4-3108
isopropylbenzene	0.999	0.011	1171	0.4-3140
n-propylbenzene	0.998	0.012	1157	0.4-3108
toluene	0.998	0.017	1028	0.4-3266
2-ethyltoluene	0.999	0.025	1128	0.4-3140
3-ethyltoluene	0.995	0.014	1084	0.4-3235
4-ethyltoluene	0.998	0.015	1102	0.4-3171
styrene	0.996	0.014	1008	0.4-3298
m+p-xylene	0.995	0.014	1754	0.4-3298
o-xylene	0.999	0.006	1087	0.4-3203

Table D.4. Calibration statistics for alkane and cycloalkane compounds measured on HP GC-FID.

VOC	Calibration r^2	LOD (ppbv)	Slope of Calibration Curve	Standard Range (ppb)
ethane	0.904	0.073	3493	1000
propane	0.999	0.069	10539	1000
i-butane	0.999	0.047	13871	1000
n-butane	0.999	0.049	13854	1000
cyclopentane	0.999	0.024	14406	1000
i-pentane	0.999	0.014	17651	1000
n-pentane	0.999	0.017	17411	1000
2,4-dimethylpentane	0.999	0.245	21116	1000
2,2,4-trimethylpentane	0.995	0.004	60829	1000
n-hexane	0.999	0.014	45754	1000
n-heptane	0.999	0.003	27050	1000
n-octane	0.997	0.012	35396	1000
cyclohexane	0.998	0.012	22689	1000

Table D.5. Calibration statistics for alkene compounds and acetylene measured on HP GC-FID.

VOC	Calibration r^2	LOD (ppbv)	Slope of Calibration Curve	Standard Range (ppb)
ethene	0.990	0.069	3393	1000
propene	0.999	0.012	19815	1000
t-2-butene	0.999	0.033	13459	1000
i-butene	0.999	0.022	17959	1000
isoprene	0.996	0.035	6705	1000
t-2-pentene	0.963	0.091	3446	1000
1-pentene	0.999	0.019	16456	1000
cis-2-pentene	0.978	0.015	22972	1000
acetylene	0.947	0.092	7022	1000

Table D.6. Calibration statistics for aromatic compounds measured on HP GC-FID.

VOC	Calibration r^2	LOD (ppbv)	Slope of Calibration Curve	Standard Range (ppb)
benzene	0.999	0.009	54563	1000
ethylbenzene	0.998	0.011	31507	1000
toluene	0.997	0.015	26110	1000
m+p-xylene	0.997	0.009	62256	1000
o-xylene	0.999	0.009	31822	1000

APPENDIX E

GC ANALYTICAL SYSTEMS INFORMATION

Tables E.1. - E.2. include the GC-FID instrumental and method parameters for analysis of VOCs from canister samples. Tables E.3. – E.4. include the five-channel GC instrumental and method parameters for the analysis of VOCs from canister samples.

Table E.1. GC-FID instrumental parameters for analysis of VOCs from canister samples.

	GC
Column Type	HP-Al_2O_3 PLOT
Column Length (m)	50
Column I.D. (mm)	0.32
Film Thickness (µm)	8
Detector Type	FID
Detector Temp (˚C)	250
Detector Gas	UHP H, zero air, UHP Helium

Table E.2. GC-FID method parameters for analysis of VOCs from canister samples

	GC
Initial Temp (˚C)	35
Initial Time (min)	4
Ramp 1 (˚C/min)	5
Final Temp (˚C)	190
Final Hold Time (min)	40
Carrier Gas	UHP Helium

Table E.3. Five-channel gas chromatograph instrumental parameters for analysis of VOCs from canister samples

	GC 1		GC 2		GC 3
Primary Analytes	C_2-C_7 NMHCs	C_6-C_{10} NMHCs	C_4-C_{10} NMHCs	C_1-C_2 halocarbons, C_1-C_5 alkyl nitrates	C_6-C_{10} NMHCs, C_1-C_2 halocarbons
Column Type	Al_2O_3/NaSO4 PLOT	(1) CP-PoraBond Q (2) Restek XTI-5	VF-1ms	OV-1701	OV-624
Column Length (m)	50	(1) 25 (2) 30	60	60	60
Column I.D. (mm)	0.53	0.25	0.32	0.25	0.25
Film Thickness (µm)	10	(1) 3 (2) 0.25	1	1	1.4
Detector Type	FID	FID	FID	ECD	MS
Detector Temp. (˚C)	250	250	250	250	250
Detector gas	N_2, UHP H, zero air	N_2, UHP H, zero air	N_2, UHP H, zero air	UHP N_2	

Table E.4. Five-channel gas chromatograph method parameters for analysis of VOCs from canister samples

	GC 1	GC 2	GC 3
Initial Temp (˚C)	40	40	40
Initial Time (min)	2	4	4
Ramp 1 (˚C/min)	15	5	9
Temp 2 (˚C)	135	60	-
Ramp 2 (˚C/min)	6	8.5	-
Final Temp (˚C)	200	190	220
Final Hold Time (min)	4	-	-
Carrier Gas	UHP Helium	UHP Helium	UHP Helium

APPENDIX F

EMISSION RATES FOR ALL VOCs

Equation F.1. was used to convert the VOC and methane emission rates from L min^{-1} to g s^{-1}.

Equation F.2. shows the unit conversion.

$$\frac{[\quad]}{[\quad]} \times \quad \times \quad \times \quad = \quad (\quad) \qquad \text{(F.1.)}$$

$$\frac{}{} \times \frac{}{} \times \frac{}{} \times \frac{}{} \times \frac{}{11} = \qquad \text{(F.2.)}$$

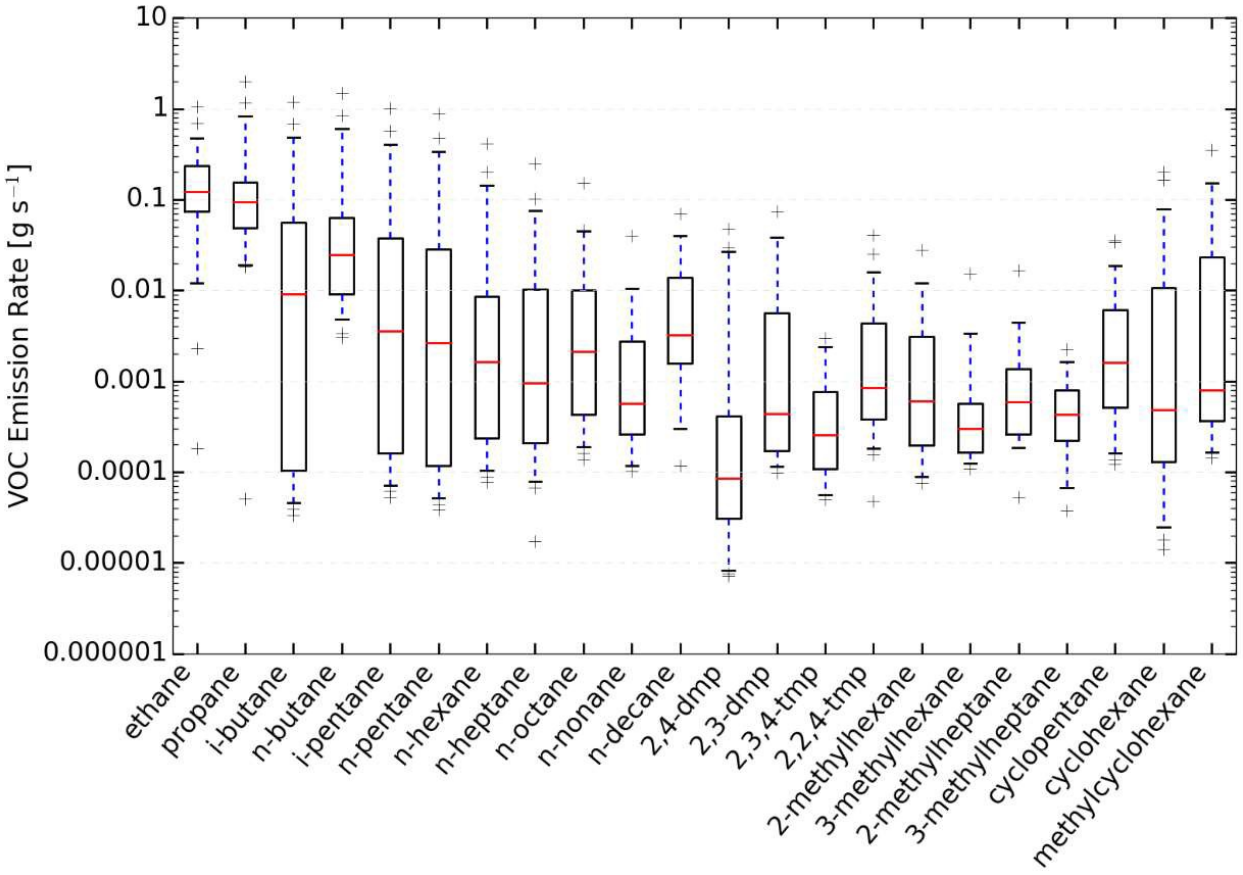

Figure F.1. Alkane emission rate distributions for drilling operations.

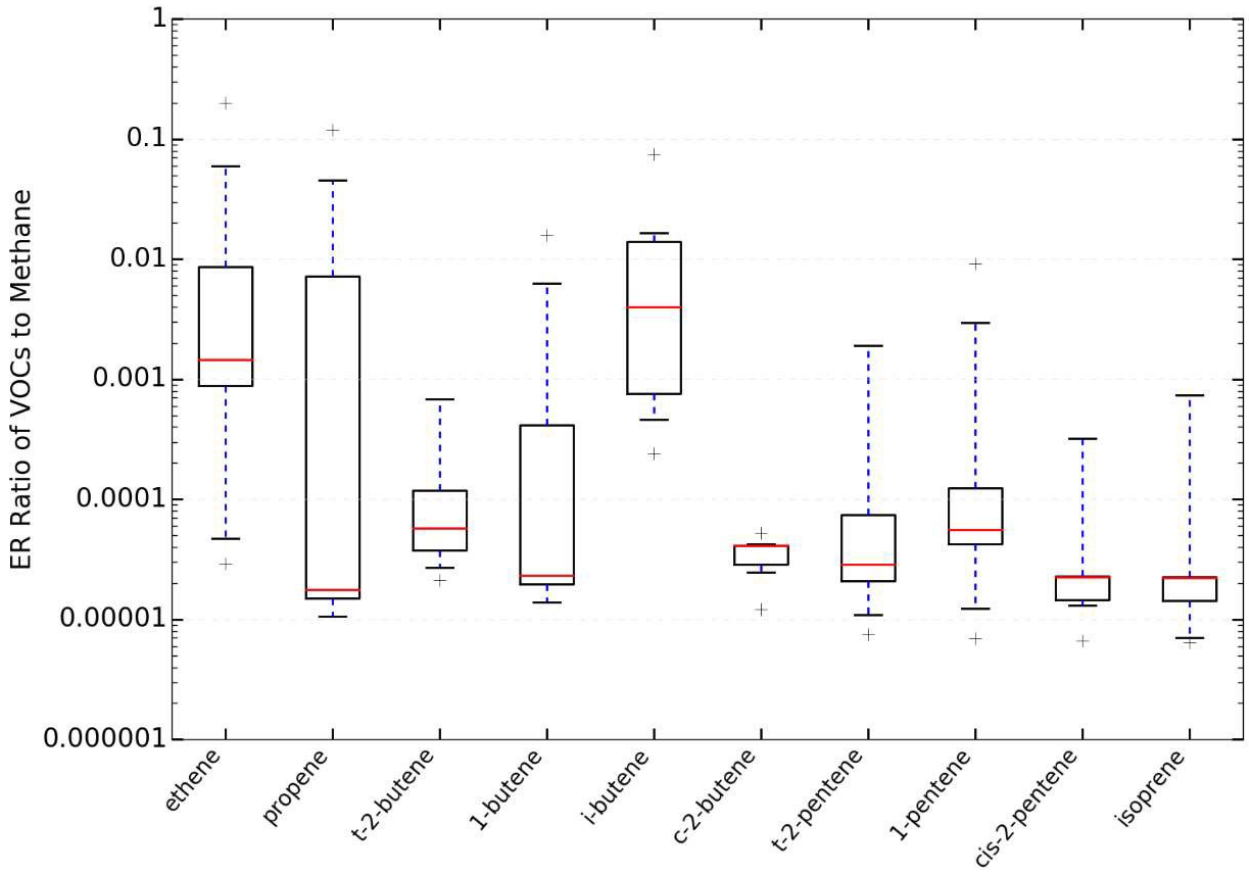

Figure F.2. Alkene emission rate distributions for drilling operations.

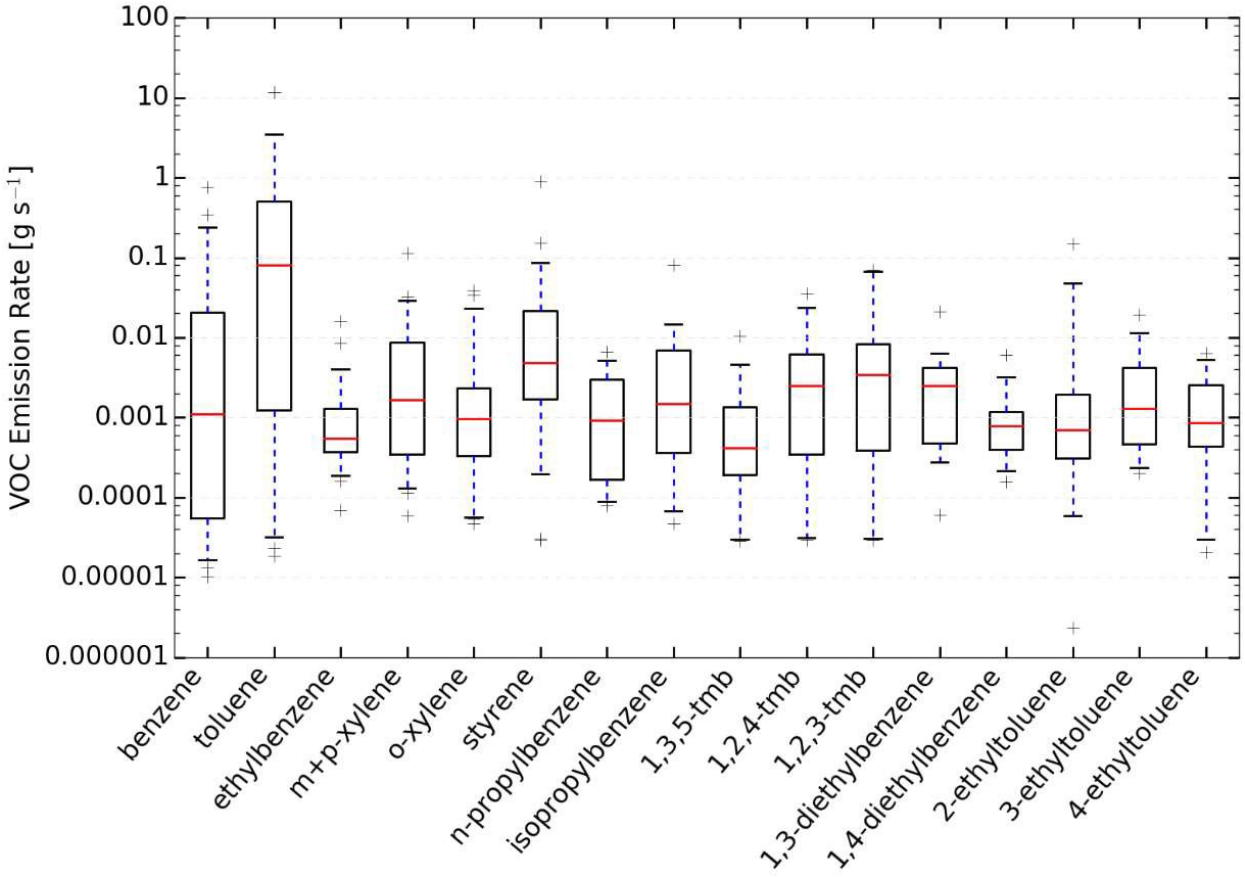

Figure F.3. Aromatic emission rate distributions for drilling operations.

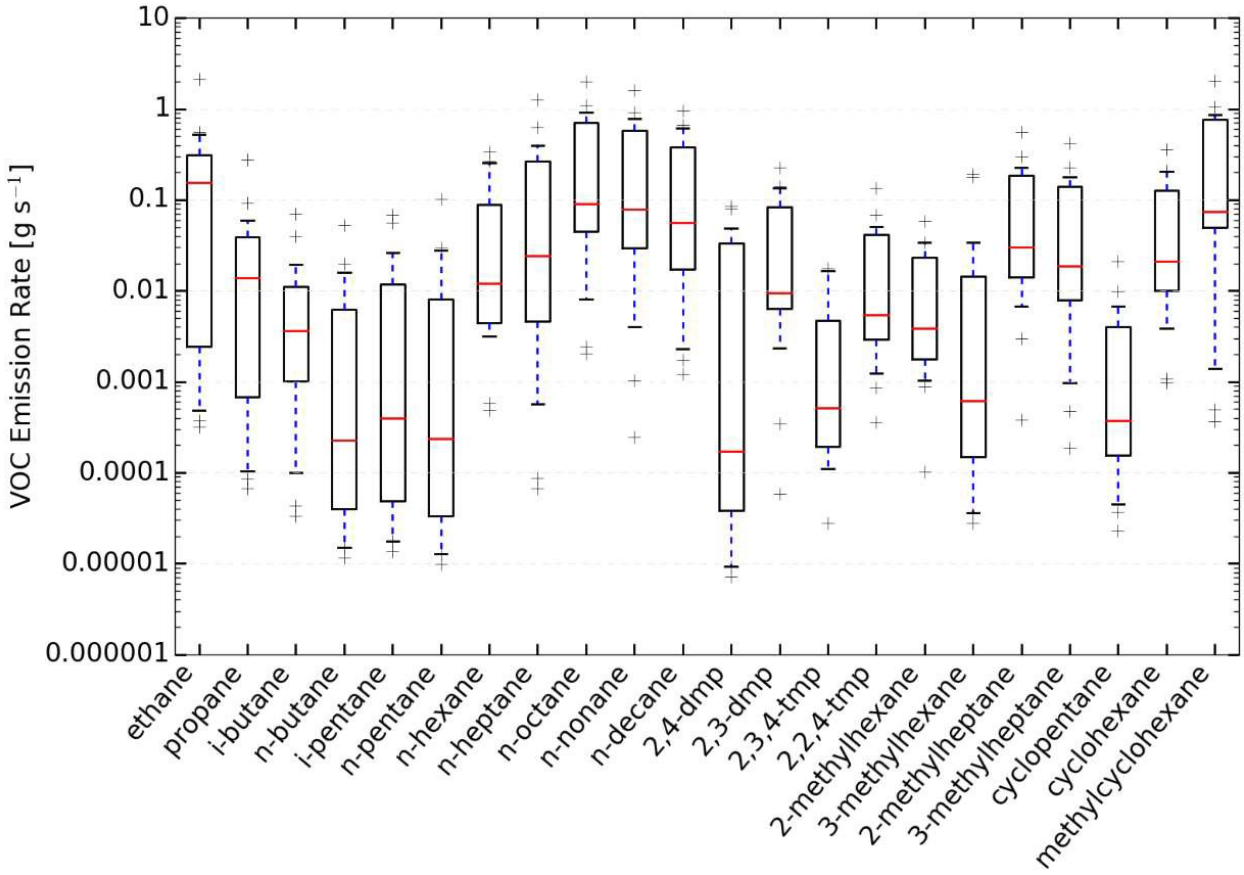

Figure F.4. Alkane emission rate distributions for fracking operations.

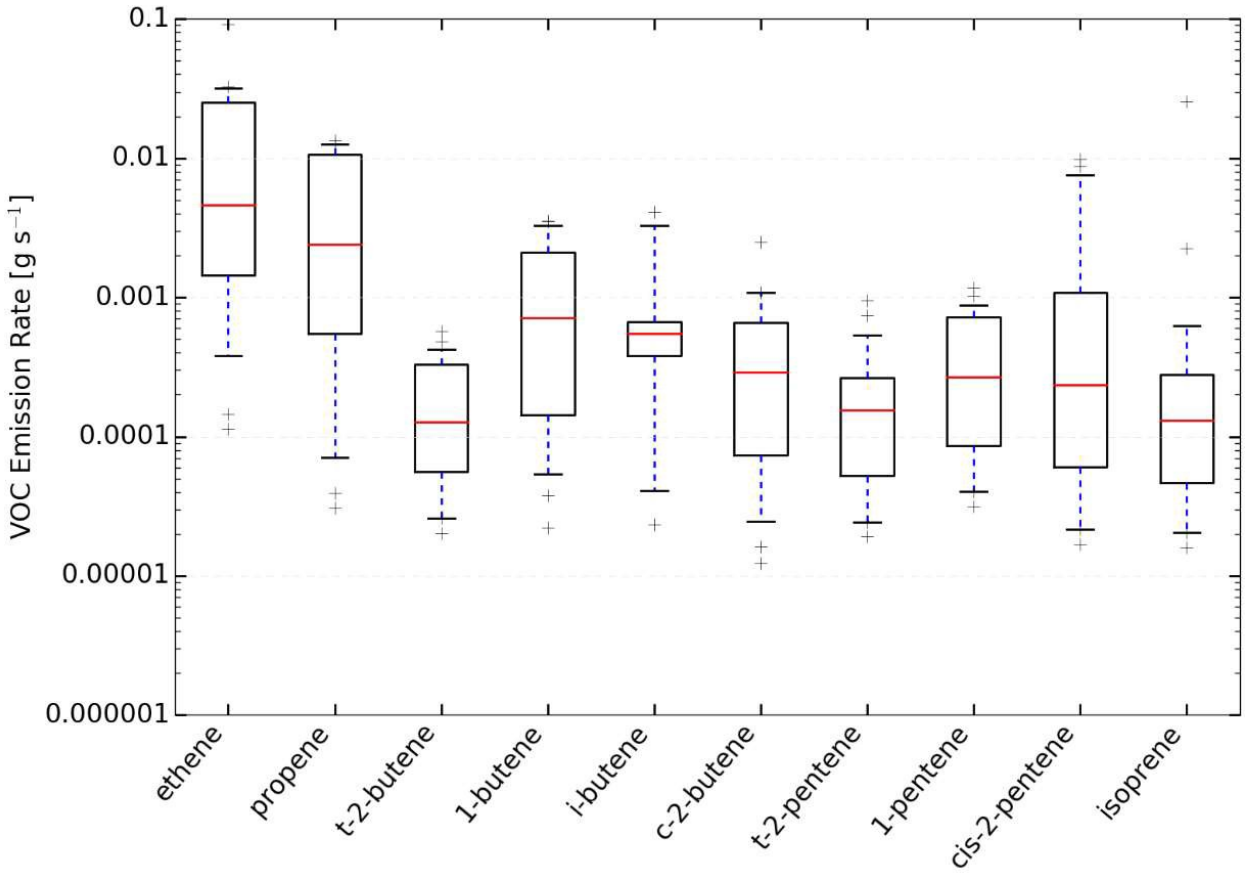

Figure F.5. Alkene emission rate distributions for fracking operations.

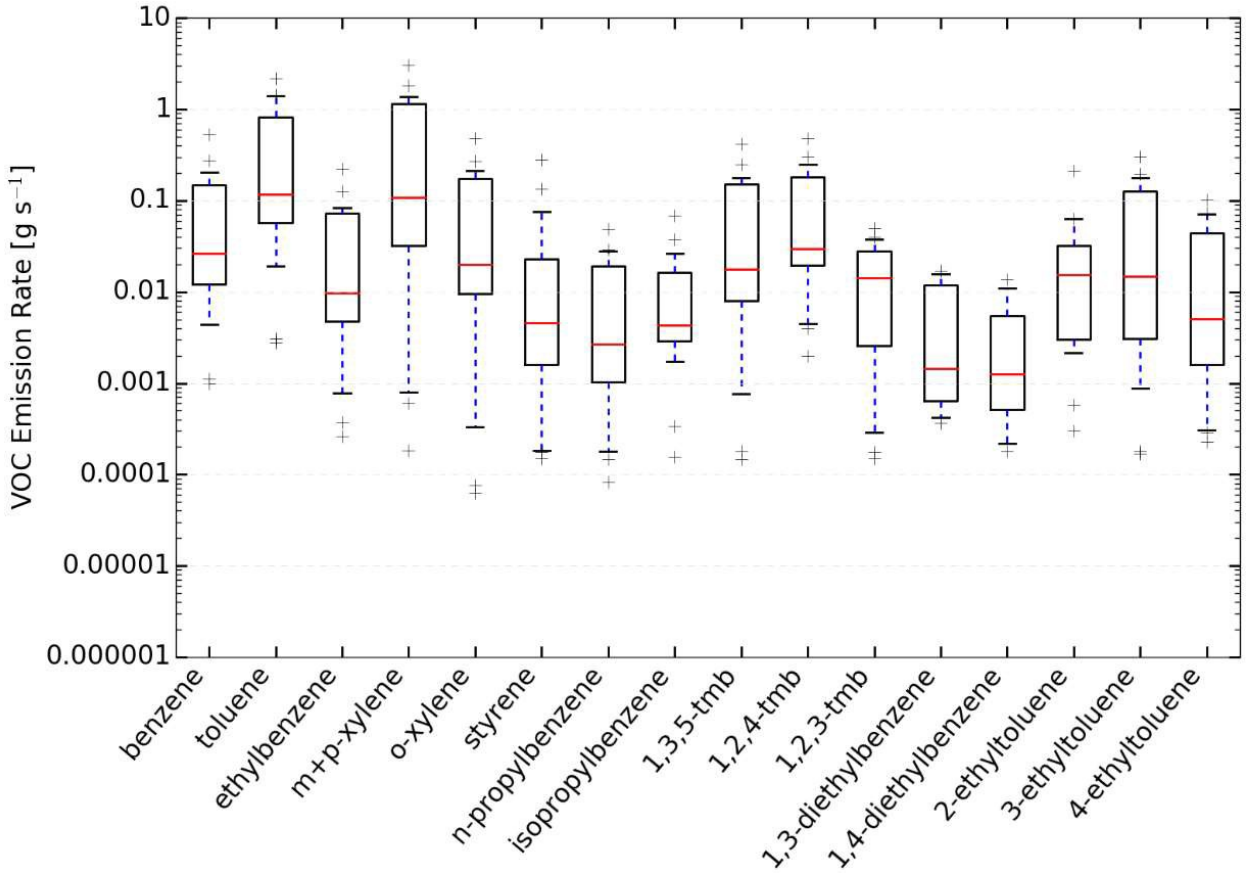

Figure F.6. Aromatic emission rate distributions for fracking operations.

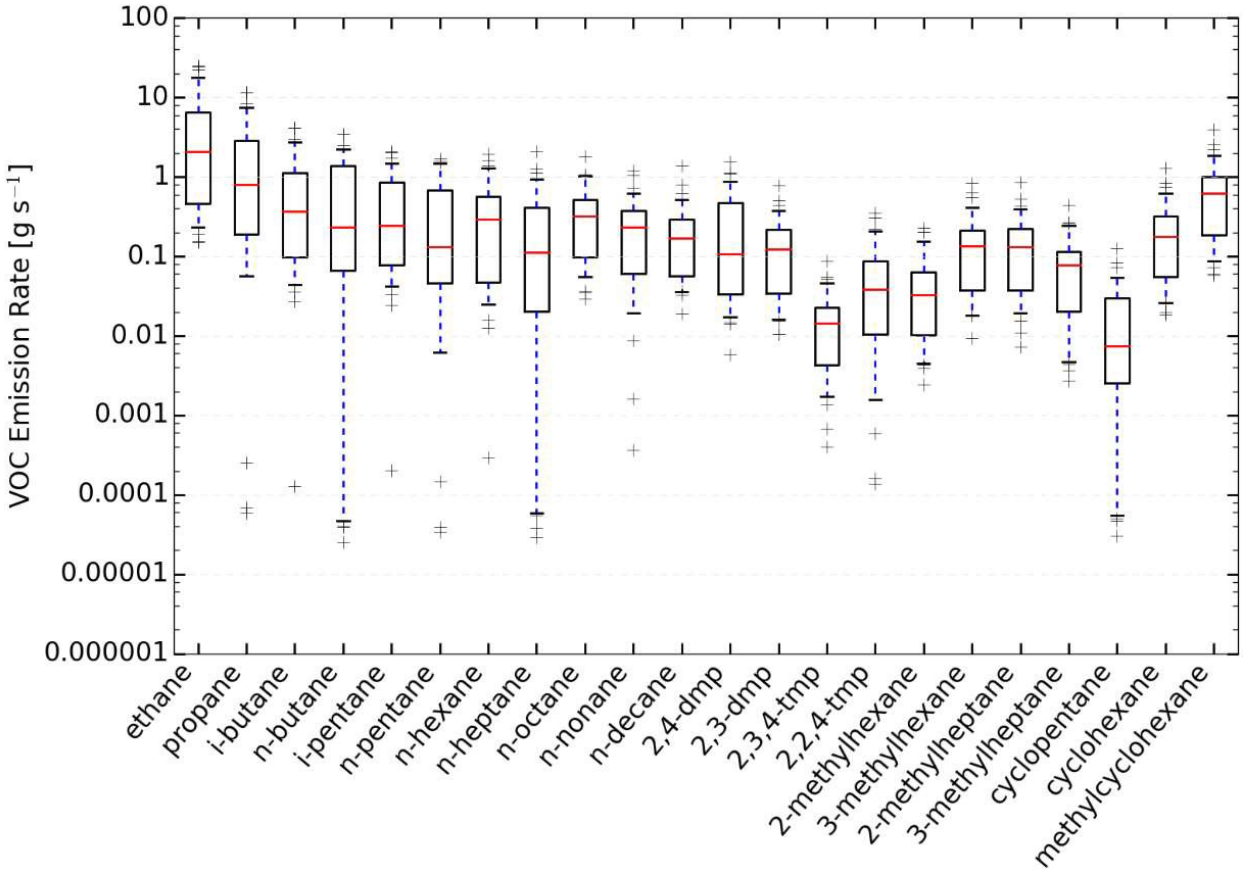

Figure F.7. Alkane emission rate distributions for flowback operations.

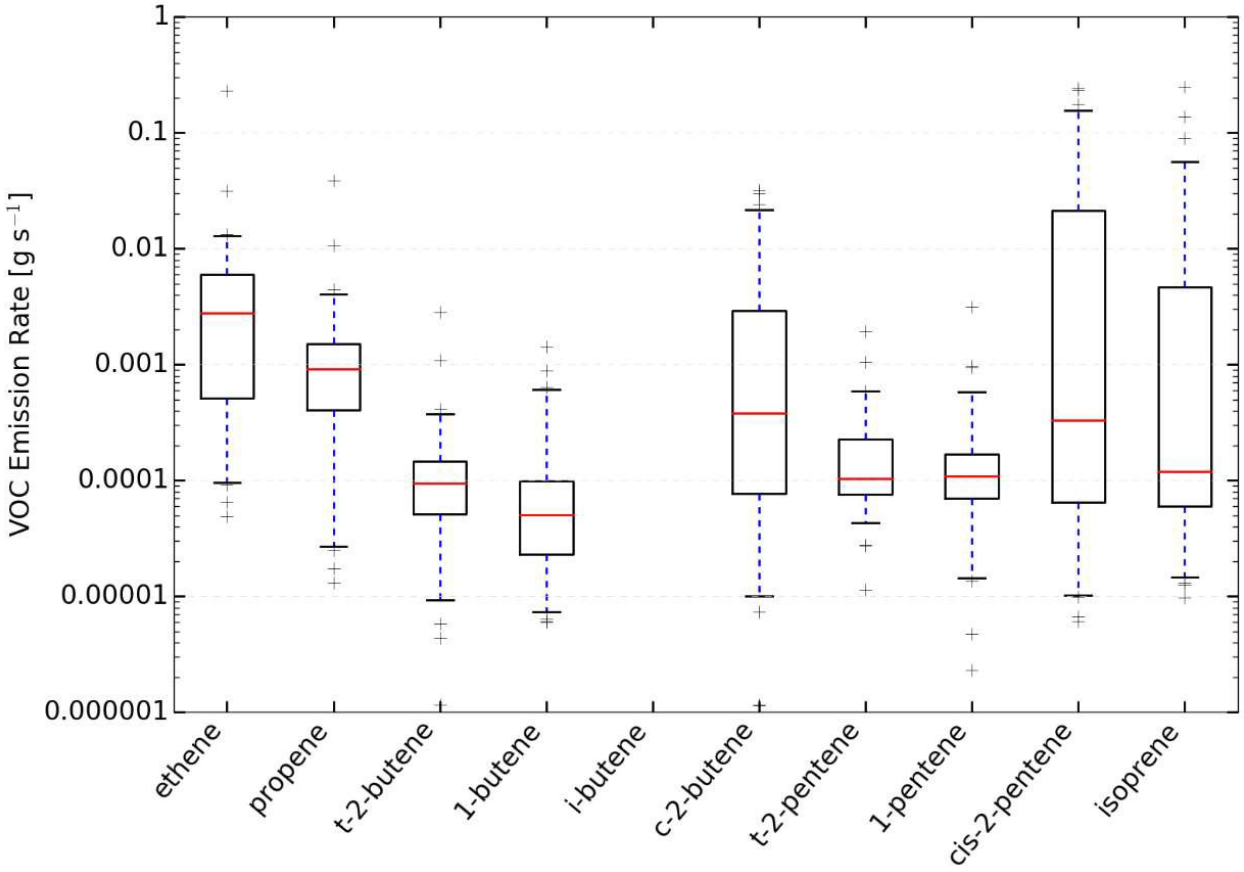

Figure F.8. Alkene emission rate distributions for flowback operations.

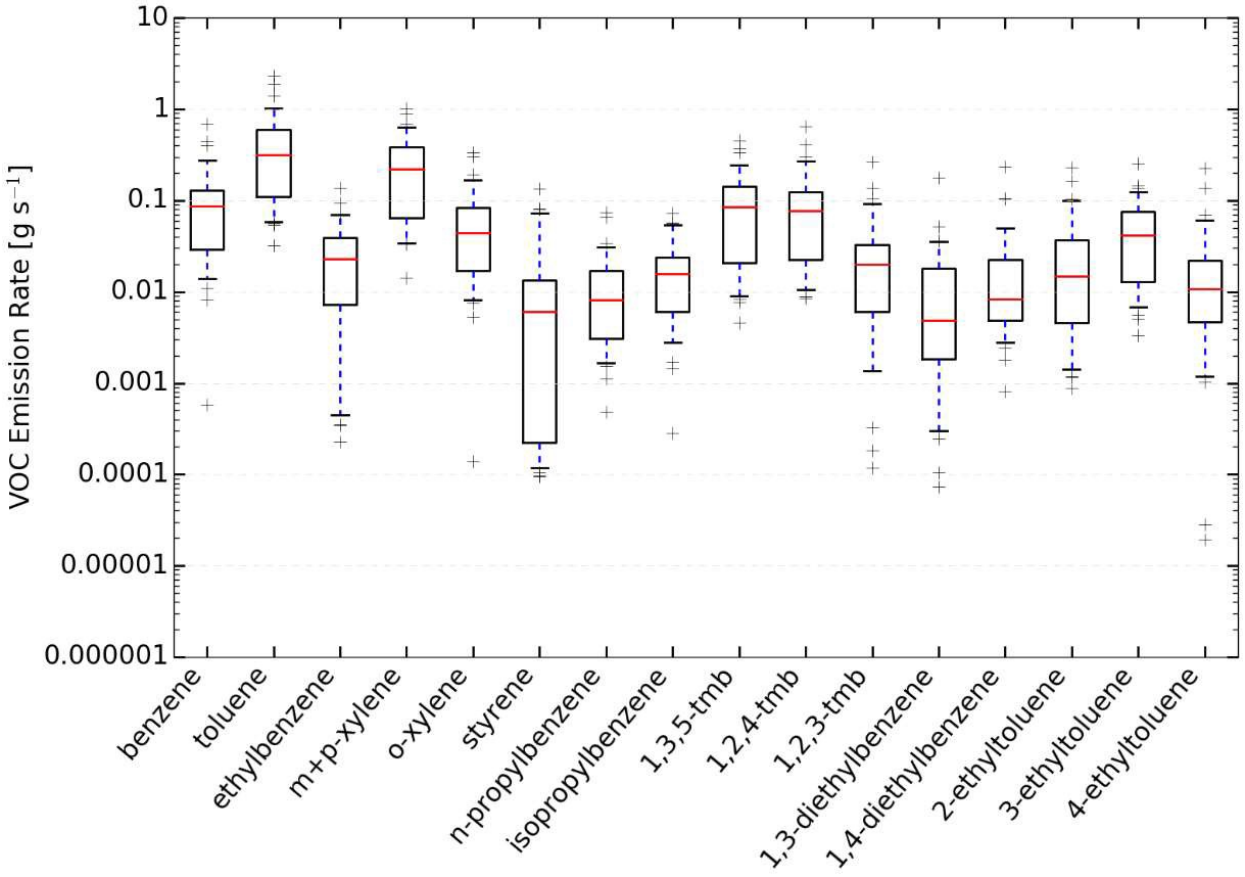

Figure F.9. Aromatic emission rate distributions for flowback operations.

APPENDIX G

ALL VOC EMISSION RATE CORRELATION MATRICES

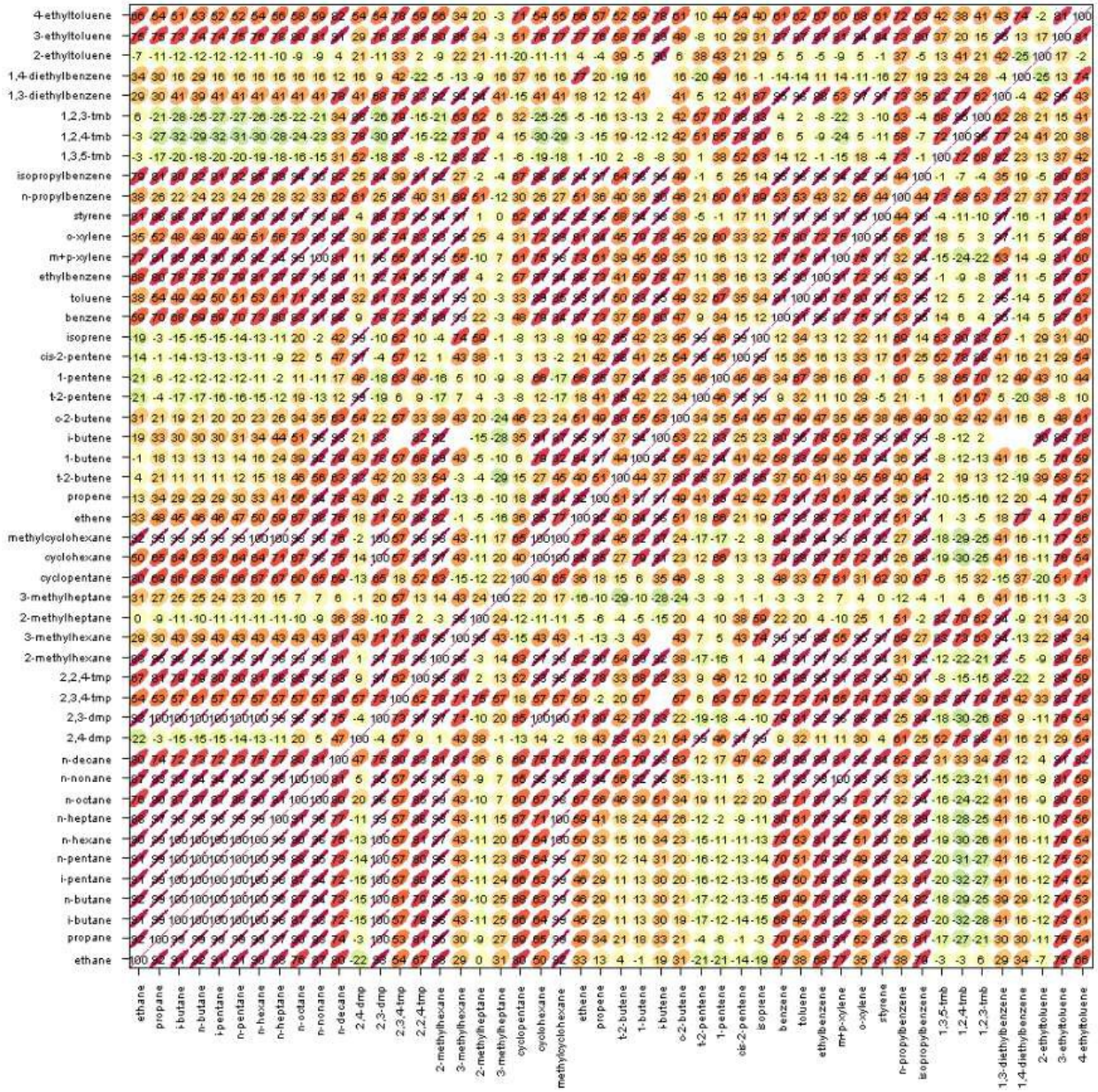

Figure G.1. Correlation matrix of VOC emission rates during drilling operations.

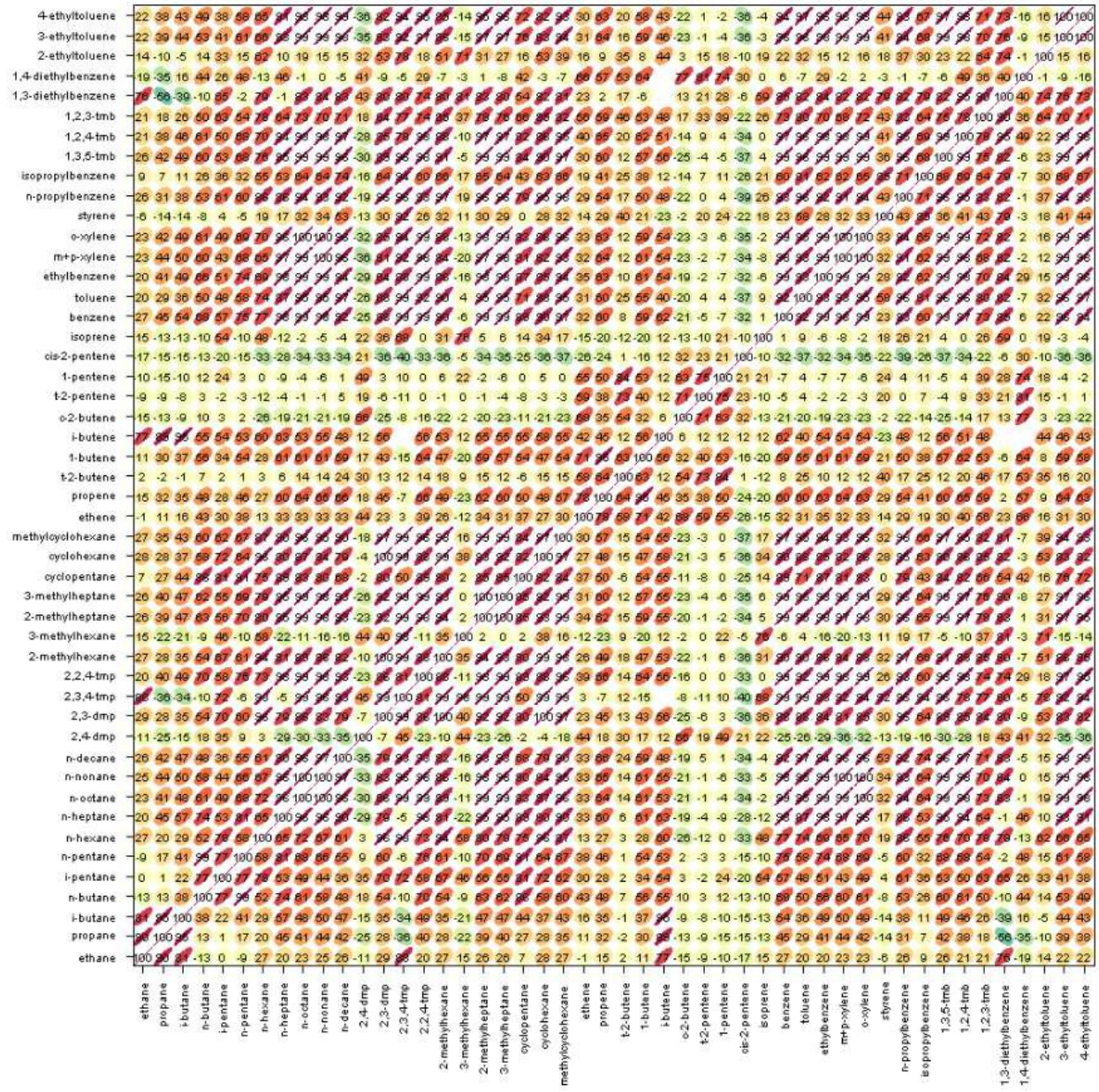

Figure G.2. Correlation matrix of VOC emission rates during fracking operations.

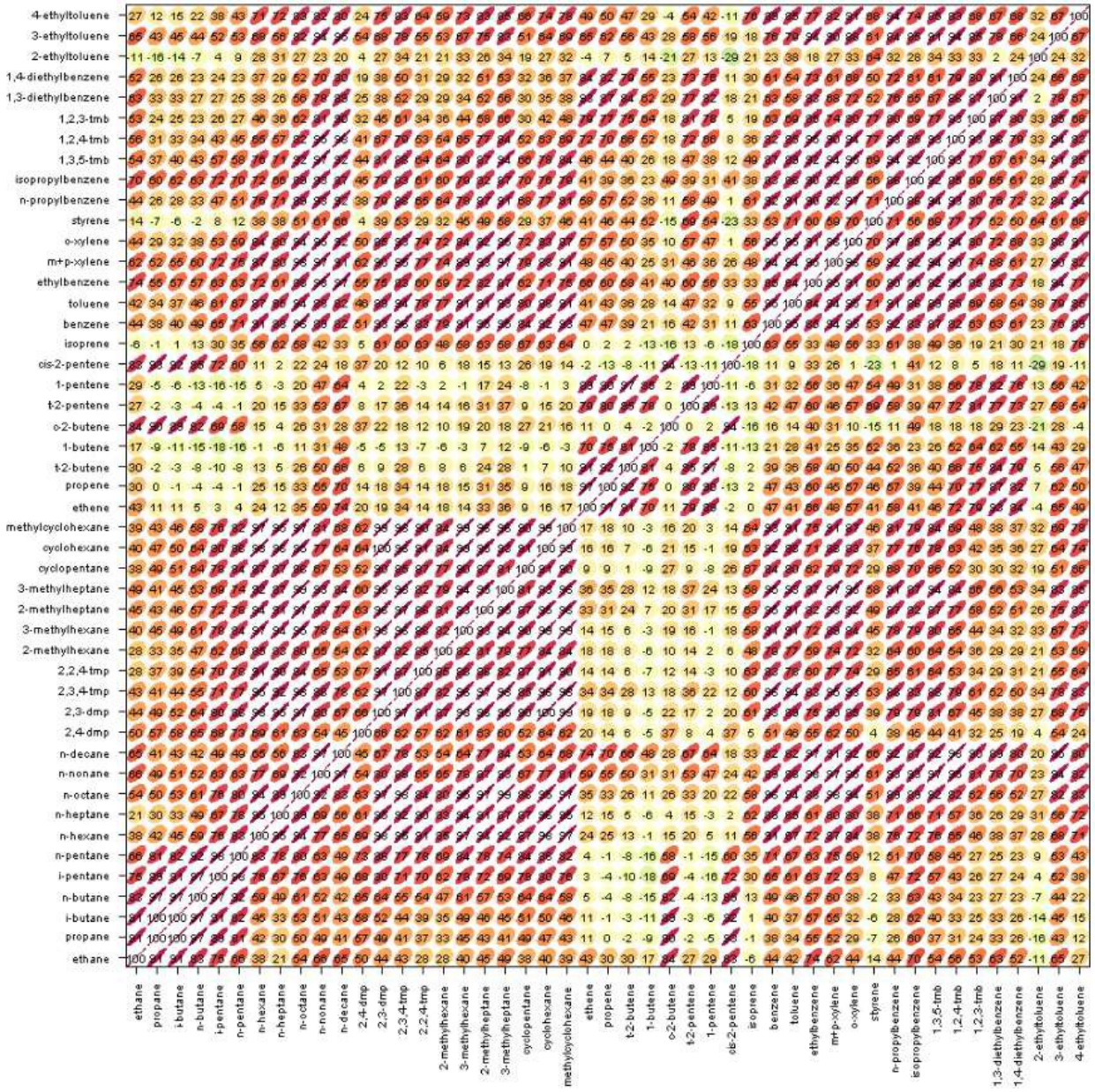

Figure G.3. Correlation matrix of VOC emission rates during flowback operations.

APPENDIX H

EMISSION RATIOS FOR ALL VOCS

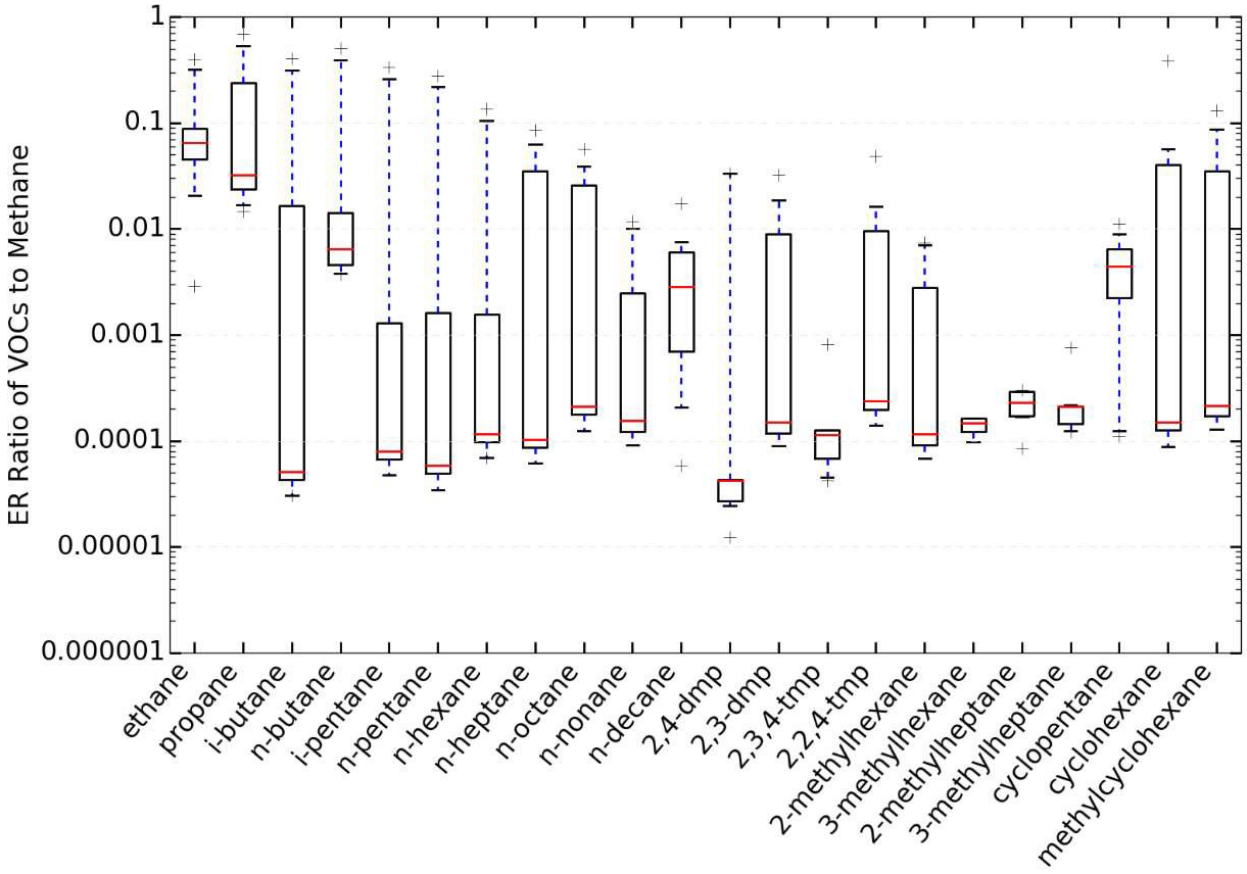

Figure H.1. Alkane emission rate ratio distributions for drilling operations.

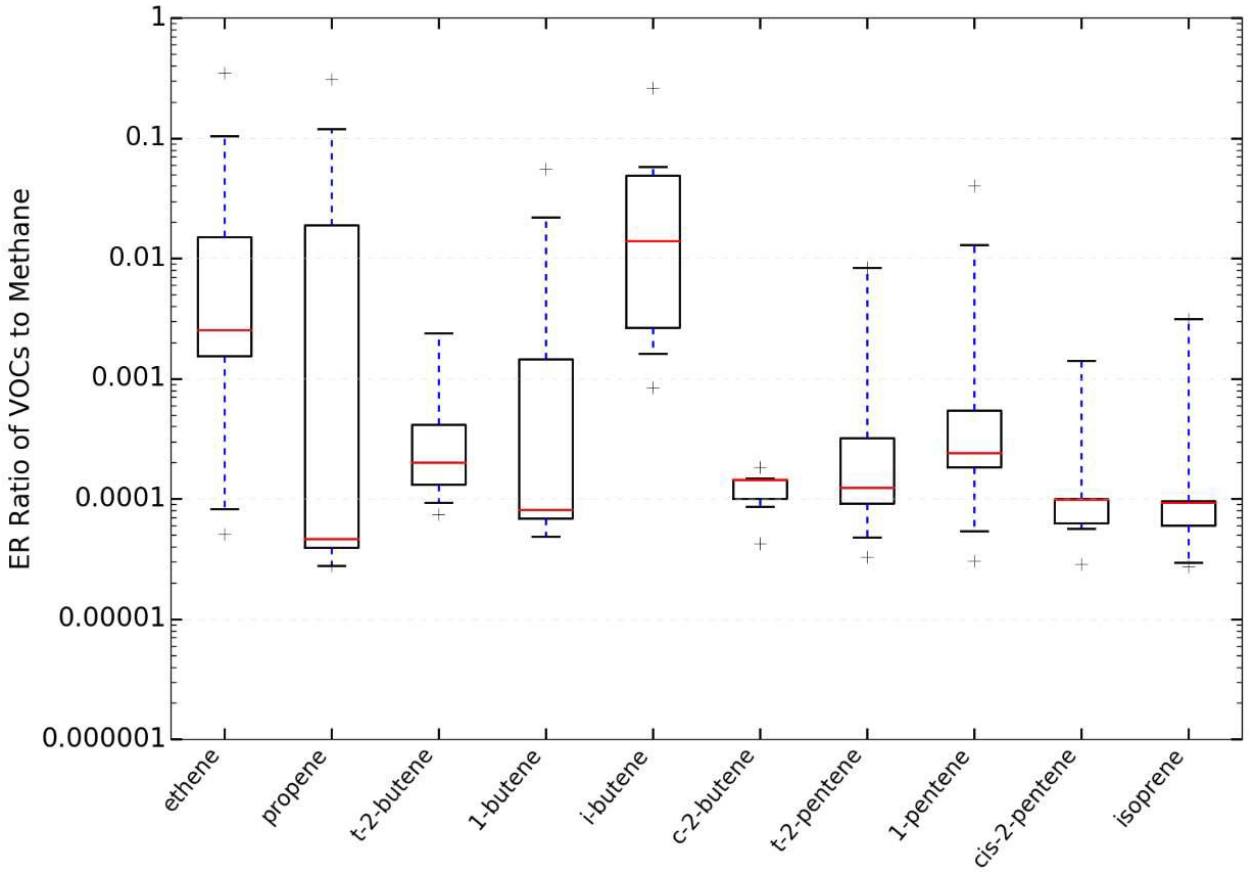

Figure H.2. Alkene emission rate ratio distributions for drilling operations.

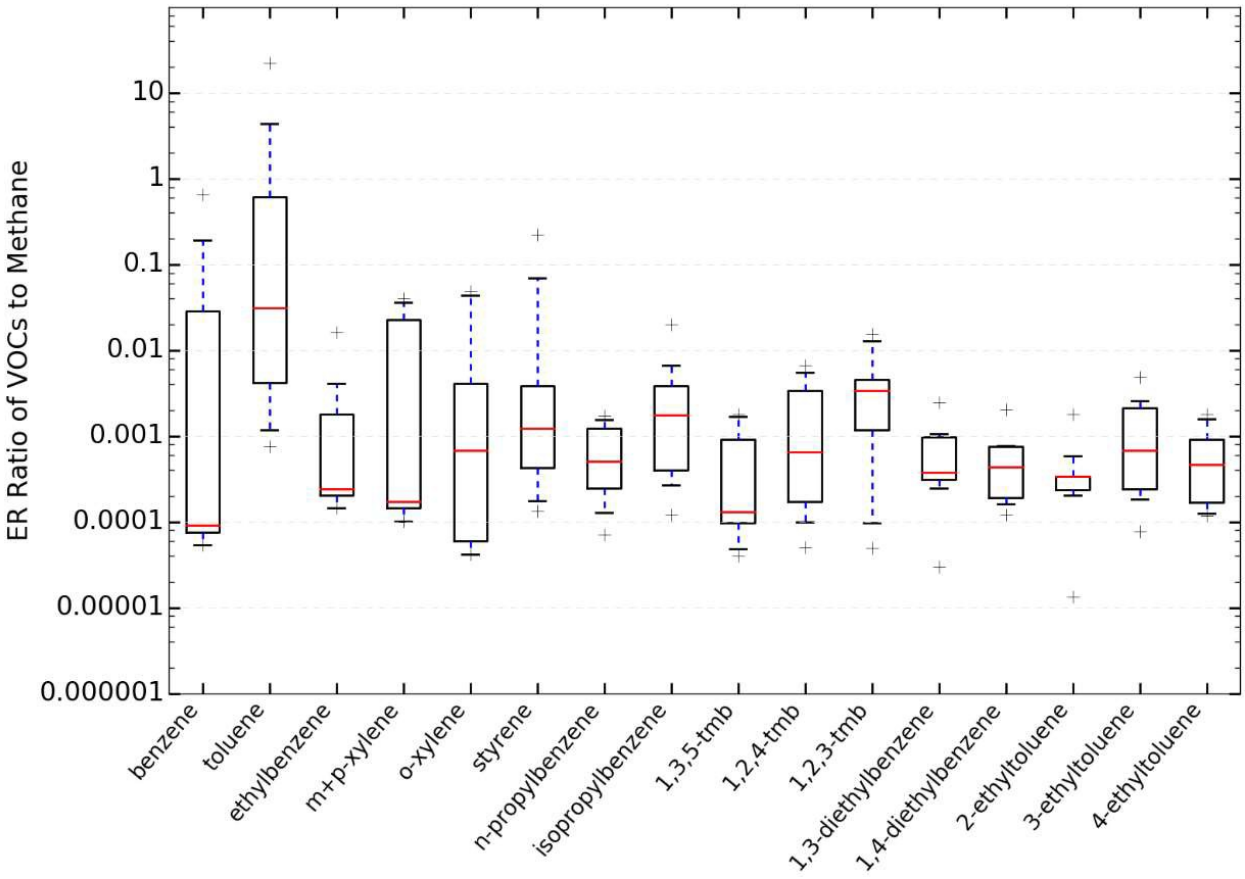

Figure H.3. Aromatic emission rate ratio distributions for drilling operations.

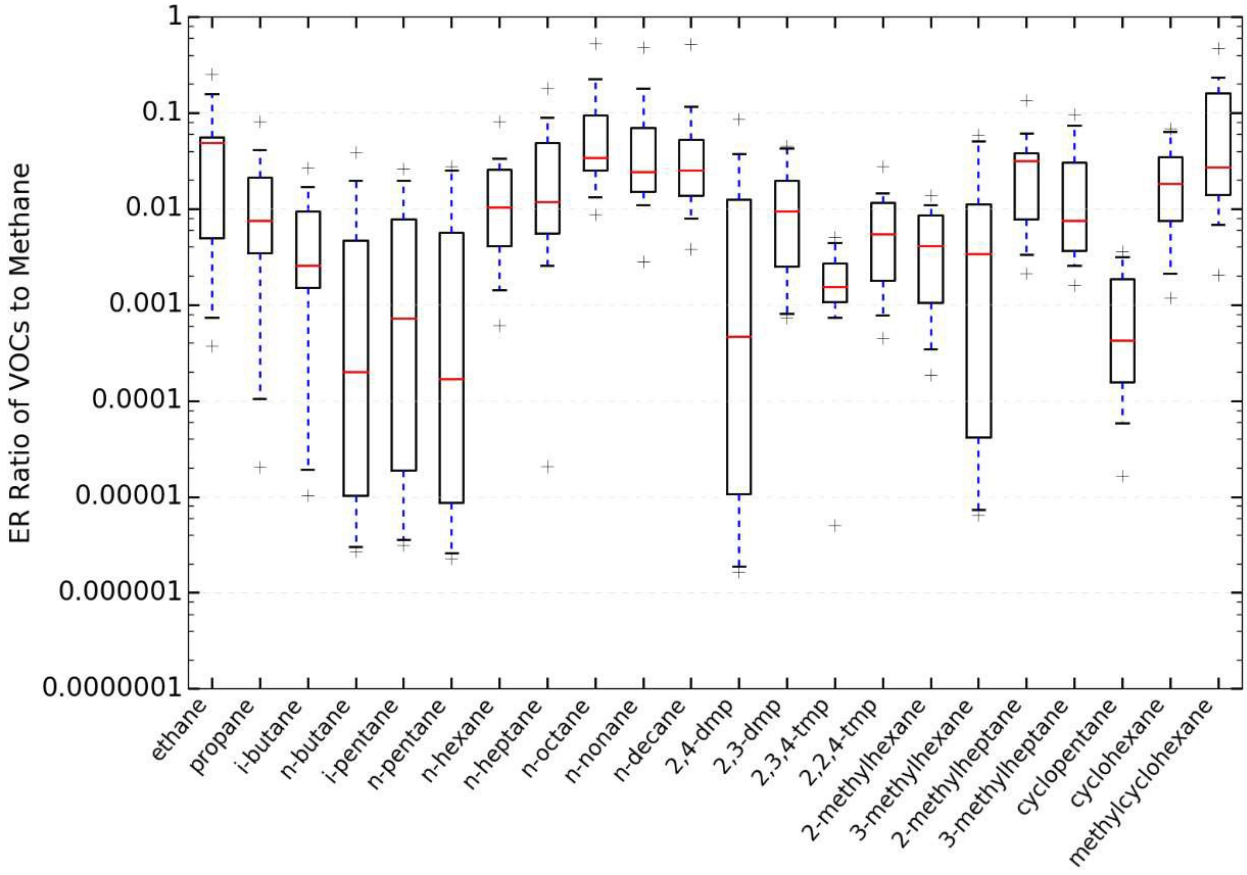

Figure H.4. Alkane emission rate ratio distributions for fracking operations.

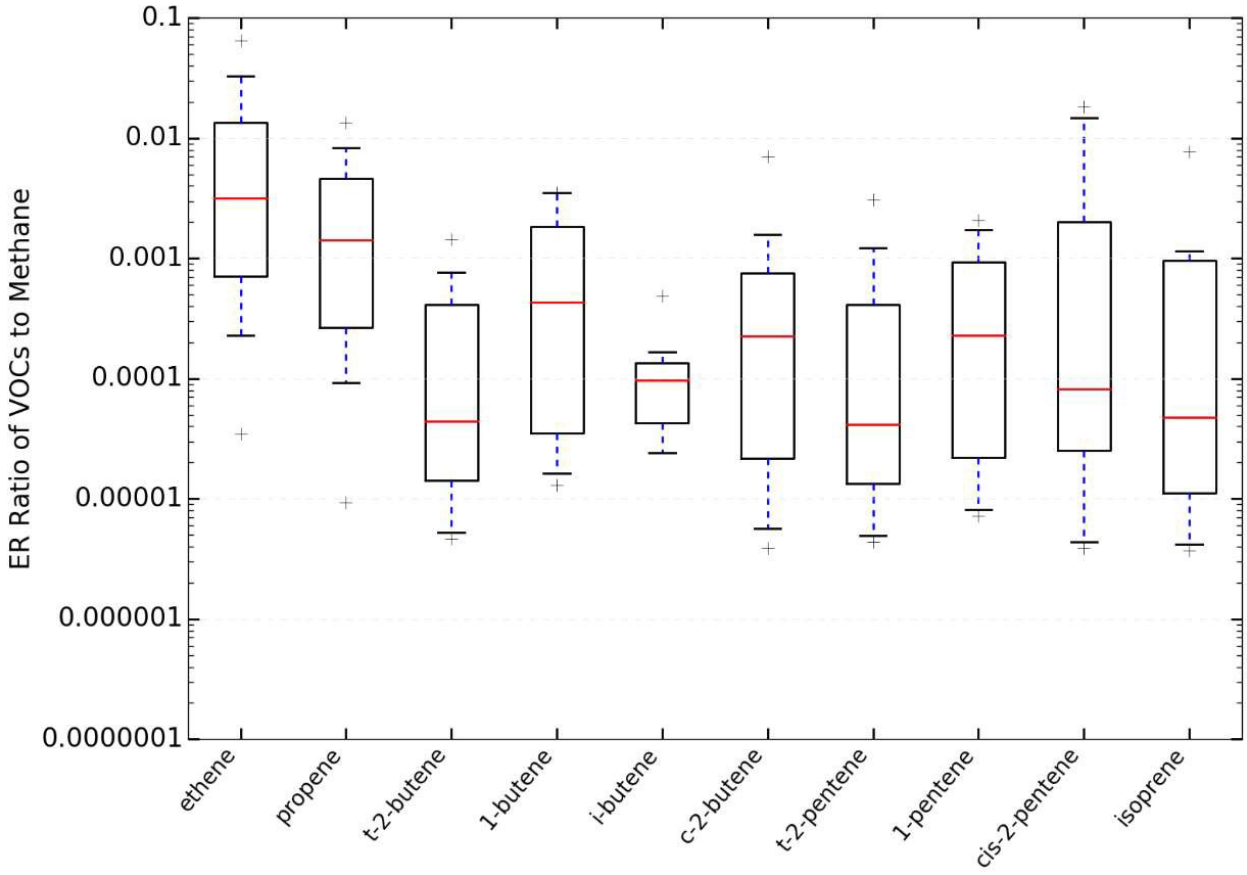

Figure H.5. Alkene emission rate ratio distributions for fracking operations.

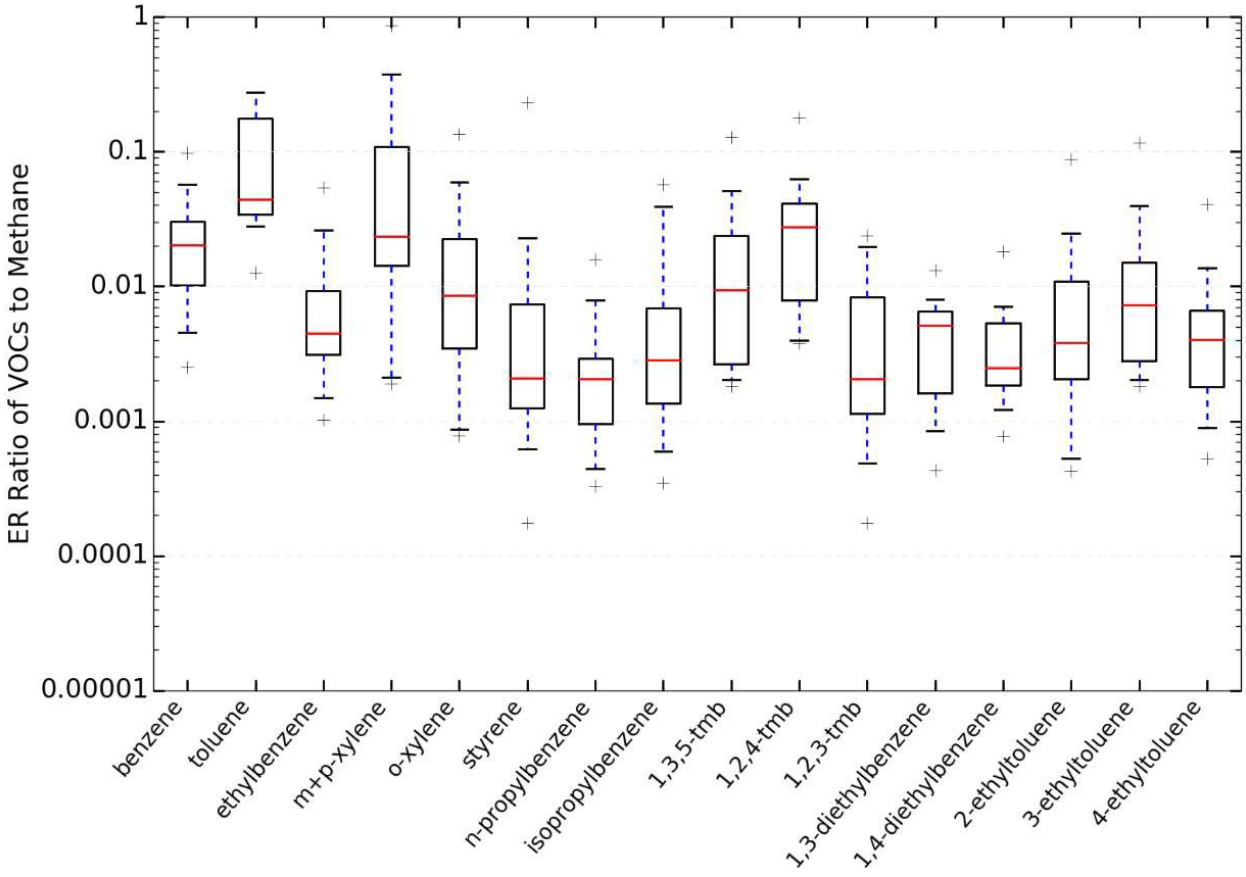

Figure H.6. Aromatic emission rate ratio distributions for fracking operations.

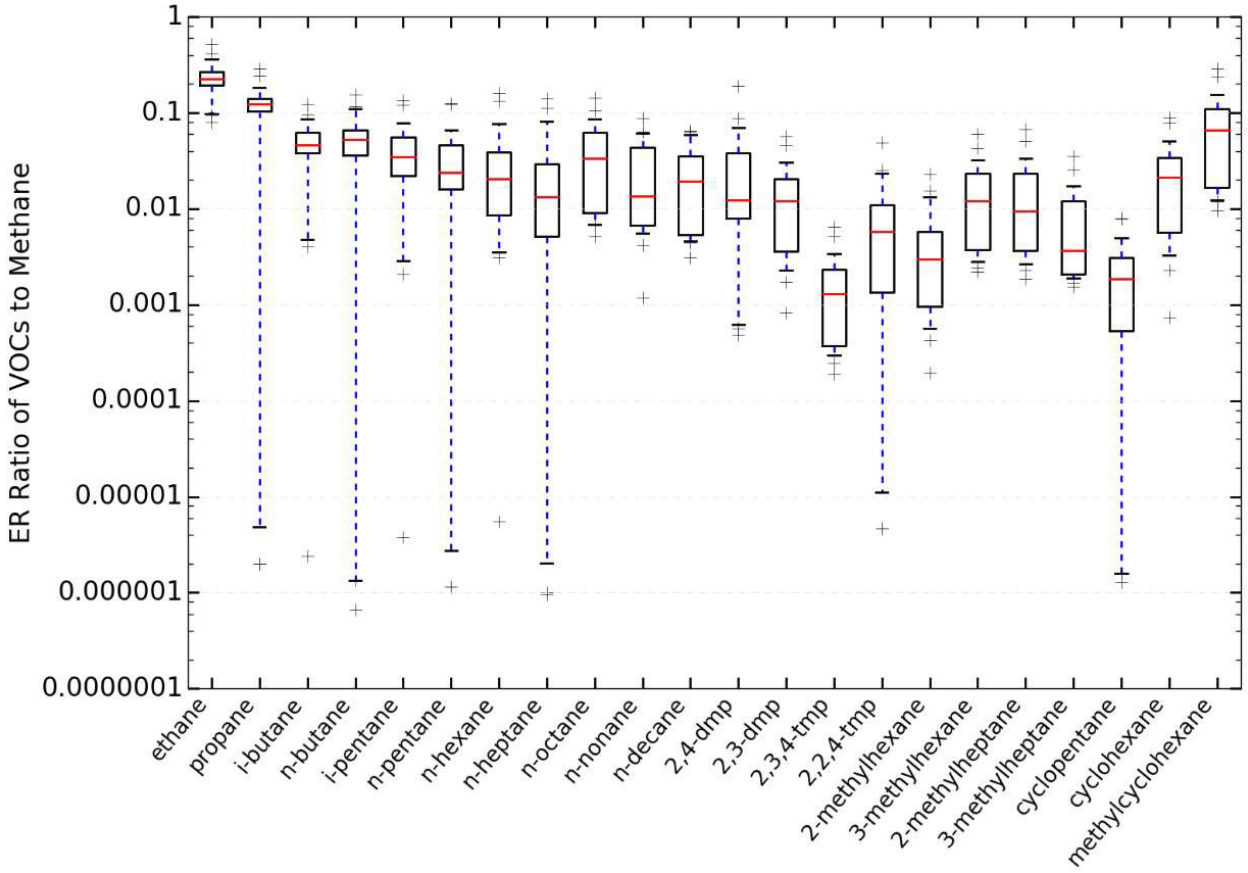

Figure H.7. Alkane emission rate ratio distributions for flowback operations.

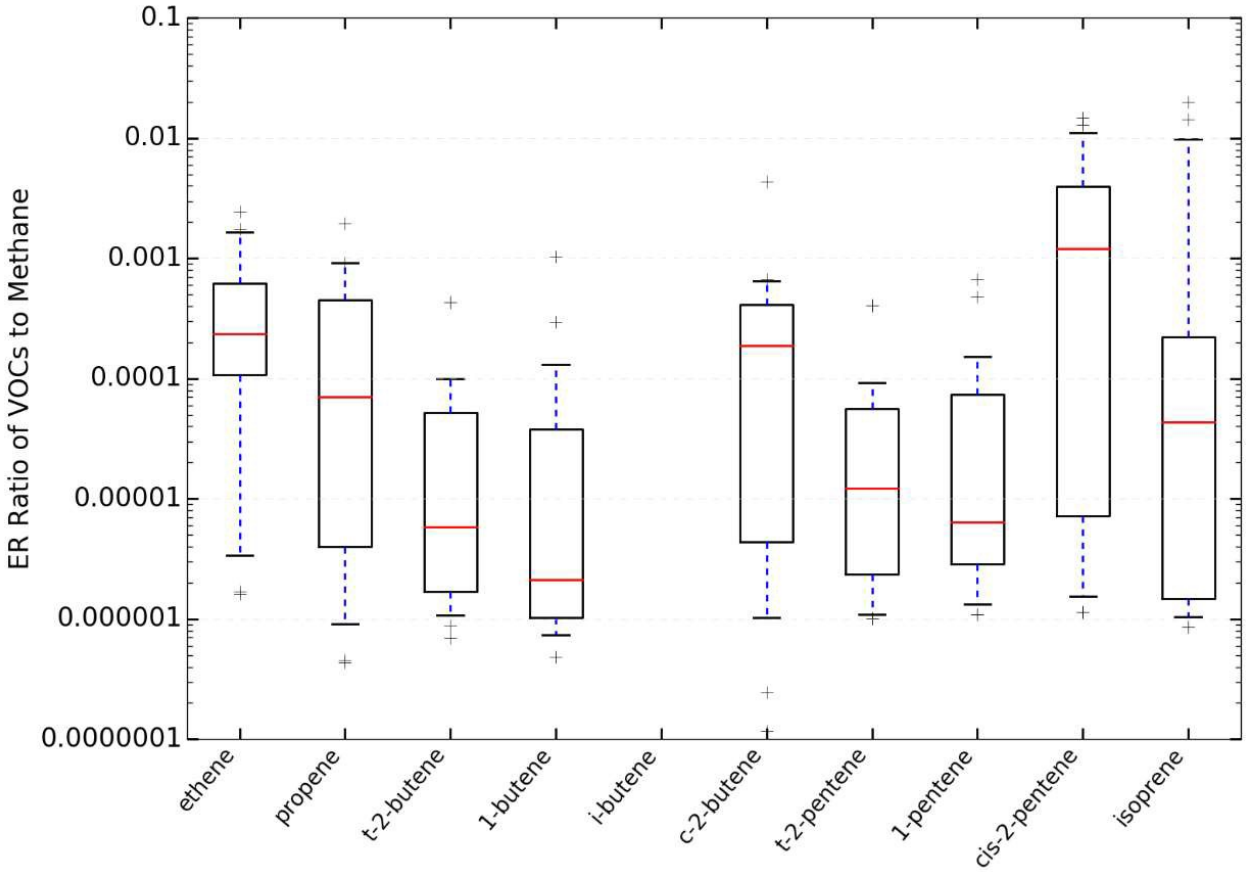

Figure H.8. Alkene emission rate ratio distributions for flowback operations.

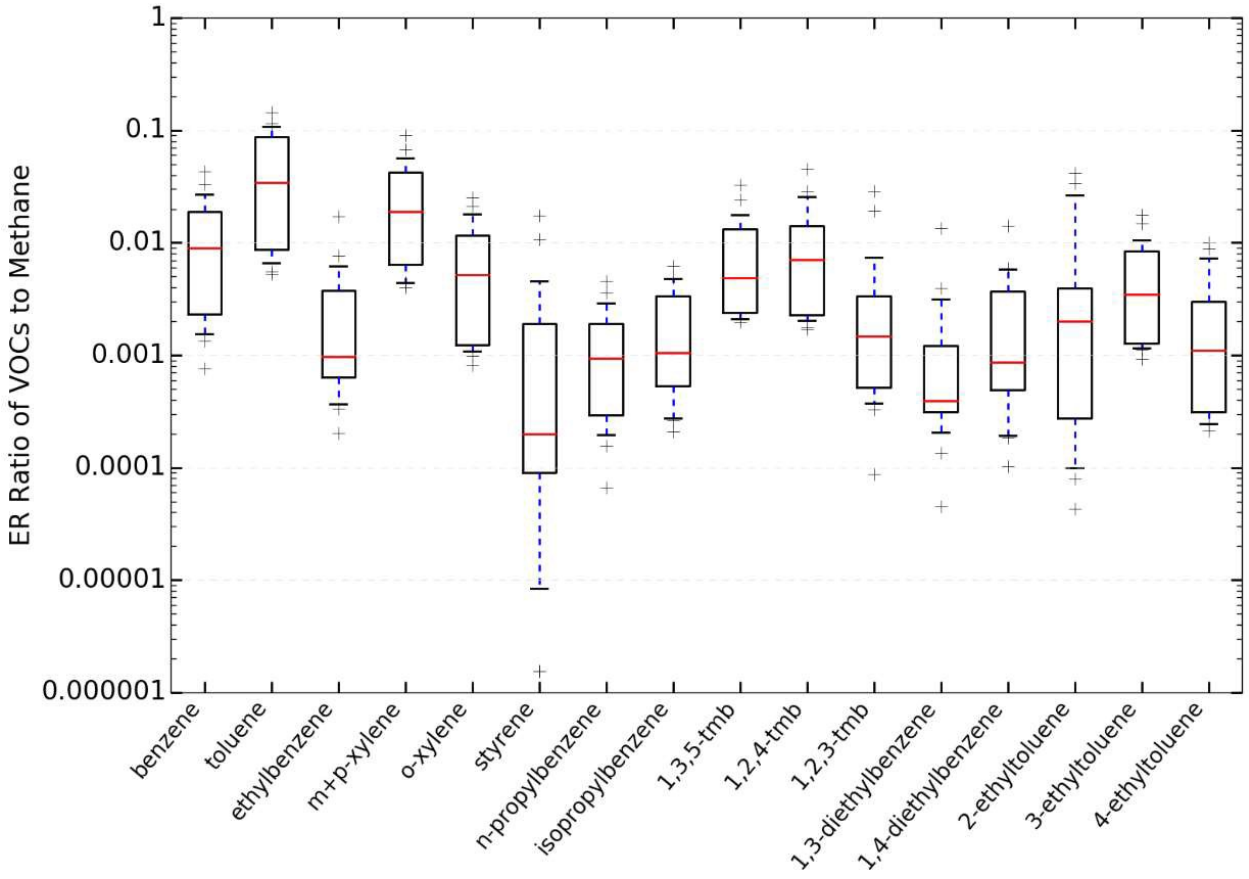

Figure H.9. Aromatic emission rate ratio distributions for flowback operations.

APPENDIX I

LIST OF EXPERIMENTS

Table I.1. List of experiments with corresponding operation type and number of canisters.

Experiment #	Type of Operation	Number of Canisters (including background)	Sets of Canisters
1	Drilling	4	2
2	Drilling	9	3
3	Drilling	6	3
4	Drilling	5	2
5	Fracking	17	6
6	Flowback	22	7
7	Fracking	2	1
8	Flowback	9	4
9	Drilling	13	4
10	Drilling, Fracking, and Flowback	10	3
11	Fracking	6	3
12	Fracking	5	4
13	Flowback	12	4
14	Flowback	15	5